

Qualitative models of intramolecular dynamics of acetylene: relation between the bending polyads of acetylene and perturbed Keplerian systems

D. A. Sadovskii and B. I. Zhilinskii

Université du Littoral—Côte d'Opale, Département de physique, 59140 Dunkerque, France

Submitted on January 29, 2018, revised April 5, 2018, accepted April 8, 2018

Abstract

We analyze qualitatively the bending vibrational polyads of the acetylene molecule (C_2H_2) in the approximation of the 1:1:1:1 resonant oscillator with axial symmetry using an effective vibrational Hamiltonian which reproduces bending vibrational energy levels computed by Michel Herman and coworkers (Herman et al., 2003). We explain how the classical limit of this quantum system for the total vibrational angular momentum $\ell = \zeta = 0$ is equivalent to a reduced perturbed Keplerian system on the classical phase space $S^2 \times S^2$, such as the hydrogen atom in external electric and magnetic fields in the Kustaanheimo–Stiefel (KS) formalism. In particular, bending vibrational N_b -polyads of C_2H_2 correspond to the n -shells of the perturbed hydrogen atom. Within this approach, using the techniques developed for the Keplerian systems and methods of the qualitative theory, we account concisely for all series of bifurcations of the classical nonlinear normal modes and their manifestations in the quantum energy level spectrum described by our predecessors Tyng and Kellman (2006). In addition to local oscillator approximations near stable equilibrium points, notably the local modes discussed by Rose and Kellman (1996); Jacobson et al. (1998, 1999a,b), we introduce two new global integrable approximations, and confirm them by constructing respective two regular complementary lattices of quantum states within one N_b, ℓ -polyad. From the stratification of the phase space, we uncover the geometrical meaning of the corresponding new good quantum numbers and define new kind of wavefunction localization in the neighborhood of two spheres S^2 in the four-dimensional space. Furthermore, we use our two approximate lattices to uncover quantum monodromy of the system through the evolution of an elementary quantum cell along a closed path in the images of the nearly integrable energy-momentum maps.

This paper appeared in the special issue of *Molecular Physics* dedicated to Prof. Michel Herman and the 2017 Colloquium on High-Resolution Molecular Spectroscopy (HRMS), Frédéric Merkt and Stefan Willitsch, Editors.

benpol 2018-05-29 22:01 ©2018 by Sadovskii & Zhilinskii

Updates at <http://purple.univ-littoral.fr/~sadovski/downloads/benpol-C2H2.pdf>

This is the final author version of the manuscript TMPH-2018-0064.

For all purposes, please refer to the published article.

With 12 figures, 9 tables, and 95 bibliography entries.

Contents

Abstract	1
1 Introduction: qualitative analysis of atomic and molecular dynamics	3
1.1 Most simple systems	3
1.2 Systems with two degrees of freedom	5
1.2.1 Molecular vibrations. Bending vibrations of acetylene	5
1.2.2 Perturbations of the hydrogen atom	6
1.2.3 Kustaanheimo-Stiefel formalism and polyads	7
1.3 Results, motivation, and purpose	7
2 Bending polyads of acetylene as a system on $\mathbb{S}^2 \times \mathbb{S}^2$	11
2.1 Perturbed Keplerian systems	12
2.2 Dynamical variables of the axially symmetric oscillator in 1:1:1:1 resonance and generators of the $\mathbb{T}_{n,\zeta}^2$ action	13
2.3 Quadratic polynomial invariants of the $\mathbb{T}_{2n,\zeta}^2$ action	14
2.3.1 Relation to the molecular system	15
2.3.2 Nonzero vibrational angular momentum ℓ	15
2.3.3 Integrity basis	15
2.4 Residual discrete symmetries and stratification of $\mathbb{S}^2 \times \mathbb{S}^2$	16
2.4.1 Stratification of $\mathbb{S}^2 \times \mathbb{S}^2$ for $\zeta = 0$	18
2.4.2 G_8 -invariant Morse functions on $\mathbb{S}^2 \times \mathbb{S}^2$	21
2.5 Bending vibrational Hamiltonian of C_2H_2	22
3 Bending relative equilibria of C_2H_2	26
3.1 Computing linear stability	26
3.2 Example of a G_8 -invariant Morse Hamiltonian on $\mathbb{S}^2 \times \mathbb{S}^2$	27
3.3 Analysis of the full C_2H_2 Hamiltonian starting at the poles	27
3.3.1 G_8 -invariant equilibria with $ K_1 = 1$	28
3.3.2 Twin equilibria at poles with $ L_1 = 1$	29
4 Classification of states within one N_b bending polyad with $\ell = 0$: third integral j and triangular lattices	29
4.1 Extending locally regular lattices with triangular patterns	30
4.2 Auxiliary quantum numbers and average values	32
4.3 Approximate dynamical symmetries. Angular momenta j' and j'' , and associated invariant spheres.	33
4.4 Phenomenological integrable $\text{SO}(4) \supset \text{SO}(3) \supset \text{SO}(2)$ and $\text{SO}(4) \supset \text{SO}(3)$ models, and their explicit realizations	36
4.5 Energy-momentum graph regularity in high N_b polyads	39
4.5.1 The $N_b = 12$ polyad. Quantum monodromy	40
4.5.2 The $N_b = 14$ polyad representation	42
4.5.3 The $N_b = 16$ polyad representation	42
5 Conclusion: types of localized bending states	42
Appendices	45

A	Reminder on the 1:1 oscillator	45
A.1	Coordinates	46
A.2	Dynamical oscillator symmetry \mathbb{S}^1	46
A.3	Coordinates of the diagonal representation	46
A.4	The Molien generating function for the invariants of the oscillator \mathbb{S}^1 symmetry	47
A.5	Reduction of the 1:1-oscillator	48
A.6	Quantum-classical correspondence	49
B	The 1:1:1:1 oscillator with axial symmetry	50
B.1	Quadratic polynomial invariants of the $\mathbb{T}_{n,\zeta}^2$ action	51
B.2	Symmetrized generating function and integrity basis	52
	References	56

1 Introduction: qualitative analysis of atomic and molecular dynamics

The qualitative approach to the study of differential equations and, in particular, of classical dynamical systems was initiated by Henri Poincaré at the end of the 19-th century, and was developed further by Lyapunov, Hopf, Andronov, Smale, Kolmogorov, Moser, Arnol'd, and many others (Abraham and Marsden, 1978). Introduction of their ideas to other fields went along with catastrophe theory, singularity theory (Arnol'd, 1992; Gilmore, 1993), and, later, with the concept of topological phase transitions (Thouless, 1998).

In general, we begin the qualitative analysis of an effective molecular Hamiltonian with the construction of the corresponding classical limit system. The subsequent study of this system involves all methods of the qualitative theory of classical dynamical systems (Arnol'd, 1989), specifically the bifurcation theory (Arnold, 1983), the idea of topological phases (Bernevig, 2013), and others. We return to the quantum system by establishing the correspondence between the qualitative characteristics of the eigenspectrum and eigenfunctions of the quantum system and their modifications under variation of one or several control parameters, and the specific qualitative features of the respective classical limit system, such as the phase space topology, equilibria and relative equilibria, their bifurcations, critical and singular fibres and their appearance/disappearance under variation of control parameters.

1.1 Most simple systems

It can be argued that one-degree-of-freedom systems with a (smooth) compact phase space without boundary and a single control parameter are the most simple systems to analyze qualitatively. In molecules, such effective systems include rotation in an isolated nondegenerate vibrational state, and two vibration modes in 1:1 resonance (Zhilinskiĭ, 2001). In atoms, we have \mathbb{S}^1 symmetric perturbations of the hydrogen atom, such as the quadratic Zeeman system (Michel and Zhilinskiĭ, 2001a; Efstathiou and Sadovskii, 2010). In all these cases, the phase space of the model system is the 2-sphere \mathbb{S}^2 or, equivalently, the complex projective line $\mathbb{C}P^1$ which is diffeomorphic to \mathbb{S}^2 . The compactness of the phase space means that (for each fixed value of the control parameter, such as the value of the momentum of the reduced \mathbb{S}^1 action) the

number of levels in the corresponding reduced quantum system is *finite*. The eigenstates can be computed by diagonalizing the matrix of the quantum Hamiltonian in an appropriate finite basis. Other advantages of such systems include the possibility to apply Morse theory to the analysis of classical Hamiltonians $H : \mathbb{S}^2 \rightarrow \mathbb{R}$. And the last, but not the least specific simplifying property of all these one-degree-of-freedom reduced systems is that energy alone is often enough to separate different dynamics. Modification, appearance, and disappearance of different dynamical regimes can be represented by regions in the energy-parameter diagram. Quite often, our parameters refer to other degrees of freedom which are reduced and described effectively. Thus, in the above examples, the length of the total angular momentum, the vibrational polyad number, and the orbital momentum, respectively, are such dynamical parameters, and the diagram corresponds to the image of the classical energy-momentum map.

The first application of the qualitative approach in molecules was the explanation of their rotational energy level clusters (Dorney and Watson, 1972; Harter and Patterson, 1984). In this case, we study the reduced classical dynamics of a freely rotating molecule with angular momentum vector \mathbf{J} whose length $j := \|\mathbf{J}\|$ and orientation in the laboratory coordinate frame are conserved (are first integrals). All other degrees of freedom, such as vibrations, are accounted for effectively, i.e., are reduced, normalized, averaged out, etc. The pure rotational molecular Hamiltonian $H(\mathbf{J})$ is a perturbation of the quadratic rigid body Hamiltonian $H_0(\mathbf{J})$ and we can call this system a reduced nonrigid Euler top. Points of \mathbb{S}^2 represent orientations of \mathbf{J} in the body fixed frame. In particular, stationary axes of rotation correspond to stationary points of H , i.e., are equilibria of the system. The value of j serves as a natural dynamical control parameter. Quantum levels for each fixed allowed value of $j = 0, 1, 2, \dots$ form rotational *multiplets*. Their internal structure, which can be particularly rich and dense in the case of (nearly) spherical top molecules, is analyzed. Modifications of this structure are related to bifurcations of stationary axes (Pavlichenkov and Zhilinskiĭ, 1985, 1988; Pavlichenkov, 1993).

Reduced systems on the phase space $\mathbb{C}P^1$ appear in the qualitative analysis of the internal structure of isolated *polyads* formed by two (quasi)-degenerate molecular vibrations in 1:1 resonance. In this case, all other motions except the two vibrations of interest are averaged out and/or separated. The analysis is very similar to that in the case of pure rotations albeit the symmetries of H (and the degrees in \mathbf{J}) can be different. In particular, polyads characterized by the polyad quantum number $n = 0, 1, 2, \dots$ are equivalent to multiplets with $j = n/2$. The most widely analyzed phenomenon in these systems is the pitchfork bifurcation leading to the appearance of so-called *local* modes and the respective energy level doublets (Lawton and Child, 1979; Jaffé and Brumer, 1980; Child and Halonen, 1984; Kellman, 1985; Mills and Robiette, 1985; Hartke et al., 1992).

Among the perturbations of the hydrogen atom by weak homogeneous static electric and magnetic fields, there is a large class of systems with the reduced phase space \mathbb{S}^2 which is obtained after removing both Keplerian and Pauliean \mathbb{S}^1 symmetries, see chap. IV.D and V.B in (Efstathiou and Sadovskii, 2010) and references therein. Historically the first system of this kind was the quadratic Zeeman effect, where the qualitative analysis explained localized states forming quasidegenerate doublets (Herrick, 1982). Within the one-parameter family of the orthogonal electric and magnetic field perturbations, whose parameter defines the relative strengths of the fields, such doublets appear very similarly to the vibrational local modes (Efstathiou et al., 2009).

At this point, several remarks may be of interest. It should be noted that the systems above are obtained by reducing Lie symmetries of different kinds. In the case of

vibrational polyads and most atomic perturbations, the symmetries are dynamical and approximate; when we study rotations, the symmetries are geometric and strict. Notice also that there are typically two approximations made in the study of resonant vibrations and perturbations of the hydrogen atom: the resonance may not exactly be 1:1 *and* the polyad integral n is not strictly conserved in the original system and becomes an integral only for the normal form which is typically divergent. In this respect, polyads of C_2H_2 are of “mixed” nature: their polyad symmetry \mathbb{S}^1 is approximate and dynamical, while the axial $SO(2) \sim \mathbb{S}^1$ symmetry is geometric. We should also mention resonances other than 1:1. They lead to reduced spaces P^* that are topologically equivalent to \mathbb{S}^2 but have singularities, i.e., these spaces are *not* diffeomorphic to \mathbb{S}^2 . Examples include Fermi resonances in molecules, typically between bending and stretching vibrations, and a class of perturbations of the hydrogen atom by electric and magnetic fields skewed to a specific angle, see (Efstathiou et al., 2008) and sec. III.C and V.C of (Efstathiou and Sadovskii, 2010). We will not consider other resonances here since they do not appear within the limited context of pure bending polyads of C_2H_2 . We can only mention that a Poisson structure-preserving singular map can make P^* into a smooth \mathbb{S}^2 and that the latter is sometimes taken confusingly for the actual phase space of the system.

1.2 Systems with two degrees of freedom

Qualitative analysis has profoundly advanced our understanding of a great number of fundamental atomic and molecular systems. We would naturally like to consider more complex systems with intrinsically larger number of degrees of freedom, i.e., with degrees of freedom that cannot be separated neither due to strict symmetries nor due to approximations based on the perturbation theory, averaging, and normalization. Specifically, we may like to study systems with two such essential degrees of freedom and retain, for simplicity, the compactness of the underlying classical four-dimensional phase space and the existence of a single control parameter. In molecular and atomic systems, we encounter phase spaces $\mathbb{C}P^2$ and $\mathbb{S}^2 \times \mathbb{S}^2$. The former occurs as a reduced phase space (or polyad space) in the study of vibrational polyads formed by 1:1:1 resonant oscillators (Zhilinskiĭ, 1989; Sadovskii and Zhilinskiĭ, 1993a), such as triply degenerate vibrational modes of tetrahedral (CH_4) or octahedral (SF_6) molecules. The latter is the classical phase space of all n -shell (or Keplerian) approximations to the perturbations of the hydrogen atom and can be traced back to the beginnings of quantum mechanics (Valent, 2003; Pauli, 1926; Fock, 1935; Bargmann, 1936). As we explain in this work, $\mathbb{S}^2 \times \mathbb{S}^2$ is also the classical phase space associated with the quantum reduced effective Hamiltonian describing bending vibrational polyads of C_2H_2 .

1.2.1 Molecular vibrations. Bending vibrations of acetylene

Vibrational polyads associated with the classical phase space $\mathbb{C}P^2$ were analyzed and described to a certain detail, see for example (Efstathiou et al., 2003, 2004; Efstathiou and Sadovskii, 2004; Crogman et al., 2007), but applications in molecules were hindered by the lack of molecular systems satisfying the necessary assumptions, specifically, that these polyads can be separated effectively from all other vibrational modes and that the polyad approximation is holding for sufficiently high polyad numbers N , for which polyads contain many levels and classical limit is feasible. Furthermore, as some known examples may suggest (Patterson et al., 1981; Sadovskii et al., 2010), such high polyad numbers are not easy to observe and interpret experimentally.

In this respect, bending polyads of acetylene $\text{H}-\text{C}\equiv\text{C}-\text{H}$ give a rare opportunity to have experimentally accessible system with two degrees of freedom which conforms our criteria. These polyads are formed by two doubly degenerate bending vibrational modes of C_2H_2 which transform according to the irreducible representation ± 1 of the axial symmetry group $\text{SO}(2)$ of this linear molecule. Being in close 1:1 resonance, these modes are strongly interacting and we should consider large polyads of an $\text{SO}(2)$ -symmetric 4-oscillator in (1:1):(1:1) resonance¹, while accounting for the three remaining nondegenerate stretching vibrational modes and the two rotational degrees of freedom effectively. As was shown in a number of detailed ground making studies by Herman and co-authors (Temsamani and Herman, 1995; Temsamani et al., 1996; Herman et al., 2003; Herman, 2007; Amyay et al., 2016) as well as in other work going back to Plíva (1972) with important contributions by Rose and Kellman (1996); Jacobson et al. (1998, 1999a,b) and more recently by Ding (2004); Tyng and Kellman (2006); Zhilinskií et al. (2000), these polyads exist and can be described effectively as isolated from each other and from all other vibrational states up to very high polyad numbers $N_b \approx 20$ with large number $(N_b/2 + 1)^2$ of vibrational components (for $\ell = 0$) and complex internal structure. Note that the $\text{SO}(2)$ symmetry implies that we have two first integrals in the system, the (1:1):(1:1) polyad integral N_b and the vibrational angular momentum ℓ associated with $\text{SO}(2)$. In other words, we have dynamical Lie symmetry \mathbb{T}^2 . The reduced system that describes internal polyad dynamics has therefore two degrees of freedom and two parameters n and ℓ . It can be analyzed qualitatively and the results can be compared to the rich vibrational energy level structure of acetylene which is reconstructed quite reliably and fully from the highly detailed experimental data on C_2H_2 accumulated over the last forty years (Herman et al., 2003; Amyay et al., 2016). This explains the continuing interest in the acetylene molecule (see, for example, the recent work by Tyng and Kellman (2009b,a, 2010); Ma et al. (2012); Larese et al. (2014)). Michel Herman is one of the key contributors to the experimental studies of the bending polyads and other vibrational states of acetylene and it is our great pleasure to contribute this paper to the special issue in his honor.

1.2.2 Perturbations of the hydrogen atom

The internal structure of the n -shells of the perturbed hydrogen atom has been studied extensively both in theory and experiment, see the recent review by Efstathiou and Sadovskii (2010). In the classical limit, the shells are described by a reduced dynamical system with two degrees of freedom and classical phase space $\mathbb{S}^2 \times \mathbb{S}^2$ equipped with the standard Lie-Poisson algebra $\mathfrak{so}(3) \times \mathfrak{so}(3)$. It is obtained from the original physical system with three degrees of freedom by averaging with regard to the Keplerian \mathbb{S}^1 action N corresponding to the principal quantum number n and by subsequent fixing the value of $N > 0$ as a dynamical control parameter. More technically (Efstathiou and Sadovskii, 2010), the original perturbed system where N is not strictly conserved is normalized with regard to the Hamiltonian flow of the Hamiltonian vector field X_N , and the normal form $H : \mathbb{S}^2 \times \mathbb{S}^2 \rightarrow \mathbb{R}$ is truncated at a certain sufficiently high order. The action N becomes first integral of the reduced system with Hamiltonian H and phase space $\mathbb{S}^2 \times \mathbb{S}^2$ for each fixed value of $N > 0$. We should remark, however, that finding a physical perturbation that preserves the approximate Keplerian dynamical symmetry of the system but removes the internal approximate Pauliean dynamical symmetry \mathbb{S}^1 of the n -shells and thus makes the n -shell dynamics anisochronous

¹Our notation implies that resonances within the parentheses are exact.

(Fontanari and Sadovskii, 2015) may not be all that straightforward. For instance, all perturbations by static homogeneous fields retain this additional \mathbb{S}^1 symmetry and we can continue reducing down to a system on \mathbb{S}^2 .

1.2.3 Kustaanheimo-Stiefel formalism and polyads

Treating perturbations of the hydrogen atom within the Kustaanheimo-Stiefel (KS) framework (see, for example, sec. IV.A of (Efstathiou and Sadovskii, 2010) and references therein, and the more recent discussion by van der Meer (2015)) makes this system most directly and explicitly related to the bending polyad system of C_2H_2 (with zero angular momentum $\ell = 0$). In the KS approach, using the singular KS map and subsequent regularization of the Coulomb potential term, the original physical system is transformed into a four-dimensional exactly 1:1:1:1 resonant oscillator subject to an additional “fictitious” exact \mathbb{S}_ζ^1 symmetry, a rotation in the coordinate space \mathbb{R}^4 with momentum ζ . The Keplerian symmetry of the original hydrogen atom in three dimensions becomes the \mathbb{S}_n^1 symmetry of the 1:1:1:1 resonant oscillator with momentum n , and together with the above additional fictitious symmetry it constitutes the symmetry \mathbb{T}^2 of the KS system. We observe readily that \mathbb{S}_ζ^1 corresponds directly to the axial $\text{SO}(2)$ symmetry of C_2H_2 and therefore, ζ is the equivalent of the vibrational angular momentum ℓ . As for the Keplerian symmetry \mathbb{S}_n^1 , it is equivalent to the polyad symmetry of C_2H_2 , albeit in the latter case we allowed for the detuning of two 1:1 modes. It follows that the shell number $n = 1, 2, \dots$ and the polyad number $N_b = 0, 1, 2, \dots$ are related as $n = N_b/2 + 1$. The hydrogen atom system corresponds to the special value of $\ell = \zeta = 0$, while for nonzero ζ we have the so-called “magnetic monopole” systems. All of them have phase spaces $\mathbb{S}^2 \times \mathbb{S}^2$, but the radii of the two \mathbb{S}^2 factors (and, consequently, their areas and symplectic volumes) differ when $\zeta \neq 0$.

1.3 Results, motivation, and purpose

The studies of bending polyads of C_2H_2 cited above, all within the detuned resonance (1:1):(1:1) oscillator model, have shaped our understanding of the dynamics of this system. Nevertheless, the description of the underlying reduced classical mechanical system remained incomplete. Most notably, the basic fact that this system has the compact phase space $\mathbb{S}^2 \times \mathbb{S}^2$ equipped with the standard Lie-Poisson algebra $\mathfrak{so}(3) \times \mathfrak{so}(3)$ and is, therefore, equivalent (for zero angular momentum $\ell = 0$) to a perturbed Keplerian system, such as the hydrogen atom in weak external fields, remained unnoticed. Similarly overlooked went the related fact that the quantum polyad Hamiltonian can be simply expressed and solved using the components of two angular momenta \mathbf{J}_1 and \mathbf{J}_2 generating the standard quantum Fock algebra $\mathfrak{so}(3) \times \mathfrak{so}(3)$. With the present work we correct this shortfall and take immediate advantage of the advanced techniques developed in the numerous studies of the hydrogen atom perturbations in order to further the qualitative analysis of bending vibrational dynamics of C_2H_2 .

We show how bending polyads of C_2H_2 are described as a system on $\mathbb{S}^2 \times \mathbb{S}^2$, more specifically, as a detuned (1:1):(1:1) resonant oscillator system reduced with respect to its \mathbb{T}^2 symmetry. Accounting for the discrete symmetries of C_2H_2 and following them into the reduced classical system, we explain how $\mathbb{S}^2 \times \mathbb{S}^2$ is stratified under the action of the resulting discrete symmetry group. The knowledge of this stratification allows an easier analysis of the respective invariant Hamiltonian functions $H : \mathbb{S}^2 \times \mathbb{S}^2 \rightarrow \mathbb{R}$ and a better understanding of the nature of particular non-generic constant h -level sets of H , such as stationary points (equilibria) and periodic orbits. We express the Hamiltonian

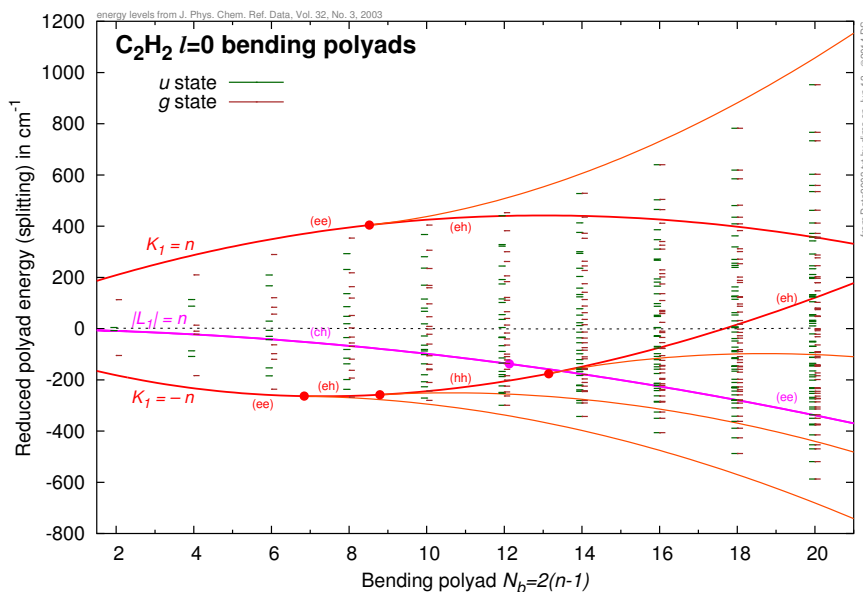


Figure 1: Energy of classical relative equilibria (solid lines) and quantum energy levels (horizontal dashes) of the bending vibrational subsystem of C_2H_2 with angular momentum $\ell = 0$ as functions of the bending polyad quantum number N_b . Opaque circles on the solid lines mark the instances of bifurcations of relative equilibria. The RE energies are computed using the Hamiltonian by Jacobson et al. (1998); quantum energies are taken from (Herman et al., 2003); a polynomial $N_b (a N_b + b)$ with $a = -0.1431$ and $b = 668.141$ is subtracted from all energies.

of Jacobson et al. (1998, 1999b) as a function H on $S^2 \times S^2$ and analyze it. In particular, we show how the equilibria on $S^2 \times S^2$ correspond to the periodic orbits studied by Ding (2004); Tyng and Kellman (2006, 2009a, 2010). Specifically, we show that they are *relative equilibria* (RE) of the four-oscillator with dynamical symmetry T^2 , or its *nonlinear normal modes*². We also adjust the parameters of the effective Hamiltonian for bending polyads in order to reproduce numerical data by Herman et al. (2003) on quantum bending energy levels, and we demonstrate subsequently in sec. 4 that these data can be interpreted as forming a rather regular lattice.

Classical RE energies (as function of parameters n and ℓ) define the energy domain allowed to the quantum system and characterize the internal structure of this domain. In sec. 3, we compute RE energies for the Hamiltonian of Jacobson et al. (1998, 1999b). Our results in fig. 1 show how all known bending quantum levels of C_2H_2 listed in

²The term *nonlinear normal mode* (NNM) was introduced by Montaldi et al. (1988, 1990). Further discussion and examples can be found in (Sadovskii and Zhilinskiĭ, 1993b; Montaldi and Roberts, 1999; Efsthathiou et al., 2004; Sadovskii et al., 2010). One can also mention *local modes* Lawton and Child (1979); Jaffé and Brumer (1980); Kellman (1985); Mills and Robiette (1985) as a particular widely known kind of NNM, see for example (Kozin et al., 2005; Crogman et al., 2007) and references therein. NNM's describe all possible basic vibrational motions of the resonant system with (quasi-)resonant normal modes and so are indispensable for describing the vibrational dynamics of resonances. They are specific *additional* periodic solutions of periods close to that of the (quasi-)degenerate normal modes. The number and stability of NNM's depends on the specific nonlinearity and symmetry of the system. Period-preserving bifurcations can increase their number, change their stability etc. The normal modes themselves become part of the set of NNM's. In the presence of Lie symmetries, such as the polyad symmetry S^1 , NNM's correspond to specific orbits of the action of that symmetry and are called *relative equilibria* (RE).

(Herman et al., 2003) are indeed contained within this domain. It can be seen that for low $N_b \leq 6$, the system has only *four* RE. By Morse theory, this is the minimal possible number on $\mathbb{S}^2 \times \mathbb{S}^2$. Two of these RE have distinct energies and are characterized by maximal absolute values of the detuning momentum ν (red lines in fig. 1). They can be interpreted as bending normal modes and their energies define maximum and minimum energy accessible to the polyad. Two other RE with $\nu = 0$ are degenerate in energy (purple line in fig. 1). They are specific bending *nonlinear* normal modes with maximal momentum μ , they define “circular” wavefunction localization pattern (Jacobson et al., 1999a; Ding, 2004; Tyng and Kellman, 2006), and they are equivalent to the motion of the hydrogen atom with maximal angular momentum L and projection $\mu = L_1 = m = \pm n$. Subsequent Morse and Hamiltonian stability analysis of these RE on $\mathbb{S}^2 \times \mathbb{S}^2$ gives information on the modifications of the internal structure of polyads in fig. 1 due to cascading bifurcations for $6 < N_b < 14$, as was observed and analyzed earlier by Tyng and Kellman (2006). Of a particular interest may be the fact, also uncovered by Tyng and Kellman (2010), that the two RE with $\mu = \pm n$ are complex hyperbolic (focus-focus) at low $N_b < 12$. This suggests a potential nontrivial organization of quantum levels known as quantum monodromy, see especially (Sadovskii and Zhilinskiĭ, 1999; Zhilinskiĭ, 2005) and references therein, as well as Efstathiou and Sadovskii (2010).

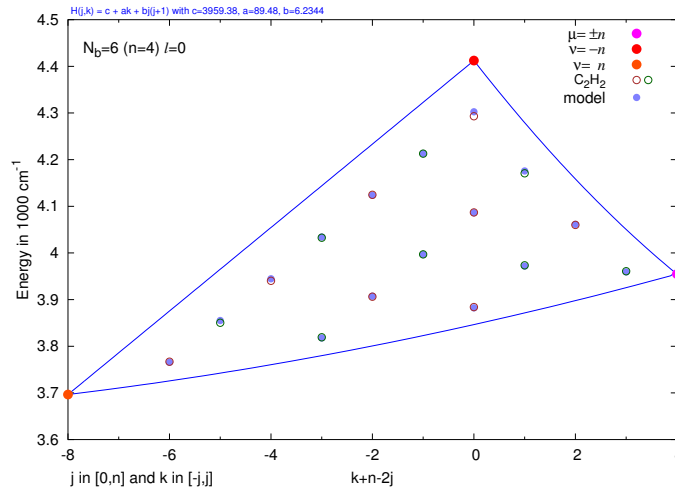


Figure 2: Internal structure of the bending vibrational polyad of C_2H_2 with quantum number $N_b = 6$ ($n = 4$) and angular momentum $\ell = 0$ as a regular lattice in the image of the classical energy-momentum map. For the simple integrable model with Hamiltonian $\mathcal{H}(j, k)$ we compute classical relative equilibria (filled circles), classical relative periodic orbits (solid blue lines), and eigenvalues of the corresponding quantum system (filled circles). The actual quantum energies from (Herman et al., 2003) are marked by red and black opaque circles.

In order to see the Hamiltonian monodromy, we need to deal with an integrable approximation for the considered system which describes the dynamics of the two-degree-of-freedom system in the region surrounding the focus-focus singularity. An integrable approximation provides further classification of quantum states within each $(N_b, \ell = 0)$ polyad through an additional good quantum number j . This can be seen as adding the third dimension to the combined plot in fig. 1. For low N_b , we came up with a simple three-parameter integrable model represented in fig. 2. This model reproduces very well the lattice of bending vibrational states within one (N_b, ℓ) polyad with low

N_b and the corresponding system of four nonlinear modes. The justification for the particular choice of the additional integrals of motion j and $\nu + n - 2j$ in the study of the internal structure of bending polyads becomes clearer when we step up N_b . We have found out that the polyad section in fig. 2 can be continued empirically to very high N_b if we take the symmetries of the quantum states into account and exploit the regularity of the corresponding local lattice patterns. This is well illustrated in fig. 3 by an empirical quantum state lattice for $N_b = 14$.

However, one such integrable approximation is not sufficient to see the presence and manifestation of Hamiltonian monodromy in a system which, as we will see, is essentially nonintegrable on a significant open neighborhood of the complex hyperbolic relative equilibrium surrounded by regular dynamics in the four-dimensional classical phase space. In section 4, we suggest two different integrable approximations which are valid near/along the boundaries of the domains of the corresponding energy-momentum maps. Our two approximations produce two sets of local classical actions and two corresponding sets of good local quantum numbers for the initial classical and quantum systems, respectively. At least one of the sets can be used near/along the boundaries of the image of the energy-momentum map, and the sets can be related in the domains where they both are valid. Considering a nontrivial closed path along the boundaries which encircles the image of the region with non-integrable dynamics, we followed the evolution of classical actions and corresponding elementary cells for the lattice of quantum states. This allowed us to uncover the monodromy of the system.

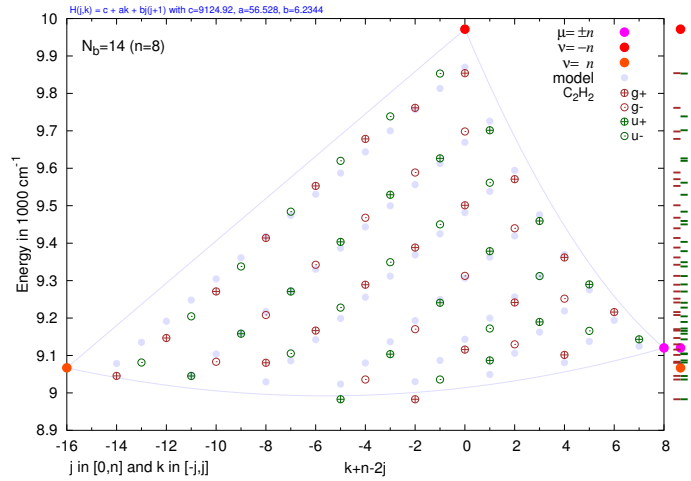


Figure 3: Empirical internal structure of the bending vibrational polyad of C_2H_2 with quantum number $N_b = 14$ ($n = 8$) and angular momentum $\ell = 0$ as a regular lattice in the image of the hypothetical “Upper Left” classical integral map, see more in sec. 4.5.2. The simple integrable model with Hamiltonian $\mathcal{H}(j, k)$ is represented by classical relative equilibria (filled circles), classical relative periodic orbits (light gray solid lines), and eigenvalues of the corresponding quantum system (light gray filled circles). The quantum energies from (Herman et al., 2003) are marked by opaque circles whose color and additional markup distinguish the four different symmetry types. The rightmost column shows the convoluted levels of the polyad similarly to the $N_b = 14$ column in fig. 1.

On the other side, the energy level pattern shown in fig. 3 clearly exhibits the consequences of the pitchfork bifurcation of the $\nu = -n$ RE at the high energy end of the polyad. According to fig. 1, this bifurcation occurs near $N_b = 9$. The quantum number

$N_b = 14$ is sufficiently large for this classical phenomenon to be reflected in the energy level structure of the polyad. And indeed, as we can see clearly in fig. 3, the diagonally (bottom left to top right) running one-dimensional sublattices of $2j + 1$ levels become doubly split towards their high energy end. Like in the case of the $\mu = \pm n$ RE, our simple model (pale gray in fig. 3) does not provide the possibility for the bifurcation of the $\nu = -n$ RE either. Nevertheless, it still reproduces fairly well the lattice section as a whole.

The existence of such regularities at very high bending excitations, essentially up to $N_b = 20$, justifies strongly the study of possible integrable approximations, and the respective description of relative equilibria, of their bifurcations and stability.

2 Bending polyads of acetylene as a system on $\mathbb{S}^2 \times \mathbb{S}^2$

Acetylene (C_2H_2) is a linear four-atomic molecule $\text{H}-\text{C}\equiv\text{C}-\text{H}$ with spatial symmetry $D_{\infty h} \sim Z_2 \times \text{O}(2)$. Small vibrations of the atoms in C_2H_2 about its linear equilibrium configuration are separated into stretching and bending displacements that are aligned with and perpendicular to the symmetry axis C_∞ , respectively. The symmetry axis is aligned with the axis of the molecule and is taken as axis z . There are seven vibrational degrees of freedom. Because the stretching and bending vibrational frequencies are sufficiently different, we can, in the simplest approximation, ignore the three stretching modes and consider two doubly degenerate bending modes ν_{4g} (*trans*, symmetric³) and ν_{5u} (*cis*, antisymmetric³). These modes transform according to the doubly degenerate irreducible representations Π_g and Π_u of $D_{\infty h}$ which are combinations of the ± 1 representations of $\text{SO}(2)$. We will denote them here as ν' and ν'' , each with components $(1, 2)$ or, equivalently, (x, y) . Thus, for example, the coordinate $(\mathfrak{z}_{1'})$ will refer to the first component of mode ν' . Since symmetry makes each mode strictly degenerate, we have two exactly 1:1 resonant oscillators (cf appendix A) which may perturb each other. Characterizing the 1:1 oscillators by the total numbers of quanta n' and n'' and the vibrational angular momenta ℓ' and ℓ'' , bending vibrational basis functions can be written as products $|n', \ell'\rangle |n'', \ell''\rangle$.

The normal mode frequencies ω_4 and ω_5 in the zero order bending vibrational Hamiltonian of C_2H_2

$$H_0 = \frac{\omega_4}{2} \sum_{i=1,2} [(q_{i'})^2 + (p_{i'})^2] + \frac{\omega_5}{2} \sum_{i=1,2} [(q_{i''})^2 + (p_{i''})^2] = \omega_4 n' + \omega_5 n''$$

are close enough to justify the 1:1:1:1 resonant oscillator model. We rewrite

$$H_0 = (\omega_4 + \omega_5) n + (\omega_4 - \omega_5) \nu, \quad (1)$$

where the standard 1:1:1:1 harmonic resonant oscillator Hamiltonian is given by

$$2n = n' + n'' \geq 0, \quad (2a)$$

and the *detuning term* is described by

$$2\nu = n' - n'', \quad \text{where } \nu \in [-n, n]. \quad (2b)$$

³With respect to inversion; under the reflection σ_h in the plane orthogonal to the axis of $\text{H}-\text{C}\equiv\text{C}-\text{H}$, the *trans* mode ν_{4g} changes sign, while the *cis* mode ν_{5u} remains invariant.

Note that the factor of 2 in the above definitions of n and ν is introduced in order to agree with similar definitions in the analysis of the perturbations of the hydrogen atom, see sec. 2.1. So n corresponds to the atomic principal quantum number.

Quantum states with the same $2n = n' + n''$, i.e., with the same total number of quanta, form bending *polyads*, whose splitting in the H_0 approximation equals $2n(\omega_4 - \omega_5)$. These polyads correspond to the atomic n -shells. Polyads are widely used by spectroscopists to describe quasi-degenerate group of vibrational states. For references, mathematical aspects, and the discussion of quantum-classical correspondence of polyads see (Pavlov-Verevkin and Zhilinskií, 1988; Xiao and Kellman, 1990; Sadovskii and Zhilinskií, 1993b, 1995). Some examples, which use our approach and techniques, can be found in (Kozin et al., 2005; Crogman et al., 2007; Sadovskii et al., 2010).

2.1 Perturbed Keplerian systems

Perturbed Keplerian systems, notably the hydrogen atom in weak external electric and magnetic fields, can also be treated as a four-oscillator system reduced with regard to the 1:1:1:1 polyad symmetry S^1 and additional “fictitious” axial symmetry (Efstathiou and Sadovskii, 2010), i.e., to a 2-torus symmetry T^2 . This approach is known as the Kustaanheimo–Stiefel (KS) formalism. We have two commuting first integrals, the principal (Keplerian) action n_{Kepler} and the momentum ζ which are generators of T^2 . After reduction, the actual Keplerian system corresponds to $\zeta = 0$ and any $n_{\text{Kepler}} > 0$. Nonzero ζ are possible, but have no physical analogues. (They require a magnetic monopole potential.)

Note here that we imply atomic units with $\hbar \equiv 1$ throughout the paper and that, unless required in the concrete context, our notation does not distinguish quantum numbers from their classical analogues (values of first integrals, classical actions). In particular recall that the principal quantum number of the hydrogen atom system $n = 1, 2, 3, \dots$ is strictly positive and that the number of levels in an n -shell is given by n^2 . At the same time, the ground state of the isotropic harmonic four-oscillator corresponds to classical action $2n_{\text{Kepler}} = 4 \times (\hbar/2)$, which suggests that the values of n_{Kepler} and n correspond exactly. On the other hand, the polyads P_{N_b} of this oscillator with $\ell = \zeta = 0$ are labeled by polyad numbers $N_b = 0, 2, \dots$ (only even nonnegative values are allowed), so that the ground state corresponds to the polyad P_0 with $N_b = 0$, and therefore, the polyad number $N_b = 2(n - 1)$, the difference between N_b and $2n$ being the action $2\hbar$ corresponding to the ground state.

There are six quadratic linearly independent polynomials in the KS oscillator variables (q, p) that Poisson commute with both n and ζ . They describe the dynamics of the reduced system. The polynomials constitute the components of the eccentricity⁴ and angular momentum vectors $\mathbf{K} = (K_1, K_2, K_3)$ and $\mathbf{L} = (L_1, L_2, L_3)$, satisfy two relations

$$\mathbf{K} \cdot \mathbf{L} = 0 \quad \text{and} \quad \mathbf{K}^2 + \mathbf{L}^2 = n^2 \quad \text{for } \zeta = 0, \quad (3)$$

and generate a Lie-Poisson algebra $\mathfrak{so}(4)$. Note that the amplitude of the classical angular momentum and the orbital quantum number l are related in the semiclassical limit as

$$\|\mathbf{L}\| = L = \sqrt{l(l+1)} \approx l + \frac{1}{2}.$$

⁴The vector \mathbf{K} is otherwise called after Laplace-Runge-Lenz and has, sometimes, even more names attached to it, see (Goldstein, 1976, 1975) and (Cushman and Bates, 1997, p. 400)

Introducing two Poisson commuting angular momenta

$$\mathbf{J}_1 = \mathbf{X} := (\mathbf{L} + \mathbf{K})/2 \quad \text{and} \quad \mathbf{J}_2 = \mathbf{Y} := (\mathbf{L} - \mathbf{K})/2, \quad (4)$$

known as Fock vectors, we come to the relations

$$\|\mathbf{J}_1\| = \|\mathbf{J}_2\| = n/2 \quad \text{for } \zeta = 0 \quad (5)$$

which show that we have a phase space $\mathbb{S}^2 \times \mathbb{S}^2$ naturally embedded into $\mathbb{R}_{\mathbf{K}, \mathbf{L}}^6$. At the same time, the above $\mathfrak{so}(4)$ algebra becomes a standard $\mathfrak{so}(3) \times \mathfrak{so}(3)$. Below we detail the exact correspondence between these systems and bending polyads of C_2H_2 .

2.2 Dynamical variables of the axially symmetric oscillator in 1:1:1:1 resonance and generators of the $\mathbb{T}_{n, \zeta}^2$ action

Similarly to the description of the hydrogen atom in the Kustaanheimo–Stiefel (KS) approach, see, for example, (Sadovskii and Zhilinskiĭ, 1998; Cushman and Sadovskii, 2000; Efstathiou and Sadovskii, 2010), consider Cartesian coordinates q and respective conjugate momenta p ,

$$q := (q_1, q_2, q_3, q_4) \quad \text{and} \quad p := (p_1, p_2, p_3, p_4), \quad (6)$$

as well as corresponding complex dynamical variables

$$z = (z_1, z_2, z_3, z_4), \quad \text{where } z_i = q_i + ip_i, \quad \bar{z}_i = q_i - ip_i, \quad \text{with } i = 1, \dots, 4. \quad (7)$$

The oscillator or polyad symmetry \mathbb{S}^1 is defined by the principal action

$$2n = \frac{1}{2} \sum_{i=1}^4 (q_i^2 + p_i^2) = \frac{1}{2} z \bar{z},$$

which is the Hamiltonian of the harmonic 4-oscillator in 1:1:1:1 resonance. The axial \mathbb{S}^1 symmetry is defined by the momentum

$$\zeta = q_1 p_4 - q_4 p_1 + q_3 p_2 - q_2 p_3. \quad (8)$$

Because ζ defines simultaneous individual rotations of the (1, 4) and (2, 3) 2-planes of the configuration space \mathbb{R}_q^4 , bending vibrational coordinates of C_2H_2 correspond to (6) as follows

$$\begin{aligned} (q_{x'}, p_{x'}) &:= (q_1, p_1), & (q_{y'}, p_{y'}) &:= (q_4, p_4), \\ (q_{x''}, p_{x''}) &:= (q_3, p_3), & (q_{y''}, p_{y''}) &:= (q_2, p_2), \end{aligned} \quad (9)$$

or, equivalently

$$(z_1, z_2, z_3, z_4) := (z_{1'}, z_{2''}, z_{1''}, z_{2'}), \quad (10)$$

and furthermore,

$$\zeta = \zeta' + \zeta'', \quad |\zeta'| = \ell', \quad |\zeta''| = \ell'', \quad |\zeta| = \ell,$$

where, following conventional molecular notation, ℓ' and ℓ'' are the absolute values of the vibrational angular momenta in each normal mode ζ' and ζ'' , and ℓ is (the absolute value of) the total vibrational angular momentum. At this point, the system becomes identical to the hydrogen atom in the KS coordinates (Efstathiou and Sadovskii, 2010),

and we rely directly on the earlier results without going into details of how they were obtained. However, it might be instructive for the reader to recall the lower dimensional case following the outline in appendix A, while some additional information on the four dimensional system can be found in appendix B. Rotating⁵ each canonical plane (q_i, p_i) as described in appendix A.3, we achieve a simultaneous diagonal representation of both ζ and n ,

$$n = \frac{1}{4}(+\mathfrak{z}_1\bar{\mathfrak{z}}_1 + \mathfrak{z}_2\bar{\mathfrak{z}}_2 + \mathfrak{z}_3\bar{\mathfrak{z}}_3 + \mathfrak{z}_4\bar{\mathfrak{z}}_4) = \frac{1}{2}(n_1 + n_2 + n_3 + n_4), \quad (11a)$$

$$\zeta = \frac{1}{2}(-\mathfrak{z}_1\bar{\mathfrak{z}}_1 - \mathfrak{z}_2\bar{\mathfrak{z}}_2 + \mathfrak{z}_3\bar{\mathfrak{z}}_3 + \mathfrak{z}_4\bar{\mathfrak{z}}_4) = -n_1 - n_2 + n_3 + n_4. \quad (11b)$$

where

$$(\mathfrak{z}_1, \mathfrak{z}_2, \mathfrak{z}_3, \mathfrak{z}_4) := (\mathfrak{z}_{2'}, \mathfrak{z}_{2''}, \mathfrak{z}_{1''}, \mathfrak{z}_{1'}) \quad (12)$$

are the new complex dynamical variables.

2.3 Quadratic polynomial invariants of the $\mathbb{T}_{2n,\zeta}^2$ action

In addition to the generators n and ζ themselves, the other six quadratic $\mathbb{T}_{2n,\zeta}^2$ invariant polynomials are constructed most straightforwardly if we use new generators

$$2x := n - \zeta/2 = n_1 + n_2 \quad \text{and} \quad 2y := n + \zeta/2 = n_3 + n_4 \quad (13)$$

and apply the usual two-mode definitions for 1:1-resonant polyads [see eq. (A.12) of appendix A] on each canonical factor space of $T\mathbb{R}^4 \sim \mathbb{R}_{(1,2)}^4 \times \mathbb{R}_{(3,4)}^4$ in order to define the Fock vectors (4) with $\|\mathbf{X}\| = x$ and $\|\mathbf{Y}\| = y$. Polynomials

$$\mathbf{J}_1 = \mathbf{X} = \frac{1}{4} \begin{pmatrix} 2(n_2 - n_1) \\ i(\mathfrak{z}_1\bar{\mathfrak{z}}_2 - \bar{\mathfrak{z}}_1\mathfrak{z}_2) \\ -(\mathfrak{z}_1\bar{\mathfrak{z}}_2 + \bar{\mathfrak{z}}_1\mathfrak{z}_2) \end{pmatrix} \quad \text{and} \quad \mathbf{J}_2 = \mathbf{Y} = \frac{1}{4} \begin{pmatrix} 2(n_4 - n_3) \\ i(\mathfrak{z}_3\bar{\mathfrak{z}}_4 - \bar{\mathfrak{z}}_3\mathfrak{z}_4) \\ -(\bar{\mathfrak{z}}_3\mathfrak{z}_4 + \mathfrak{z}_3\bar{\mathfrak{z}}_4) \end{pmatrix} \quad (14)$$

were introduced in our earlier work⁶ on the hydrogen atom perturbations by orthogonal homogeneous constant electric and magnetic fields (Sadovskii and Zhilinskiĭ, 1998; Cushman and Sadovskii, 1999, 2000) and, subsequently, on generic field configurations (Efstathiou et al., 2007, 2008, 2009). In particular, combining the first components of (14) according to (4) gives momenta

$$L_1 = \frac{1}{2}(-n_1 + n_2 - n_3 + n_4) \quad \text{and} \quad K_1 = \frac{1}{2}(-n_1 + n_2 + n_3 - n_4). \quad (15)$$

Back in the legacy KS variables (6), the \mathbf{K} and \mathbf{L} vectors in (4) are expressed as

$$\mathbf{L} = \frac{1}{2} \begin{pmatrix} 2(q_2p_3 - q_3p_2) \\ q_2p_4 - q_4p_2 + q_3p_1 - q_1p_3 \\ q_1p_2 - q_2p_1 + q_3p_4 - q_4p_3 \end{pmatrix} \quad (16a)$$

and

$$\mathbf{K} = \frac{1}{2} \begin{pmatrix} (q_2^2 + p_2^2 + q_3^2 + p_3^2)/2 - (q_1^2 + p_1^2 + q_4^2 + p_4^2)/2 \\ -q_1q_2 - p_1p_2 + q_3q_4 + p_3p_4 \\ -p_2p_4 - p_1p_3 - q_2q_4 - q_1q_3 \end{pmatrix}, \quad (16b)$$

⁵In order to reproduce the notation of Sadovskii and Zhilinskiĭ (1998); Cushman and Sadovskii (2000); Efstathiou and Sadovskii (2010), an additional rotation of the plane (1, 4) is required.

⁶Sadovskii and Zhilinskiĭ (1998) in eqs. (14) and (22) use indices (e, b, p) to distinguish vector components in the physical 3-space, meaning b along the magnetic field and e along the electric field; axis b is also often taken for the vertical (first) axis in the physical three-dimensional space of the hydrogen atom system.

see, for example, equations (14) and (22) of [Sadovskii and Zhilinskiĭ \(1998\)](#)⁶. Expressions (16) together with (9) are most useful to explore further the correspondence to the C₂H₂ system in sec. 2.2; they are exploited in sec. 2.4.

2.3.1 Relation to the molecular system

We recall from sec. 2.1 that the Keplerian integral n and the length $L := \|\mathbf{L}\|$ correspond to the principal quantum number n and the orbital momentum l of the hydrogen atom. On the other hand, for the 1:1:1 bending polyads of C₂H₂ in sec. 2.2, the quantity $2(n - 1)$ corresponds to the total number of bending quanta N_b in (2a), and $|\zeta|$ gives the total vibrational angular momentum ℓ . Furthermore, polynomials

$$\nu = -K_1 \quad \text{and} \quad \mu = L_1, \quad (17)$$

give, respectively, the *detuning* (2b) and the difference of the angular momenta of the two 1:1 resonant bending normal mode subsystems. The fact that the reduced bending Hamiltonian H is a function on $\mathbb{S}^2 \times \mathbb{S}^2$ implies, among other things, that the typical system has *four* relative equilibria (RE, see footnote 2). We discuss these implications in more detail later in sec. 2.4.2.

2.3.2 Nonzero vibrational angular momentum ℓ

While we focus in this paper primarily on the $\zeta = 0$ case, we can notice that eqs. (13) imply that systems with nonzero $|\zeta| = \ell$ have a classical phase space $\mathbb{S}^2 \times \mathbb{S}^2$ whose x and y factors have different respective radii ($n \pm \ell/2$). Furthermore, studying, as it is customary in molecular applications, the whole subsystem with $\ell = |\zeta| > 0$ requires considering the disjoint union

$$(\mathbb{S}^2 \times \mathbb{S}^2)_{\zeta=-\ell} \cup (\mathbb{S}^2 \times \mathbb{S}^2)_{\zeta=+\ell}.$$

Reversing symmetry operations (see sec. 2.4) map points between the disjoint components of this union. Classical dynamics is, of course, confined to one of the components, but quantum eigenstates with $\zeta = \pm\ell$ are degenerate in energy and they can be seen as stationary combinations of rotating waves with $\zeta = \ell$ and $\zeta = -\ell$, i.e., as delocalized between the components. The number of doubly degenerate quantum states for arbitrary $\zeta = \ell \neq 0$ can be expressed as $[(N_b + \zeta)/2 + 1][(N_b - \zeta)/2 + 1]$.

2.3.3 Integrity basis

Any $\mathbb{T}_{2n,\zeta}^2$ -invariant function $\mathbb{C}_3^4 \rightarrow \mathbb{R}$ can be expressed using six $\mathbb{T}_{2n,\zeta}^2$ -invariant polynomials (14) or (16) and two *parameters* $n \geq 0$ and $\zeta \in [-n, n]$. This produces a function $\mathbb{R}_{(\mathbf{X}, \mathbf{Y})}^6 \rightarrow \mathbb{R}$, and by (5) or (13), a function on the reduced phase space $(\mathbb{S}^2 \times \mathbb{S}^2)_{n,\zeta}$. In particular, we may consider power series in all these quantities and classify the terms of the series according to their combined degree in $(\mathbf{X}, \mathbf{Y}, n, \zeta)$, so that, introducing a formal smallness parameter ϵ , all terms of the same degree s can be considered to be of order ϵ^s . Such formal series are obtained after normalizing in \mathbb{C}_3^4 with respect to the Hamiltonian flow of $2n$. The molecular Hamiltonians used by spectroscopists to describe bending polyads of C₂H₂ are already in this normalized form truncated to some degree s_{\max} , see sec. 2.5.

Expressions using (\mathbf{X}, \mathbf{Y}) for degrees $s > 1$ cannot, obviously, be unique because these six variables are related algebraically by quadratic restrictions (5) or (13) defining

the embedding of $\mathbb{S}^2 \times \mathbb{S}^2$ in \mathbb{R}^6 . To construct such expressions uniquely for any degree $s > 1$, we use the *integrity basis* (see (Michel and Zhilinskií, 2001b,a) and (Efstathiou and Sadovskii, 2010)). It can be shown (see appendix B.2) that this basis for the \mathbb{T}^2 invariants has six principal (denominator) and two auxiliary (numerator) invariants, all of degree 1 in $(\mathbf{X}, \mathbf{Y}; n, \zeta)$, and there is one auxiliary invariant of degree 2. Furthermore, these invariants should be constructed in a certain way: we must use the Casimirs n and ζ (or their linear combinations) as two principal invariants, while the remaining four include two of the three components of \mathbf{X} and \mathbf{Y} each. Thus, the principal invariants (cf appendix A.5) can be chosen as

$$\|\mathbf{X}\|, \|\mathbf{Y}\|, X_1, X_3, Y_1, \text{ and } Y_2,$$

with the corresponding auxiliary invariants

$$X_2, Y_3, \text{ and } X_2 Y_3.$$

Then the ring of all \mathbb{T}^2 -invariant polynomials can be represented as

$$\mathcal{R}(\|\mathbf{X}\|, \|\mathbf{Y}\|, X_1, X_3, Y_1, Y_2) \bullet \{1, X_2, Y_3, X_2 Y_3\}, \quad (18a)$$

or, equivalently, recombining linearly its principal invariants, as

$$\mathcal{R}(n, \zeta, \nu, \mu, X_3, Y_2) \bullet \{1, X_2, Y_3, X_2 Y_3\}. \quad (18b)$$

Here \mathcal{R} is a free module generated multiplicatively by principal invariants, while the degree in the auxiliary polynomials from $\{\}$ is one. Note that in order to express concrete molecular bending vibrational Hamiltonians of C_2H_2 , the additional discrete symmetry G_8 of the reduced system (sec. 2.4) should be taken into account and the integrity basis (18) should be modified accordingly (Appendix B.2).

2.4 Residual discrete symmetries and stratification of $\mathbb{S}^2 \times \mathbb{S}^2$

The spatial symmetry group⁷ of C_2H_2 is $D_{\infty h}$. Combining it with time reversal or, more concretely, momentum reversal $\mathcal{T} : (q, p) \mapsto (q, -p)$, we obtain the full symmetry group $D_{\infty h} \wedge \mathcal{T}$ of the original 4-oscillator system. Reduction removes the continuous component $C_\infty \sim \mathbb{S}^1 \sim \text{SO}(2)$ of this group: the image of $D_{\infty h} \wedge \mathcal{T}$ under the \mathbb{T}^2 symmetry reduction map is an order eight Abelian group G_8 which is isomorphic to an abstract group $Z_2 \times Z_2 \times Z_2$ and to the point group D_{2h} . We give its characters in table 1. Note that G_8 has an order four spatial subgroup $G_4 = \{1, \sigma, i, C_2\}$; its other operations are *reversal*⁸, they involve \mathcal{T} and toggle the sign of the symplectic form and the direction of the flow of all Hamiltonian fields. Such operations can be used along with the spatial operations to study the Hamiltonian H of the system as a G_8 invariant function (for example, to find additional constraints on the number, position, and type of stationary points of H), to understand the stratification of the phase space $\mathbb{S}^2 \times \mathbb{S}^2$, but they are less useful in the analysis of the dynamics on $\mathbb{S}^2 \times \mathbb{S}^2$. G_4 is of particular importance to the quantum analogue system whose eigenstates transform according to the irreducible representations of G_4 and are labeled g^\pm or A_g/B_g and u^\pm or A_u/B_u .

⁷We use Schönflies notation for the groups of transformations in \mathbb{R}^3 which are subgroups of $O(3)$, see their discussion in (Landau and Lifshitz, 2002, Chap. XII).

⁸Reversal properties in $\mathbb{R}_{q,p}^8$ and $\mathbb{R}_{\mathbf{X}, \mathbf{Y}}^6$ are reciprocal. To verify, consider the action of operations in table 1 on \mathbf{X} and \mathbf{Y} . So the operation $C_2 : (\mathbf{X}, \mathbf{Y}) \mapsto (-Y_1, -Y_2, Y_3, -X_1, -X_2, X_3)$ interchanges the two factor spheres and rotates them by π about axis 3. This operation is, clearly, nonreversal.

Table 1: Characters of the symmetry group G_8 and its action on the \mathbb{T}^2 -invariant variables (11) and (16). Irreducible representations Γ are denoted similarly to those of the isomorphic point group D_{2h} . Notation for the elements of G_8 corresponds to the action of the corresponding elements in the preimage G_8^θ on the original variables (q, p) . The last row gives invariant two-dimensional manifolds of the G_8 action on $\mathbb{S}^2 \times \mathbb{S}^2$ for $\zeta = 0$ whose stabilizer is the order two subgroup of G_8 corresponding to the class in the first row, see sec. 2.4.1.

Γ	1	C_2	\mathcal{T}	\mathcal{T}_2	i	σ	\mathcal{T}_i	\mathcal{T}_v	variables
A_g	1	1	1	1	1	1	1	1	K_1, n, ν
B_{1g}	1	1	-1	-1	1	1	-1	-1	
B_{2g}	1	-1	1	-1	1	-1	1	-1	
B_{3g}	1	-1	-1	1	1	-1	-1	1	L_1, ζ, μ
A_u	1	1	1	1	-1	-1	-1	-1	K_2
B_{1u}	1	1	-1	-1	-1	-1	1	1	L_3
B_{2u}	1	-1	1	-1	-1	1	-1	1	K_3
B_{3u}	1	-1	-1	1	-1	1	1	-1	L_2
Space	$\mathbb{S}^2 \times \mathbb{S}^2$	\mathbb{S}^2	\mathbb{S}^2	\mathbb{T}^2	4pt	\mathbb{S}^2	\mathbb{S}^2	\mathbb{T}^2	

The last column of table 1 gives the action of G_8 on the \mathbb{T}^2 -invariant polynomials (11) and (16), and, as a consequence, on $\mathbb{S}^2 \times \mathbb{S}^2 \subset \mathbb{R}_{K,L}^6$. Below we explain how this action was derived.

Strictly speaking, G_8 belongs to the reduced system. The *preimage* of G_8 is a continuous one-parameter family of order-8 subgroups $G_8^\theta \subset D_{\infty h} \wedge \mathcal{T}$ with $\theta \in [0, \pi)$ which act on the dynamical variables of the full system in sec. 2.2. For our purposes, we can consider any concrete member of this family. Specifically, we can take G_8^0 generated by the reflection $\sigma := \sigma_v^{xz}$ in the plane xz (a representative of the class σ_v of $D_{\infty h}$), the spatial inversion i , and the time reversal \mathcal{T} . The other four nontrivial operations in G_8^0 are

$$C_2 := C_2^y = \sigma_v^{xz} \circ i, \quad \mathcal{T}_v = \mathcal{T} \circ \sigma_v^{xz}, \quad \mathcal{T}_i = \mathcal{T} \circ i, \quad \text{and} \quad \mathcal{T}_2 = \mathcal{T} \circ C_2^y.$$

The action of G_8^0 on the vibrational dynamical variables of the full system in sec. 2.2 is summarized in table 2. It follows directly from the definition of the normal vibrations ν_4 and ν_5 of acetylene. Using the correspondence (9) between the vibrational normal mode variables and the KS coordinates (6) together with the explicit definitions of all quadratic $\mathbb{T}_{2n,\zeta}^2$ invariants (11) and (16), we derive the following transformation properties of these variables under the generators of G_8^0 and the action of G_8 in table 1.

variables	σ	i	\mathcal{T}
n, ν or K_1	+	+	+
ζ, μ or L_1	-	+	-
L_2	+	-	-
L_3	-	-	-
K_2	-	-	+
K_3	+	-	+

Since the reduced phase space $\mathbb{S}^2 \times \mathbb{S}^2$ is naturally embedded in \mathbb{R}^6 with coordinates (\mathbf{X}, \mathbf{Y}) , we can subsequently uncover (in sec. 2.4.1) the action of G_8 on $\mathbb{R}_{K,L}^6 \supset \mathbb{S}^2 \times \mathbb{S}^2$ for any fixed nonzero (n, ζ) and the resulting stratification of $\mathbb{S}^2 \times \mathbb{S}^2$.

Table 2: Action of the discrete symmetry group G_8^0 on the bending vibrational dynamical variables of acetylene in sec. 2.2; operations in G_8^0 are explained in sec. 2.4. The C_2H_2 -variables, their symmetry (u, g) with respect to spatial inversion i , and the corresponding KS variables used by Sadvovskii and Zhilinskiĭ (1998) and in the later work (Efstathiou and Sadvovskii, 2010; Efstathiou et al., 2009) appear in columns C_2H_2 and KS, respectively; in all subsequent columns, the + or – signs indicate whether the variable remains invariant or changes sign.

Variables			Symmetry operations in the group G_8							
C_2H_2	KS	Type	1	σ	i	C_2	\mathcal{T}	\mathcal{T}_v	\mathcal{T}_i	\mathcal{T}_2
q_{4x}	$q_{1'}$	q_1	g	+	+	+	+	+	+	+
p_{4x}	$p_{1'}$	p_1	g	+	+	+	+	–	–	–
q_{4y}	$q_{2'}$	q_4	g	+	–	+	–	+	–	+
p_{4y}	$p_{2'}$	p_4	g	+	–	+	–	–	+	–
q_{5x}	$q_{1''}$	q_3	u	+	+	–	–	+	+	–
p_{5x}	$p_{1''}$	p_3	u	+	+	–	–	–	–	+
q_{5y}	$q_{2''}$	q_2	u	+	–	–	+	+	–	–
p_{5y}	$p_{2''}$	p_2	u	+	–	–	+	–	+	–

Knowing the strata on $\mathbb{S}^2 \times \mathbb{S}^2$ helps greatly in the analysis of the equilibria of the reduced system, i.e., the \mathbb{T}^2 -relative equilibria of the original 4-oscillator, corresponding to the stationary points of the G_8 -symmetric reduced Hamiltonian $H : \mathbb{S}^2 \times \mathbb{S}^2 \rightarrow \mathbb{R}$.

2.4.1 Stratification of $\mathbb{S}^2 \times \mathbb{S}^2$ for $\zeta = 0$

We can specify points on $\mathbb{S}^2 \times \mathbb{S}^2$ using coordinates $(\mathbf{K}, \mathbf{L}) = (K_1, K_2, K_3, L_1, L_2, L_3)$ in \mathbb{R}^6 and assuming that \mathbf{K} and \mathbf{L} satisfy (3), or, alternatively, using the linear combinations (\mathbf{X}, \mathbf{Y}) and the respective relation (5). We describe invariant manifolds of the G_8 action on $\mathbb{S}^2 \times \mathbb{S}^2$ whose stabilizers (or isotropy groups) G are different subgroups of the total symmetry group G_8 . Note that the abelian group $G_8 \sim Z_2 \times Z_2 \times Z_2$ has subgroups of order 2, 4, and 8 (the group itself). In particular, each class of conjugated elements (each column) in table 1 corresponds to just one element which defines a Z_2 subgroup, e.g., $\{1, i\}$. For each stabilizer $G \subseteq G_8$ the *invariant manifold* consists of all points which are simultaneously invariant (map to itself) with respect to all nontrivial elements of G . The (union of) G -invariant manifold(s) can contain points with higher isotropy group G' such that $G \subset G' \subseteq G_8$. The *stratum* of type G is obtained after excluding all such points.

Isolated fixed points (poles). From the rightmost column of table 1, we can see immediately that the two points⁹ $(\pm n, 0, 0, 0, 0, 0)$ with $\nu = \mp n$ and $\mathbf{L} = 0$ satisfying (3) are fully symmetric (their stabilizer is the whole of G_8). Furthermore, since K_1 is the only fully symmetric component of (\mathbf{K}, \mathbf{L}) , any small deviation from point $(\pm n, 0, 0, 0, 0, 0)$ in $\mathbb{S}^2 \times \mathbb{S}^2$ breaks (lowers) its isotropy symmetry G_8 . So it follows that points with $\nu = \pm n$ are isolated in their stratum which consists precisely of these two points. It is worth recalling that maximum $|\nu|$ corresponds to maximum detuning and that therefore points with $\nu = n$ and $\nu = -n$ represent the limits of pure normal modes ν' (or ν_4) and ν'' (or ν_5), respectively.

⁹Tyng and Kellman (2009a,b, 2006) seem to call fully symmetric points with $K_1 = n$ and $K_1 = -n$ as B and A , respectively; they do not analyze and make use of symmetries.

We can also see that the two points $(0, 0, 0, \pm n, 0, 0)$ with maximal $|\mu| = n$ are also isolated. These points are interchanged by operations C_2 and σ_v and form a stratum consisting of one two-point orbit of G_8 with stabilizer $\{1, i, T_2, T_v\}$, an order-4 reversal subgroup of G_8 . The points $|\mu| = n$ lift to relative equilibria of the \mathbb{T}^2 action, or nonlinear normal modes with maximal difference of vibrational angular momenta ℓ' and ℓ'' . As was understood essentially by [Jacobson et al. \(1999a\)](#) and later by [Ding \(2004\)](#); [Tyng and Kellman \(2006\)](#), such modes correspond to “circularly polarized” combinations of the original normal modes.

Note that the existence of the precisely four isolated fixed points can be seen as the consequence of the presence of the i element¹⁰, which *rotates* both \mathbf{X} and \mathbf{Y} simultaneously about axis 1 by π . As can be understood from visualizing the action of such rotation on each 2-sphere factor of $\mathbb{S}^2 \times \mathbb{S}^2$, the action of $\{1, i\} \subset G_8$ has four fixed points with maximal absolute values of either ν or μ which can be called *poles*. To obtain the poles algebraically, we can see from the i column in table 1 that their defining equation is $K_2 = K_3 = L_2 = L_3 = 0$. Together with (3) it gives

$$K_1 L_1 = 0 \quad \text{and} \quad K_1^2 + L_1^2 = n^2$$

satisfied in four points $\{K_1 = \pm n, L_1 = 0\} \cup \{K_1 = 0, L_1 = \pm n\}$. Any small departure from a pole breaks its $\{1, i\}$ isotropy and therefore, poles are isolated.

It is interesting to consider briefly how the poles extend to the case of nonzero vibrational angular momentum $\ell = |\zeta|$. When $\zeta \neq 0$, the two fully symmetric points and $\nu = \pm n$ form naturally two pairs with $\zeta = \pm \ell$, while at same time, the pair $\{L_1 = \pm n, K_1 = 0\}$ turns into four points splitting into two pairs¹¹ $\{L_1 = \mp n, \zeta = \pm \ell\}$ and $\{L_1 = \pm n, \zeta = \pm \ell\}$.

Two-dimensional invariant manifolds with stabilizers of order 2. The topology of the invariant manifolds of the G_8 action on $\mathbb{S}^2 \times \mathbb{S}^2$ (for $\zeta = 0$) whose stabilizers are order-two subgroups of G_8 are listed in the last row of table 1. It turns out that except for $\{1, i\}$, all other nontrivial subgroups of G_8 stabilize precisely one invariant two-dimensional subspace of $\mathbb{S}^2 \times \mathbb{S}^2$, either a 2-sphere or a 2-torus. For example, the second column of table 1 tells that the $\{1, C_2\}$ invariant manifold is a sphere \mathbb{S}^2 . Indeed, we can see that all C_2 invariant points (\mathbf{K}, \mathbf{L}) obey $K_3 = L_1 = L_2 = 0$. Satisfying restrictions (3), we obtain the two-sphere

$$\mathbb{S}^2 \times \mathbb{S}^2 \Big|_{K_3=L_1=L_2=0} = \{(K_1, K_2, 0, 0, 0, L_3); K_1^2 + K_2^2 + L_3^2 = n^2\} = \mathbb{S}^2.$$

Similarly, we uncover the topology of the $\{1, T_2\}$ invariant manifold by combining its defining equation $K_2 = L_2 = 0$ with (5) and obtain equations

$$X_1^2 + X_3^2 = Y_1^2 + Y_3^2 = n^2/4$$

which define a two-dimensional torus $\mathbb{T}^2 = \mathbb{S}^1 \times \mathbb{S}^1$.

Invariant circles \mathbb{S}^1 . We have examined subgroups of order 2 and 8 (the group itself). It remains to find invariant manifolds for stabilizers $Z_2 \times Z_2 \subset G_8$ of order 4. From

¹⁰Our notation of the group elements in table 1 follows their original action on the bending vibrational normal mode coordinates $q'_{1,2}, p'_{1,2}, q''_{1,2}, p''_{1,2}$ of C_2H_2 . In regard to the induced action on $\mathbb{R}_{\mathbf{X}, \mathbf{Y}}^6$, this notation becomes somewhat confusing. Thus, contrary to what it may imply literally, the i element is a simultaneous rotation in $\mathbb{R}_{\mathbf{X}}^3$ and $\mathbb{R}_{\mathbf{Y}}^3$ and *not* an inversion which it originally was in \mathbb{R}_q^4 .

¹¹It is likely that [Tyng and Kellman \(2009a,b\)](#) call one pair C and the other D .

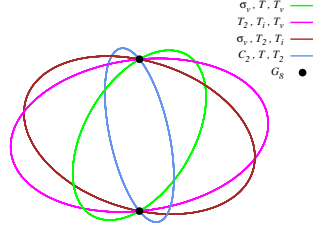






Figure 4: Invariant circles \mathbb{S}^1 of the G_8 group action on $\mathbb{S}^2 \times \mathbb{S}^2$ including all one-dimensional strata (colored lines) and fully symmetric zero-dimensional stratum (opaque circles), see table 3.

Table 3: Invariant circles \mathbb{S}^1 of the G_8 group action on the reduced phase space $(\mathbb{S}^2 \times \mathbb{S}^2)_{n, \zeta=0}$

Restriction	Stabilizer	Definition	figs. 4, 5
$K_3 = L = 0$	$\{1, C_2, \mathcal{T}, \mathcal{T}_2\}$	$K_1^2 + K_2^2 = n^2$	
$K_2 = L = 0$	$\{1, \sigma_v, \mathcal{T}, \mathcal{T}_v\}$	$K_1^2 + K_3^2 = n^2$	
$K_3 = K_2 = L_1 = L_2 = 0$	$\{1, C_2, \mathcal{T}_i, \mathcal{T}_v\}$	$K_1^2 + L_3^2 = n^2$	
$K_3 = K_2 = L_1 = L_3 = 0$	$\{1, \sigma_v, \mathcal{T}_2, \mathcal{T}_i\}$	$K_1^2 + L_2^2 = n^2$	

the total of seven candidates, we can exclude the three containing $\{1, i\}$ because they will stabilize only isolated fixed points. Considering the four other stabilizers, we find that each is an isotropy group of a manifold of dimension one, and that this manifold has the topology of a circle. The resulting full description of the four invariant circles¹² of the G_8 action on $\mathbb{S}^2 \times \mathbb{S}^2$ can be found in table 3.

Intersections of invariant manifolds. Strata. Residual group action. We should now determine how various low-dimensional G invariant manifolds with $G \subseteq G_8$ fit together in the four-dimensional compact space $\mathbb{S}^2 \times \mathbb{S}^2$. Each stabilizer of order 4 has two order 2 subgroups which can in turn be stabilizers of 2-manifolds. This means that the invariant manifolds have common points, i.e., they intersect. First of all, we note that the totally symmetric poles with $|K_1|=n$ are the intersection of *all* low-dimensional invariant manifolds, namely the four circles \mathbb{S}^1 , four spheres \mathbb{S}^2 , and two tori \mathbb{T}^2 . Thus, as illustrated in fig. 4, the four invariant circles in table 3 intersect at the two poles. Furthermore, six different pairs of invariant circles are related to six different two-dimensional invariant manifolds (table 1, last row). So each circle belongs to three two-dimensional invariant manifolds, two spheres \mathbb{S}^2 and one torus \mathbb{T}^2 , while each two-dimensional invariant manifold contains two circles. The spheres are drawn schematically in fig. 5. It follows that the four invariant spheres intersect pairwise on a circle. Each of the two two-dimensional tori \mathbb{T}^2 with stabilizers \mathcal{T}_2 and \mathcal{T}_v intersects all four spheres, specifically, two spheres on each of the two invariant circles it contains. The poles $\{|K_1|=n\}$ are common to both tori, and furthermore, the tori also intersect each other at the two isolated points with maximal $|L_1| = n$ which otherwise stay apart from all other manifolds.

The residual group action on the circles in table 3 is formally equivalent to the action of the C_2 point group on a circle $\{(x, y) \in \mathbb{R}^2; x^2 + y^2 = 1\}$ with the G_8 invariant poles on the vertical axis C_2 . Removing the poles, we obtain the stratum $\mathbb{S}^1 \setminus \{|K_1| = n\}$ which consists of two-point orbits. For example, the stratum with

¹²Tyng and Kellman (2009a,b, 2006) call them “grand circles”.

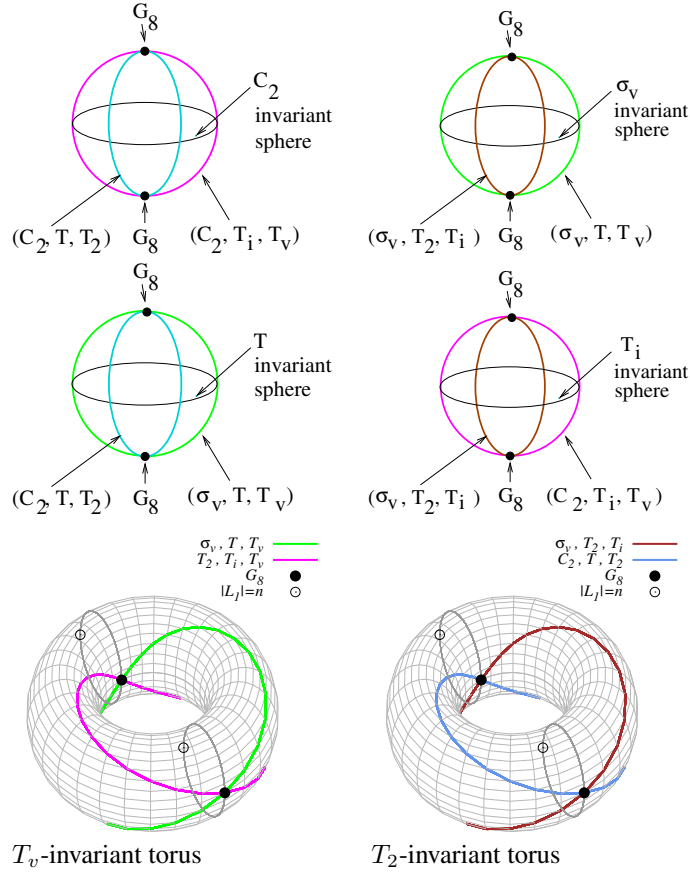


Figure 5: Two-dimensional invariant manifolds of the G_8 action on $\mathbb{S}^2 \times \mathbb{S}^2$ (cf table 1, bottom row) and their intersection with higher symmetry strata, see table 3 and sec. 2.4.1.

stabilizer $\{1, C_2, T, T_2\}$ has orbits with

$$K_1 = n \sin \theta, \quad K_2 = \pm n \cos \theta, \quad \text{with } -\pi/2 < \theta < \pi/2.$$

The residual group action on each of the spheres is formally equivalent to the action of the $C_{2v} \sim Z_2 \times Z_2$ point group on a two-dimensional sphere $\{(x, y, z) \in \mathbb{R}^3; x^2 + y^2 + z^2 = 1\}$ with the G_8 invariant poles on the vertical axis C_2 and the two invariant circles \mathbb{S}^1 lying in the symmetry planes.

2.4.2 G_8 -invariant Morse functions on $\mathbb{S}^2 \times \mathbb{S}^2$

We can naturally assume that the Hamiltonian of the reduced system $H : \mathbb{S}^2 \times \mathbb{S}^2 \rightarrow \mathbb{R}$ is a Morse function: a smooth function without degenerate stationary points. Such function remains stable under small deformations due to the change of its parameters and can be considered as generic. The topology of $\mathbb{S}^2 \times \mathbb{S}^2$ imposes certain restrictions on H (Michel and Zhilinskiĭ, 2001a). Notably, H should have at least four stationary points. The simplest Morse function H has exactly four stationary points. To conform with topology, these points must include an absolute maximum and minimum of Morse indices 4 and 0 and Hessian signatures $(+, +, +, +)$ and $(-, -, -, -)$, respectively, and two index-2 points with signature $(-, -, +, +)$. In a dynamical system

with Hamiltonian function H , the two former points are, necessarily, stable (elliptic-elliptic, ee) equilibria, while several possibilities exist for the Hamiltonian stability of the two $(-, -, +, +)$ points, which can be either hyperbolic-hyperbolic, elliptic-elliptic, or complex hyperbolic, with the frequencies of the linearization near these points (see sec. 3.1) being imaginary, real, or complex.

Stratification of $\mathbb{S}^2 \times \mathbb{S}^2$ under the action of G_8 imposes further restrictions. Any G_8 -invariant Morse function should have stationary points at the isolated fixed points of this action, and furthermore, points with $\mu = \pm n$ are equivalent, i.e., the value of H at, and the stability of these points are exactly the same. Combining with the topological requirements, we conclude that the *simplest* G_8 -invariant Hamiltonian function H on $\mathbb{S}^2 \times \mathbb{S}^2$ can have four stationary points, a maximum and a minimum at the poles with $\nu = \pm n$, and a pair of equivalent index-2 points at the poles with $\nu = \pm n$. Because all stationary points are located on (isolated) critical orbits of the group action, such function is called *perfect*. So we have two elliptic RE and a pair of equivalent RE, whose stability remains to be investigated (sec. 3.1).

More complex systems of stationary points can be obtained after bifurcations of these initial four points. The typical bifurcations are also affected by stratification. Thus we should anticipate various pitchfork bifurcations at the G_8 -invariant poles $\{\nu = \pm n\}$ which break generically *one* of the three Z_2 factor groups of G_8 . This means that the new stationary points would depart from the pole on one of the four invariant circles with stabilizer $Z_2 \times Z_2$ (cf fig. 4).

Table 4: Parameters (cm^{-1}) of the effective vibrational Hamiltonian used to fit spectroscopic data on bending vibrational levels of C_2H_2 by Jacobson et al. (1998)

Parameter	Value cm^{-1}	Parameter	Value cm^{-1}
ω_4	608.657		
ω_5	729.137		
x_{44}	3.483	y_{444}	-0.03060
x_{45}	-2.256	y_{445}	0.0242
x_{55}	-2.389	y_{455}	0.0072
g_{44}	0.677	y_{555}	0.00955
g_{45}	6.670		
g_{55}	3.535		
S_{45}	-8.574	r_{445}	0.0304
r_{45}	-6.193	r_{545}	0.0110

2.5 Bending vibrational Hamiltonian of C_2H_2

The quantum vibrational Hamiltonian

$$H_{\text{bend}} = H_0 + H_{\text{diag}} + V_{\text{DD1}} + V_\ell + V_{\text{DD2}} \quad (19)$$

with numerical values of parameters in Table 4 used by Jacobson et al. (1998) and other spectroscopists¹³ to fit their data on the bending vibrational levels of C_2H_2 is defined implicitly through its matrix elements. We can recover the classical analogue of (19) using the correspondence of the quantum creation-annihilation operators a^\pm

¹³This Hamiltonian goes back to Plíva (1972), who introduced the explicit matrix elements, and it was used repeatedly later by Temsamani and Herman (1995); Temsamani et al. (1996) with minor improvements. See also (Ding, 2004).

and a defining matrix elements of (19) and complex dynamical variables $\bar{3}/\sqrt{2}$ and $\bar{3}'/\sqrt{2}$, see appendix A.6. In addition to the zero order harmonic Hamiltonian (1)

$$H_0 = \omega_4(n - K_1) + \omega_5(n + K_1),$$

higher order diagonal terms in (19)

$$\begin{aligned} H_{\text{diag}} &= x_{44}(n')^2 + x_{45} n' n'' + x_{55}(n'')^2 \\ &+ g_{44}(\ell')^2 + g_{45} \ell' \ell'' + g_{55}(\ell'')^2 \\ &+ y_{444}(n')^3 + y_{445}(n')^2 n'' + y_{455} n' (n'')^2 + y_{555}(n'')^3 \end{aligned}$$

can be easily rewritten in terms of n and ν in (2), (15), (17), and (11), and

$$\zeta = \ell' + \ell'', \quad \mu = (\ell' - \ell'')/2,$$

where we assume consistent signs of ℓ' and ℓ'' . To order 2 we obtain

$$\begin{aligned} H_{\text{diag}} &= (x_{44} + x_{45} + x_{55})n^2 + 2(x_{44} - x_{55})n\nu + (x_{44} - x_{45} + x_{55})\nu^2 \\ &+ (g_{44} + g_{45} + g_{55})(\zeta/2)^2 + (g_{44} - g_{55})\zeta\mu + (g_{44} - g_{45} + g_{55})\mu^2 \\ &+ \dots \end{aligned} \quad (20)$$

From the definition of the first nondiagonal term (Darling-Dennyson, DD1)

$$\begin{aligned} \langle n', l' | \langle n'', l'' | \hat{V}_{\text{DD1}} | n' - 2, l' \rangle | n'' + 2, l'' \rangle = \\ \frac{S_{45}}{4} \sqrt{(n' - l')(n' + l')(n'' + 2 + l'')(n'' + 2 - l'')} \end{aligned} \quad (21)$$

in (Jacobson et al., 1998, p. 125), parameterizing

$$V_{\text{DD1}} = S_{45} H_{\text{DD1}}, \quad (22a)$$

and comparing to (A.15), we see immediately that

$$\hat{H}_{\text{DD1}} = a_{1'} a_{2'} a_{1''}^{\dagger} a_{2''}^{\dagger} + a_{1'}^{\dagger} a_{2''}^{\dagger} a_{1''} a_{2''}, \quad (22b)$$

and that its classical analogue is

$$H_{\text{DD1}} = \frac{1}{4} (\bar{3}_{1'} \bar{3}_{2'} \bar{3}_{1''} \bar{3}_{2''} + \bar{3}_{1'} \bar{3}_{2'} \bar{3}_{1''} \bar{3}_{2''}) = \frac{1}{4} (\bar{3}_4 \bar{3}_1 \bar{3}_3 \bar{3}_2 + \bar{3}_4 \bar{3}_1 \bar{3}_3 \bar{3}_2). \quad (22c)$$

The same result (22b) follows from the expression for the matrix element of \hat{V}_{DD1}

$$S_{45} \sqrt{n_2' n_1' (n_1'' + 1)(n_2'' + 1)}$$

in terms of 1-oscillator numbers n_1' , n_2' , n_1'' , and n_2'' . The correspondence of H_{DD1} and \hat{H}_{DD1} is exact because all monomial factors in \hat{H}_{DD1} commute. Note also that the conjugate term (c.c.) is added automatically to have the symmetric matrix element.

Similarly, the so-called “ ℓ -resonance” or “vibrational ℓ -doubling” term

$$\begin{aligned} \langle n', l' | \langle n'', l'' | \hat{V}_{\ell} | n', l' \pm 2 \rangle | n'', l'' \mp 2 \rangle = \\ \frac{R_{45}}{4} \sqrt{(n' \mp l')(n' \pm l' + 2)(n'' \pm l'')(n'' \mp l'' + 2)} \end{aligned} \quad (23)$$

which leaves $n' - n''$ unaltered, can be parameterized as $V_\ell = R_{45} \hat{H}_\ell$ where

$$\hat{H}_\ell = a_1^\dagger a_2' a_1'' a_2''^\dagger + a_1' a_2^\dagger a_1'' a_2'' \quad (24a)$$

with the exact classical analogue

$$H_\ell = \frac{1}{4} (\bar{\mathfrak{z}}_1' \mathfrak{z}_2' \bar{\mathfrak{z}}_1'' \bar{\mathfrak{z}}_2'' + \mathfrak{z}_1' \bar{\mathfrak{z}}_2' \bar{\mathfrak{z}}_1'' \mathfrak{z}_2'') = \frac{1}{4} (\mathfrak{z}_4 \bar{\mathfrak{z}}_1 \bar{\mathfrak{z}}_3 \mathfrak{z}_2 + \bar{\mathfrak{z}}_4 \mathfrak{z}_1 \mathfrak{z}_3 \bar{\mathfrak{z}}_2). \quad (24b)$$

Since [Jacobson et al. \(1998\)](#) use high order corrections such that

$$R_{45} = r_{45} + r_{445}(n' - 1) + r_{545}(n'' - 1), \quad (25)$$

the complete analogue of their ℓ -coupling term is

$$V_\ell = (r_{45} - r_{445} - r_{545}) H_\ell + (r_{445} + r_{545}) n H_\ell + (r_{445} - r_{545}) \nu H_\ell. \quad (26)$$

The last off-diagonal term of [Jacobson et al. \(1998\)](#) is defined by

$$\begin{aligned} \langle n', l' | \langle n'', l'' | \hat{V}_{\text{DD2}} | n' - 2, l' \mp 2 \rangle | n'' + 2, l'' \pm 2 \rangle = \\ \frac{R_{45} + 2g_{45}}{16} \sqrt{(n' \pm l')(n' \pm l' - 2)(n'' \pm l'' + 2)(n'' \pm l'' + 4)}. \end{aligned} \quad (27)$$

Introducing

$$\hat{V}_{\text{DD2}} = \frac{R_{45} + 2g_{45}}{4} \hat{H}_{\text{DD2}}, \quad (28a)$$

which after substituting (25) gives

$$\begin{aligned} \hat{V}_{\text{DD2}} = \frac{r_{45} - r_{445} - r_{545} + 2g_{45}}{4} \hat{H}_{\text{DD2}} \\ + \frac{1}{4} [(r_{445} + r_{545}) n + (r_{445} - r_{545}) \nu] \hat{H}_{\text{DD2}}, \end{aligned} \quad (28b)$$

we can see that

$$\hat{H}_{\text{DD2}} = [(a_1^\dagger)^2 (a_1'')^2 + (a_2^\dagger)^2 (a_2'')^2 + \text{c.c.}], \quad (28c)$$

with the exact classical analogue

$$H_{\text{DD2}} = \frac{1}{4} (\bar{\mathfrak{z}}_1^2 \mathfrak{z}_1'^2 + \bar{\mathfrak{z}}_2^2 \mathfrak{z}_2''^2 + \text{c.c.}) = \frac{1}{4} (\bar{\mathfrak{z}}_4^2 \mathfrak{z}_3^2 + \bar{\mathfrak{z}}_1^2 \mathfrak{z}_2^2 + \text{c.c.}). \quad (28d)$$

Note, however, that replacing quantum operator \hat{H}_{DD2} in (28b) for its classical analogue (28d) is ambiguous because ν and \hat{H}_{DD2} do not commute. We can verify directly that the nondiagonal terms (22c), (24b), and (28d) Poisson commute with n and ζ , and that, therefore, they are $\mathbb{T}_{2n, \zeta}^2$ invariants¹⁴. Consequently, these terms can be expressed as polynomials in \mathbf{K} and \mathbf{L} using the integrity basis (18) or, more specifically, its fully symmetrized version (see appendix B.2). We obtain

$$H_{\text{DD1}} = 2(X_3 Y_3 + X_2 Y_2) = \frac{1}{2}(L_3^2 + L_2^2 - K_2^2 - K_3^2) = \frac{1}{2}\xi, \quad (29a)$$

$$H_\ell = 2(X_2 Y_2 - X_3 Y_3) = \frac{1}{2}(K_3^2 - K_2^2 - L_3^2 + L_2^2), \quad (29b)$$

$$H_{\text{DD2}} = 2(X_2^2 - X_3^2 + Y_2^2 - Y_3^2) = K_2^2 - K_3^2 + L_2^2 - L_3^2. \quad (29c)$$

¹⁴The invariance can be also verified directly using expressions (A.3) and (A.6).

Starting with parameters in (Jacobson et al., 1998), we have computed parameters of the effective bending Hamiltonian (19) written in terms of our integrity basis with 19 adjustable parameters and adjusted these parameters in order to reproduce quantum energy levels tabulated by Herman et al. (2003). In our fit, we used complete set of numerical data for all 545 levels with $N_b \leq 10$ and all possible $\ell = \zeta$, and achieved the standard deviation of 0.05 cm^{-1} . Given that Herman et al. (2003) provide only one decimal digit, the matching can be considered exact. Our resulting parameters, along with the corresponding Hamiltonian terms represented in terms of single oscillator mode creation and annihilation operators, are given in table 5. Table 6 gives an example of the correspondence between the energies calculated with our parameters in Table 5 and those in (Herman et al., 2003).

Table 5: Parameters (cm^{-1}) of the effective Hamiltonian (19) used to reproduce bending vibrational energy levels of C_2H_2 in (Herman et al., 2003).

Parameter cm^{-1}	Operator	Parameter cm^{-1}	Operator
1337.8242	n	-11.655622	$n k$
120.33648	k	3.3069468	k^2
-8.3286063	$a_2^+ a_3^+ a_1 a_4 + \text{c.c.}$	-1.1416802	n^2
-5.7662075	$a_2^+ a_4^+ a_1 a_3 + \text{c.c.}$	2.7080975	ζ^2
-0.10280552	$n a_2^+ a_4^+ a_1 a_3 + \text{c.c.}$	-3.0114943	$\zeta \mu$
-0.10606887	$k a_2^+ a_4^+ a_1 a_3 + \text{c.c.}$	-2.8204543	μ^2
1.9976205	$(a_3^+)^2 a_4^2 + (a_1^+)^2 a_2^2 + \text{c.c.}$	0.067089051	n^3
-0.028191724	$n ((a_3^+)^2 a_4^2 + (a_1^+)^2 a_2^2) + \text{c.c.}$	0.17006851	$n^2 k$
-0.027675688	$k ((a_3^+)^2 a_4^2 + (a_1^+)^2 a_2^2) + \text{c.c.}$	-0.1686278	$n k^2$
		-0.06839412	k^3

Table 6: Comparison of energies h (cm^{-1}) calculated using the effective Hamiltonian (19) with parameters in table 5 for the $N_b = 6$ polyad (second last column) and the numerical data by Herman et al. (2003) (last column).

N_b	ζ	sym	$h \text{ cm}^{-1}$	data	N_b	ζ	sym	$h \text{ cm}^{-1}$	data
6	0	g^+	4293.1310	4293.1	6	2	g	4306.8073	4306.8
6	0	u^-	4212.8058	4212.8	6	2	u	4224.9183	4224.9
6	0	u^+	4170.7879	4170.8	6	2	u	4185.4213	4185.4
6	0	g^+	4124.6383	4124.6	6	2	g	4135.0799	4135.1
6	0	g^-	4086.8834	4086.9	6	2	g	4099.7227	4099.7
6	0	g^+	4060.0145	4060.0	6	2	g	4076.0384	4076.0
6	0	u^-	4032.7446	4032.7	6	2	u	4041.5134	4041.5
6	0	u^+	3996.9549	3996.9	6	2	u	4005.7029	4005.7
6	0	u^-	3973.4736	3973.5	6	2	u	3978.0606	3978.1
6	0	u^+	3960.7863	3960.8	6	2	g	3947.3908	3947.4
6	0	g^+	3940.2675	3940.3	6	2	g	3911.4735	3911.5
6	0	g^-	3906.1730	3906.2	6	2	g	3880.3704	3880.4
6	0	g^+	3884.0345	3884.0	6	2	u	3855.5976	3855.6
6	0	u^-	3850.3211	3850.3	6	2	u	3819.3650	3819.4
6	0	u^+	3819.3235	3919.3	6	2	g	3769.3823	3769.4
6	0	g^+	3766.0277	3767.0					

3 Bending relative equilibria of C_2H_2

The bending vibrational Hamiltonian (19), expressed as a function of (\mathbf{K}, \mathbf{L}) and dynamical parameters ($n = N_b/2 + 1, \zeta = \ell$) using (20) and (29), can have a number of equilibrium points on $\mathbb{S}^2 \times \mathbb{S}^2$ for fixed $n = N_b/2 + 1$ and $\zeta = \ell$. For the original system of four bending vibrations, these equilibria represent *relative equilibria* lifting to $\mathbb{T}_{2n, \zeta}^2$ tori in the original phase space $T\mathbb{R}_{q,p}^4 \sim \mathbb{C}_3^4$. In this section, we consider the stationary points of (19) on $\mathbb{S}^2 \times \mathbb{S}^2$ and study the stability of the respective equilibria as function of the polyad number n for fixed $\ell = \zeta = 0$ following the outline in sec. 3.1.

As explained in sec. 2.4.1 and sec. 2.4.2, there are precisely four isolated fixed points on $\mathbb{S}^2 \times \mathbb{S}^2$ in the presence of the G_8 symmetry which we called *poles*. Any G_8 -invariant Hamiltonian dynamical system should have equilibria at these points. Furthermore, as our example below in sec. 3.2 shows, it is possible to have the simplest Morse Hamiltonian function $H : \mathbb{S}^2 \times \mathbb{S}^2 \rightarrow \mathbb{R}$ whose only stationary points lie at these points. So, naturally, in sec. 3.3, we begin our analysis of the equilibria of the system with concrete Hamiltonian (19) at the poles. We give the results which are essentially overlapping with previous studies by [Rose and Kellman \(1996\)](#); [Ding \(2004\)](#); [Tyng and Kellman \(2006, 2009a,b, 2010\)](#); the computation is explained in sec. 3.2.

3.1 Computing linear stability

The Morse index of the stationary point $s \in \mathbb{S}^2 \times \mathbb{S}^2$ of function $H : \mathbb{S}^2 \times \mathbb{S}^2 \rightarrow \mathbb{R}$ is obtained from the eigenvalues of the Hessian matrix of H at s . The general way to analyze the linear stability of an equilibrium point $s \in \mathbb{S}^2 \times \mathbb{S}^2$ of the Euler-Poisson dynamical system on the phase space $\mathbb{S}^2 \times \mathbb{S}^2$ with Hamiltonian H is as follows: (i) find a tangent 4-plane $T_s(\mathbb{S}^2 \times \mathbb{S}^2)$ with standard symplectic coordinates (q_x, p_x, q_y, p_y) ; (ii) express H locally near the origin in $T_s(\mathbb{S}^2 \times \mathbb{S}^2)$ as $\mathcal{H}(q_x, p_x, q_y, p_y)$; (iii) compute with this \mathcal{H} the linearized equations of motion near the origin; (iv) find the eigenvalues of the matrix of these equations; (v) if, additionally, local canonical coordinates are of interest, ensure that the transformation to the eigenbasis is symplectic.

The specific fixed position of the poles simplifies the analysis. The plane $T_s(\mathbb{S}^2 \times \mathbb{S}^2)$ is orthogonal to axis 1, and the components 2 and 3 of \mathbf{X} and \mathbf{Y} serve as local coordinates. Considering their Poisson brackets at each pole, we have (for $\zeta = 0$)

Pole s on $\mathbb{S}^2 \times \mathbb{S}^2$				Local symplectic coordinates in $T_s \mathbb{S}^2 \times \mathbb{S}^2$	
K_1	L_1	X_1	Y_1	$(q_\alpha, p_\alpha, q_\beta, p_\beta)$	(q_x, p_x, q_y, p_y)
n	0	$n/2$	$-n/2$	$(K_2, L_3, L_2, K_3)/n$	$(X_2, X_3, Y_3, Y_2)/(n/2)$
$-n$	0	$-n/2$	$n/2$	$(L_3, K_2, K_3, L_2)/n$	$(X_3, X_2, Y_2, Y_3)/(n/2)$
0	n	$n/2$	$n/2$	$(K_2, K_3, L_2, L_3)/n$	$(X_2, X_3, Y_2, Y_3)/(n/2)$
0	$-n$	$-n/2$	$-n/2$	$(K_3, K_2, L_3, L_2)/n$	$(X_3, X_2, Y_3, Y_2)/(n/2)$

It is important to warn that in its simple form, the calculation applies only at the origin $0 \in T_s \mathbb{S}^2 \times \mathbb{S}^2$. In order to extend the analysis to the neighbourhood of 0 beyond linearization, the symplectic 2-form $\omega(K_3, K_2, L_3, L_2)$ should first be flattened at 0.

All interaction terms (29) are large away from the poles, at the “equator”, and can be immediately rewritten in terms of (q_x, p_x, q_y, p_y) , while X_1 and Y_1 with $|X_1| \approx \|\mathbf{X}\| = x$ and $|Y_1| \approx \|\mathbf{Y}\| = y$ are found from (13) by choosing the appropriate branch of the square root and Taylor expanding in (q_x, p_x, q_y, p_y) at 0.

For stationary points s other than poles, we should first rotate our coordinates (\mathbf{X}, \mathbf{Y}) so that components \tilde{X}_1 and \tilde{Y}_1 of the rotated vectors $(\tilde{\mathbf{X}}, \tilde{\mathbf{Y}})$ point at s , and

then proceed with the analysis as detailed above. Note also that we can work on \mathbb{C}_3^4 , thus avoiding having to deal with the nonflat 2-form ω at $s \in \mathbb{S}^2 \times \mathbb{S}^2$. To this end, we lift s to $\tilde{s} \in \mathbb{C}_3^4$, pullback H using (4) and (14), and then proceed in Cartesian complex coordinates $(\mathfrak{J}, \bar{\mathfrak{J}})$. After finding the eigenvalues of the matrix of the linearized Hamiltonian equations at \tilde{s} , we exclude four zeros that correspond to the directions of the Hamiltonian flows defined by the first integrals $2n$ and ζ in (11).

3.2 Example of a G_8 -invariant Morse Hamiltonian on $\mathbb{S}^2 \times \mathbb{S}^2$

Let us give a simple example of the analysis of a G_8 invariant Morse Hamiltonian function on $\mathbb{S}^2 \times \mathbb{S}^2$ for which the system may have complex hyperbolic equilibrium. Consider, to a factor and a constant, the linear Hamiltonian (1) plus an ϵ -small quadratic perturbation. Specifically, consider

$$H = K_1 + \epsilon (a H_\ell + b L_1^2/2), \quad \text{with } a^2 + b^2 \leq 1$$

and H_ℓ defined in (24). We can see from (4) that momentum K_1 induces a linear Hamiltonian \mathbb{S}^1 flow on $\mathbb{S}^2 \times \mathbb{S}^2$ which amounts to a simultaneous opposite sense rotation on each factor sphere of $\mathbb{S}^2 \times \mathbb{S}^2$ about its axis 1. Such rotation has four fixed isolated points which we called *poles* in sec. 2.4.1. The poles lie on the axis of rotation where the absolute values of $|X_1|$ and $|Y_1|$ in (13) are maximal, and where all other components of \mathbf{X} and \mathbf{Y} vanish, i.e., where $|X_1| = \|\mathbf{X}\| = x$ and $|Y_1| = \|\mathbf{Y}\| = y$. For sufficiently small ϵ , they are the *only* equilibria of the system with Hamiltonian H .

The $K_1 = \pm n$ equilibria of our example system continue from the minimum and maximum of H_0 and for small ϵ , they remain stable (elliptic). At the equivalent points with $L_1 = \pm n$, the eigenvalues are

$$\pm(\epsilon n \sqrt{a^2 - b^2} + i) \text{ and } \pm(\epsilon n \sqrt{a^2 - b^2} - i).$$

So for any $|a| > |b| \geq 0$ these equilibria are complex hyperbolic. Otherwise, they are stable, and for small ϵ , they have frequencies of opposite signs. In particular, for $a = b = 0$, the frequencies are ± 1 .

The above system of equilibria conforms to the Euler characteristics of $\mathbb{S}^2 \times \mathbb{S}^2$ (cf sec. 2.4.2). In fact, H_0 and its ϵ -small perturbation H are the simplest Morse functions on $\mathbb{S}^2 \times \mathbb{S}^2$ with the minimum number of stationary points, similar to the “height” function $X_1 : \mathbb{S}^2 \rightarrow \mathbb{R}$, which is the simplest Morse function on \mathbb{S}^2 with one maximum and one minimum.

3.3 Analysis of the full C_2H_2 Hamiltonian starting at the poles

At low n , the zero order H_0 of the reduced bending Hamiltonian (19) dominates, and the only equilibria of the system lie at the poles of $\mathbb{S}^2 \times \mathbb{S}^2$, cf sec. 3.2. The value of (19) at the poles is a function of n and ζ which defines the domain of classically allowed energies as shown in fig. 1. With regard to the original system, the respective relative equilibria (RE) correspond to its most basic vibrational modes. Specifically, the stable RE with $\nu = -n$ and $\nu = n$ correspond to the antisymmetric ν_{5u} and symmetric ν_{4g} normal modes at the upper and lower end of the energy spectrum, respectively (see fig. 1). The pair of RE with $|\mu| = n$ and energy close to the minimal energy is hyperbolic unstable. This RE is a specific “precessional” (Rose and Kellman, 1996) nonlinear normal mode, a resonant combination of the two normal modes giving maximal absolute value of the vibrational angular momentum projection on the $H-C \equiv C-H$

Table 7: Two-dimensional (pitchfork) bifurcations of G_8 -invariant equilibria at poles with $|\nu| = |K_1| = n$, see figs. 1, 4, and sec. 3.3.1. For each bifurcation, we point to the invariant circle from table 3 on which new equilibria depart. The circles are characterized by their stabilizers and the non-zero (\mathbf{K}, \mathbf{L}) component which emerges in addition to K_1 . The third column (type) gives the new Hamiltonian stability of the pole equilibrium. (Recall that $N_b = 2(n - 1)$.)

n_{crit}	Energy cm^{-1}	K_1	Type	Invariant circle
5.262	7420.104	n	ee \rightarrow eh	$K_3 \{1, \sigma, \mathcal{T}, \mathcal{T}_v\}$
4.422	5634.479	$-n$	ee \rightarrow eh	$L_3 \{1, C_2, \mathcal{T}_i, \mathcal{T}_v\}$
5.397	6936.850	$-n$	eh \rightarrow hh	$L_2 \{1, \sigma, \mathcal{T}_2, \mathcal{T}_i\}$
7.571	9907.990	$-n$	hh \rightarrow eh	$K_2 \{1, C_2, \mathcal{T}, \mathcal{T}_2\}$

axis. At larger n , the terms of order 2 in (19) become more important, and we observe a transition from the “normal mode” structure of H_0 to the polyad structure defined by the nonlinear terms in H_1 . As we increase n , this transition manifests itself through cascading pitchfork bifurcations at the normal mode poles (fig. 1) which we describe below in sec. 3.3.1, and the Hopf bifurcation of the precessional RE (sec. 3.3.2).

3.3.1 G_8 -invariant equilibria with $|K_1| = 1$

The two G_8 -invariant equilibria at the poles with $|K_1| = n$ undergo a number of Hamiltonian pitchfork bifurcations in a close sequence. One bifurcation happens at the $K_1 = 1$ pole (at the upper energy end), while three others occur at the $K_1 = -1$ pole (near the lower energy end), see table 7. Each time, one of the Z_2 symmetry subgroups of $G_8 \sim Z_2 \times Z_2 \times Z_2$ is involved (broken), and each time the bifurcation can be regarded as a two-dimensional event involving one of the two degrees of freedom of the near equilibrium dynamics. These bifurcations and the new equilibria they create can be found easily by exploiting the stratification of $\mathbb{S}^2 \times \mathbb{S}^2$ under the action G_8 , see sec. 2.4.1. Recall from fig. 4 and table 3 that there are four invariant circles crossing at each of the G_8 -invariant pole. The pair of the new equivalent stationary points of H which are created in a pitchfork bifurcation at either G_8 -invariant pole depart on the \mathbb{S}^1 circle whose stabilizer $Z_2 \times Z_2$ corresponds to the symmetries retained by the new equilibrium points.

Table 7 lists also the new Hamiltonian stability of the pole equilibrium and this allows to reconstruct the phenomenon as a whole. Originally, at low n , both the $K_1 = n$ and $K_1 = -n$ poles are stable (elliptic-elliptic, ee). So, when they first bifurcate, they become unstable (elliptic-hyperbolic, eh) in the direction defined by the respective invariant circle, and the pair of new stable (ee) equilibria depart on this circle. In other words, we have a supercritical (or local) Hamiltonian pitchfork bifurcation. The energy of the new stable paired equilibria becomes, respectively, the maximal and minimal energy of the system at given n . In the quantum system, this is reflected by energy level doublets which form near each end of the spectrum, see fig. 1.

After that, the $K_1 = -n$ equilibrium undergoes a second supercritical bifurcation and becomes hyperbolic unstable (hh) in both degrees of freedom, sending out a pair of (eh) equilibria. And finally, a third bifurcation, now subcritical, turns the stability of this point back to (eh). So we end up having precisely one pair of additional equilibria on each invariant circle in table 3 and 7. [Rose and Kellman \(1996\)](#); [Jacobson et al. \(1999a\)](#); [Tyng and Kellman \(2006\)](#) call the corresponding new modes as *local* and *anharmonic*, and interpret the respective vibrational motion of C_2H_2 . Since the periods of all these RE are close to that of the Hamiltonian flow defined by the polyad integral

$2n$, they all fall into the category of nonlinear normal modes.

3.3.2 Twin equilibria at poles with $|L_1| = 1$

To look for possible one degree of freedom bifurcations at the $L_1 = n$ pole and its symmetric twin $L_1 = -n$ on $\mathbb{S}^2 \times \mathbb{S}^2$, we can simply search for real roots of the determinant of the Hessian of $H|_{L_1=n}$. In this way we can verify that, no such bifurcations happen, at least not within the reasonable interval of the values of n covered by our model Hamiltonian. Checking for four-dimensional events that involve *both* degrees of freedom is more involved. We compute the eigenvalues of the matrix of the linearized equations of motion at $L_1 = n$ using $(K_3, K_2, L_3, L_2)/n$ as standard symplectic coordinates (see sec. 3.2). It turns out that for $n < 7$, the eigenvalues are complex, while for $n > 7$ they are imaginary. The bifurcation which occurs¹⁵ at $n = 7.0635$ ($N_b \approx 12.1$), see the mark on the $|L_1| = n$ curve in fig. 1, is, therefore, likely to be a Hamiltonian Hopf bifurcation¹⁶. Our computation showed that at $n > 7$ the equilibrium becomes elliptic (ee) with two different frequencies of the same (positive) sign.

Within this simple approach, we cannot determine precisely the kind of the Hopf bifurcation that happens (because the computation has to extend away from the origin). We may suppose that it is of the “weak” (subcritical) kind that involves a family of periodic orbits which is not coming out from the origin $L_1 = n$. These periodic orbits may be in some way related to the $K_1 = -n$ equilibrium or its “children” that are close in energy and undergo several bifurcations at approximately the same values of n .

In conclusion, it is tempting to remark on an increased level density in the triangle formed by the $L_1 = n$ (purple) and $K_1 = -n$ (red) lines for $\approx N_b > 13$. This may indicate two overlapping systems of states. One (smaller) system corresponds to states localized near the $|L_1| = 1$ equilibrium (it is now elliptic and the dynamics in its neighbourhood can be approximated by two degenerate anisotropic 2-oscillators, so that the quantum levels should form two kinds of doublets). The sequences of these states seem to ascend and end below the $K_1 = -n$ line. In other words, if there was an integrable approximation, we would have an “island” (like the one in LiCN (Joyeux et al., 2003) or in the hydrogen atom perturbed in nearly perpendicular static homogeneous fields with a sufficiently strong magnetic field component (Efstathiou et al., 2007)).

4 Classification of states within one N_b bending polyad with $\ell = 0$: third integral j and triangular lattices

The classical dynamical system corresponding to the vibrational polyad $N_b > 0$ and $\ell = 0$ has two degrees of freedom and the classical phase space $\mathbb{S}^2 \times \mathbb{S}^2$. Generically, this system is not integrable, i.e., we do not have an “additional” integral of motion j which is a function on $\mathbb{S}^2 \times \mathbb{S}^2$ in involution with energy H . One of our main purposes in this section will be to look for *integrable approximations* to our system. We investigate whether an approximate integral j can be used to characterize adequately the classical dynamics of our system on the whole or on a part of the phase space $\mathbb{S}^2 \times \mathbb{S}^2$ within a reasonably large and interesting interval of polyad numbers N_b . We

¹⁵For easier comparison to previous results, notably by Tyng and Kellman (2006), we use the parameters in (Jacobson et al., 1998, 1999a) to compute critical values of n . Using the Hamiltonian that reproduces the data by Herman et al. (2003) almost exactly gives slightly different values.

¹⁶For an introduction on Hamiltonian Hopf bifurcations, see, for example, (Buono et al., 2005).

will call an approximation *global* or *partial* if it covers all or part of the eigenstates of the corresponding quantum system, respectively. So a global integral j makes possible to arrange *all* quantum states with the same fixed N_b and ℓ into a regular, locally \mathbb{Z}^2 -equivalent lattice of points in the 2-plane \mathbb{R}^2 with coordinates given by the values of H and j . Pulled back to the original system of four bending vibrations (see sec. 2.2), j becomes a function of (6) that Poisson commutes with energy H and integrals $(2n, \zeta)$ in (11), namely the polyad integral with values $N_b + 2$ and the vibrational angular momentum. This is why we call j the “third” integral.

At low values of N_b , the system of n^2 quantum energy levels with $\ell = 0$ exhibits a clear regular behavior, especially so, if we distinguish the four symmetry types g^\pm and u^\pm of the corresponding wavefunctions, cf. fig. 2. To uncover and describe such regular patterns of quantum energies at larger N_b , we can search for an additional phenomenological quantum number, which we expect to interpret subsequently as a “good” quantum number associated with an approximate dynamical symmetry and corresponding to a classical integral j whose value is approximately conserved. The search can exploit a number of ideas, namely (a) introducing local quantum numbers corresponding to local classical actions and extending locally regular patterns of quantum energies for at least as far as the semiclassical requirements apply, see sec. 4.1; (b) studying expectation values $\langle K_1 \rangle$, $\langle L_1^2 \rangle$, and others (sec. 4.2); (c) restricting on dynamically invariant subspaces with nontrivial spatial stabilizers, cf. sec. 2.4.1; (d) constructing explicit approximate integrals as functions on $\mathbb{S}^2 \times \mathbb{S}^2$ (sec. 4.3 and 4.4); (e) describing quantum energies phenomenologically in terms of j and K_1 , cf. fig. 2 and 3, see sec. 4.4; (f) applying additional normalization (averaging).

4.1 Extending locally regular lattices with triangular patterns

First of all, we note that starting from one particular quantum state (which can be, for instance, of totally symmetric type g^+), we can reach all other states within the one chosen N_b, ℓ -polyad through a sequence of excitations/de-excitations of the u^- and u^+ symmetry types. The u^- (de-)excitation steps to a neighbour state which has both symmetry types toggled as $g \leftrightarrow u$ and $[+] \leftrightarrow [-]$ and is closest below or above in energy; the u^+ works similarly but preserves the \pm symmetry. These (de-)excitations define a certain local lattice pattern of neighbour state symmetries that we continue throughout all our constructions. Note that in the classical analogue system, they correspond to stepping local classical actions (momenta) I by \hbar . Their properties are related to the symmetry properties of the actions. The procedure should reconstruct I as long as the semiclassical conditions apply locally.

Denoting the number of (de-)excitations of type u^- and u^+ as $n(u^-)$ and $n(u^+)$, respectively, we can represent all states within the polyad by constructing a two-dimensional graph with energy as its vertical axis and with a specific linear function of $n(u^-), n(u^+)$ along its horizontal axis. Associating the latter function with a *reconstructed momentum* \mathcal{M} , makes our graph the *reconstructed energy-momentum* (\mathcal{EM}) *lattice*. This graph may, naturally, be not unique because of many existing different sequences of u^\pm (de-)excitations that lead to the same final state.

To make our construction unique, we first consider states that can be obtained from the *highest energy state* by a pure sequence of consecutive u^- de-excitations. Then, starting again with the topmost state, we step down once using the u^+ de-excitation and continue by the u^- ones. We continue, every time increasing by one the number $n(u^+)$ of initial u^+ de-excitations. We call such construction “Upper Left” or “ L ” for brevity, and we denote by $[n^L(u^+), n^L(u^-)]$ the number of de-excitations required to

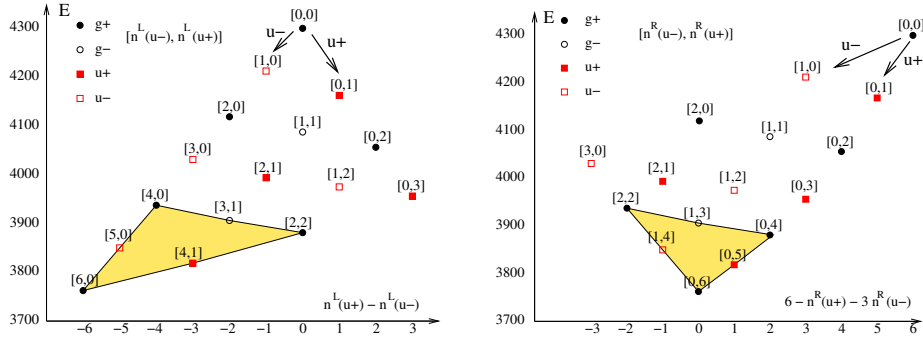


Figure 6: “Upper Left” (left) and “Upper Right” (right), or “ L ” and “ R ” triangular graphs (reconstructed \mathcal{EM} lattices) of energy levels of the $N_b = 6, \ell = 0$ bending polyad of C_2H_2 . Each quantum state is characterized by de-excitation numbers $[n^L(u^-), n^L(u^+)]$ and $[n^R(u^-), n^R(u^+)]$, while the horizontal axes use additional quantum numbers $n^L(u^+) - n^L(u^-)$ and $N_b - n^R(u^+) - 3n^R(u^-)$, respectively. States of different symmetry types are marked by different symbols. States within the shadowed domains have different L and R labels; labeling of all other states is the same.

reach each state from the topmost state. We use the “Left” momentum coordinate

$$\mathcal{M}^L = n^L(u^+) - n^L(u^-)$$

as the additional quantum number. For our example polyad with $N_b = 6$ and $\ell = 0$, we obtain the *triangular* lattice in fig. 6, left.

As an alternative “Upper Right” or “ R ” scheme, consider states which can be obtained from the topmost state by a pure series of consecutive u^+ de-excitations. Then, starting again with the highest energy state, use one u^- de-excitation followed by u^+ ones, etc. As can be seen in fig. 6, right, this procedure also yields a triangular pattern. The corresponding de-excitation numbers are denoted as $[n^R(u^-), n^R(u^+)]$, and the particular choice of momentum

$$\mathcal{M}^R = N_b - n^R(u^+) - 3n^R(u^-)$$

makes it easier to see the regularity of the reconstructed \mathcal{EM}^R -lattice.

Naturally, as we can see in fig. 6, left and right, both reconstructed \mathcal{EM}^L - and \mathcal{EM}^R -lattices are quite regular for low $N_b = 6$. One should be warned, however, that even for such low N_b , semiclassical conditions may not be valid throughout the complete reconstruction. In fact, they are likely to fail away from the “founding” boundary of the reconstructed \mathcal{EM}^L - and \mathcal{EM}^R -lattices, which is the initial sequence of states along their upper left and upper right boundaries, respectively. So, in particular, the \mathcal{EM}^L -lattice is unstable near its lower right corner, and its regularity there may rather be an artifact of the low density of available states than reflecting the actual underlying classical dynamics. So, in general, we can only assume that these lattices cover a number of the states of the polyad, see more in sec. 4.5. The main interest of our construction is that, as we will see below, we can follow the same scheme and obtain similar, rather regular L - and R -patterns for polyads with significantly higher values of N_b , where “almost chaotic behavior” has been previously believed to prevail largely.

4.2 Auxiliary quantum numbers and average values

Before extending our analysis to higher- N_b polyads, let us investigate the physical meaning of the introduced auxiliary “ L ” and “ R ” quantum numbers and suggest possible candidates for the momentum j of the approximate dynamical symmetry. To obtain the dynamical information on each quantum state labeled within a \mathcal{EM}^L - or \mathcal{EM}^R -lattice, we can calculate average values of certain physical quantities and represent the distribution of these values over the reconstructed \mathcal{EM} -lattice of quantum states. Below we use the simple $N_b = 6$ pattern in fig. 6 to illustrate the regularities in this distribution.

We begin with the average values $\langle K_1 \rangle$. Their distribution for the \mathcal{EM}^L - and \mathcal{EM}^R -lattices is shown in fig. 7. We can see immediately that the whole set of quantum levels is split into subsets with nearly constant, almost integer values of $\langle K_1 \rangle \in [-3, 3]$ aligned on almost straight lines so that

$$\langle K_1 \rangle \approx N_b/2 - n^L(u^-) - n^L(u^+) \quad \text{for the “Upper Left” choice,} \quad (30a)$$

$$\langle K_1 \rangle \approx N_b/2 - n^R(u^-) - n^R(u^+) \quad \text{for the “Upper Right” choice.} \quad (30b)$$

We observe the similarities of the “Upper Left” and “Upper Right” distributions of $\langle K_1 \rangle$. Maximal and minimal values of $K_1 = \pm 3$ are associated with states of maximal and minimal energy. These correspond, obviously, to the classical motion localized near fully symmetric normal mode poles on the $\mathbb{S}^2 \times \mathbb{S}^2$ phase space with $K_1 = \pm n$ and $K_2 = K_3 = \|\mathbf{L}\| = 0$, see sec. 2.4.1 and 3.3. Turning to the distributions of $\sqrt{\langle L_1^2 \rangle}$ over the triangular \mathcal{EM} -graphs in fig. 7, we can see that their maximum lies *inside* the lattices. This maximum marks the neighbourhood of the $L_1 = \pm n$ poles on $\mathbb{S}^2 \times \mathbb{S}^2$ with $\|\mathbf{K}\| = L_2 = L_3 = 0$. As we saw in sec. 3.3.2, the equilibria at these poles are complex unstable at low N_b .

After visualizing the average values $\langle K_1 \rangle$ and $\sqrt{\langle L_1^2 \rangle}$, we can easily *relate* the “Upper Left” quantum numbers $[n^L(u^-), n^L(u^+)]$ and the “Upper Right” quantum numbers $[n^R(u^-), n^R(u^+)]$. The two average values (and energy) are entirely sufficient to identify quantum states uniquely and to compare “Left” and “Right” lattices. We give below the correspondence between $[n^L(u^-), n^L(u^+)]$ and $[n^R(u^-), n^R(u^+)]$ in a form valid for an arbitrary N_b rather than for the particular example with $N_b = 6$ that we use currently for illustration. The correspondence between the “Left” and “Right” quantum numbers consists of two rules:

- For $n(u^-) + n(u^+) \leq N_b/2$ both sets of numbers are identical

$$[n^R(u^-), n^R(u^+)] = [n^L(u^-), n^L(u^+)]. \quad (31a)$$

- For $n(u^-) + n(u^+) = N_b/2 + t$, where $t > 0$ we have

$$[n^R(u^-), n^R(u^+)] = [n^L(u^-) - 2t, n^L(u^+) + 2t]. \quad (31b)$$

In fig. 6, the domain where quantum states have different labels in the “Left” and “Right” versions is highlighted. Note that the $-2t$ shift is responsible for the monodromy which can be computed along a circular path that follows the boundaries of the energy-momentum graph and transfers between different local lattices in order to avoid singularities where the lattices are poorly defined (see sec. 4.5.1).

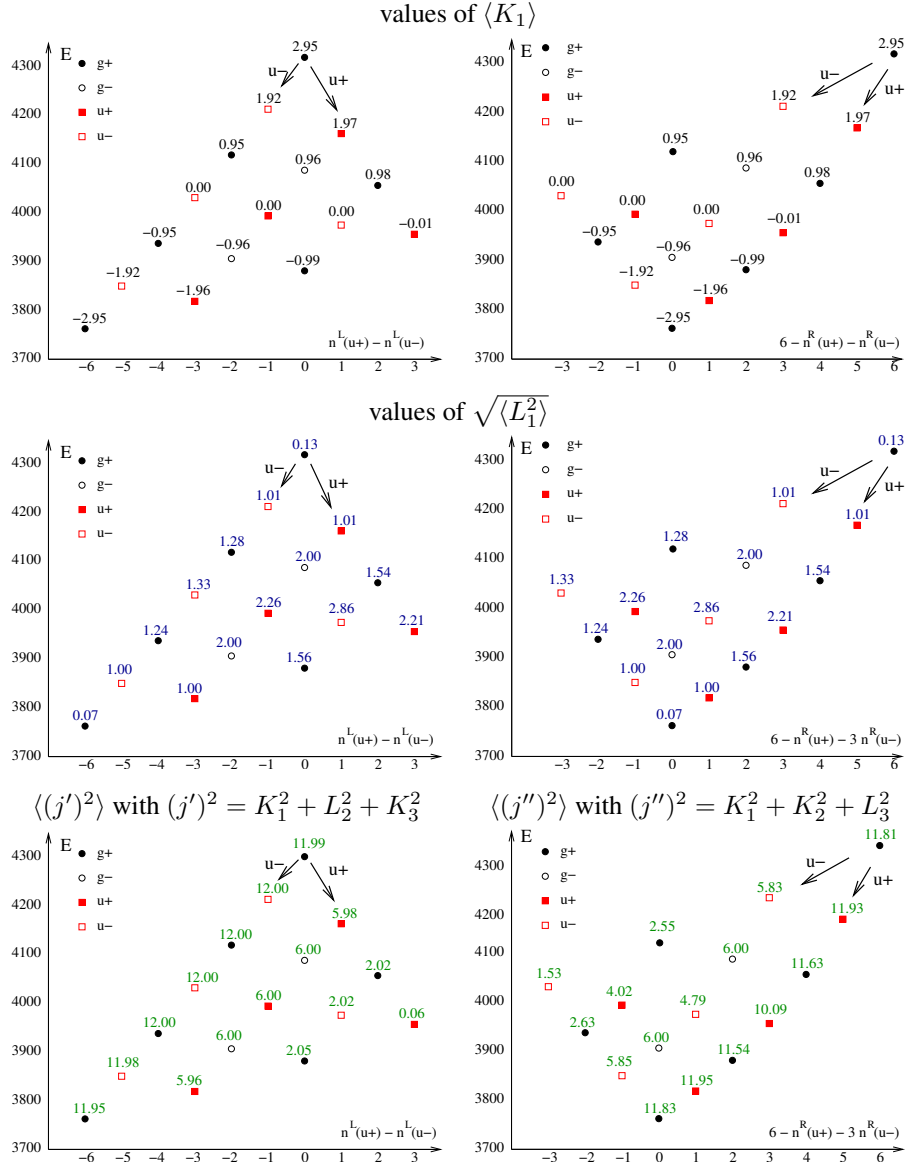


Figure 7: “Upper Left” (left column) and “Upper Right” (right column) patterns of energy levels for the $N_b = 6$, $\ell = 0$ polyad of C_2H_2 , see fig. 6. Average values $\langle K_1 \rangle$ (upper row), $\sqrt{\langle L_1^2 \rangle}$ (middle row), $\langle (j')^2 \rangle$ (bottom left), and $\langle (j'')^2 \rangle$ (bottom right) are given for each quantum state.

4.3 Approximate dynamical symmetries. Angular momenta j' and j'' , and associated invariant spheres.

We continue to investigate the nature and the physical origins of the “Left” and “Right” choices of global quantum numbers. This requires understanding the parallel constructions in the classical analogue Hamiltonian dynamical system on $S^2 \times S^2$.

Starting at the well pronounced global maximum of energy H in both “Left” and

“Right” definitions, we make sure to begin near an elliptic equilibrium where dynamics occurs on invariant two-tori labeled by two local classical oscillator actions I_{u^+} and I_{u^-} quantizing as $\hbar n(u^\pm) + \hbar/2$. The tori corresponding to quantized (integer) actions form a regular \mathbb{Z}^2 lattice near the origin of the local action space. Stepping integers $n(u^\pm)$, we explore this lattice. When we manage to find energy levels that comply with our $n(u^\pm)$ steps, we extend the lattice, and at the same time, we globalize our local actions which become actions on a domain $D \subseteq \mathbb{S}^2 \times \mathbb{S}^2$ foliated by the tori that we represent by our constructed lattice. If the steps are sufficiently (infinitesimally for $\hbar \rightarrow 0$) small, we can assure continuity and keep semiclassical conditions satisfied, but it is more difficult to have smoothness and to exclude multivaluedness (branching). It follows that we obtain generalized “actions” which are not necessarily, or not globally smooth momenta (i.e., generators of proper \mathbb{S}^1 actions) on D . The reduced Euler top and other systems on \mathbb{S}^2 with local modes (cf. appendix A) can serve as pertinent examples. Thus we can introduce a continuous action for the Euler top, a pendular action k , that allows to label and quantize tori throughout the whole energy span of the system, from the minimum to the maximum energy, but this action corresponds neither to the j_1 nor to the j_3 component of the angular momentum j which are local actions near maximum and minimum energies. Nevertheless, it might happen that at least one action in either “Left” or “Right” construction is a global momentum. To explore this possibility, we can study expectation values of known momenta and pay particular attention to the founding boundaries of “Left” and “Right” lattices where one of the constructed actions remains \hbar -small.

Considering the distribution of $\langle K_1 \rangle$ along the upper left boundary of the “Left” \mathcal{EM} graph, which is formed by states that correspond to the pure u^- sequence of de-excitations in one local “Left” action (fig. 6, left), we can naturally assume that this sequence constitutes a multiplet of states $|k\rangle$ with $k = 3, 2, 1, 0, -1, -2, -3$ which transform according to the irreducible representation of the $SU(2)$ or $SO(3)$ group of rank 3. Let us introduce the corresponding integer quantum number j' , such that for the maximal $j' = N_b/2 = 3$, it gives the value $j'(j' + 1) = 12$ of the square of the corresponding angular momentum j' . In the same manner, we can observe that the sequence of states forming the upper right boundary of the “Right” energy-momentum graph can, in turn, be characterized using $j'' = 3$ with $j''(j'' + 1) = 12$. We can further observe, that the sequence of states with single u^+ de-excitation form in the “Left” graph a string of five states one step below the left boundary. We can conjecture that these states correspond to $j' = 2$. And so forth. We can further conjecture that our lattice reconstructions are reliable as long as j' and j'' remain large (close to $N_b/2$).

Stratification of the classical phase space $\mathbb{S}^2 \times \mathbb{S}^2$ under the action of G_8 (sec. 2.4.1) gives a clue to the explicit form of j' and j'' . Among all invariant two-dimensional subspaces in table 1 and fig. 5, we can single out *two* spheres whose stabilizers are spatial (non-reversal) subgroups $\{1, C_2\}$ and $\{1, \sigma\}$ of G_8 . The particular importance of these isolated spheres is that due to their exceptional symmetry they house self-contained dynamical one-degree-of-freedom subsystems, and they can, therefore, serve as a *dynamical limit* near a one-dimensional boundary of the \mathcal{EM} -domain. We can see from sec. 2.4.1 and table 1 that the spheres are defined as

$$\begin{aligned} \mathbb{S}_{C_2}^2 &= \mathbb{S}^2 \times \mathbb{S}^2 \Big|_{K_3=L_1=L_2=0} = \{(K_1, K_2, 0, 0, 0, L_3); (j')^2 = n^2\}, \\ \mathbb{S}_\sigma^2 &= \mathbb{S}^2 \times \mathbb{S}^2 \Big|_{K_2=L_1=L_3=0} = \{(K_1, 0, K_3, 0, L_2, 0); (j'')^2 = n^2\}. \end{aligned}$$

with

$$(j')^2 := K_1^2 + K_2^2 + L_3^2 \quad \text{and} \quad (j'')^2 := K_1^2 + K_3^2 + L_2^2. \quad (32)$$

Furthermore, we can verify on either sphere that the nonvanishing (\mathbf{L}, \mathbf{K}) components generate Poisson subalgebras¹⁷ $\mathfrak{so}(3)$ of $\mathfrak{so}(4)$ with Casimirs (32), and that

$$\mathbf{j}' := (K_1, K_2, L_3) \quad \text{and} \quad \mathbf{j}'' := (K_1, K_3, L_2) \quad (33)$$

play the role of angular momenta. In other words, after restricting $H(\mathbf{L}, \mathbf{K})$ on either sphere, we have Euler-Poisson Hamiltonian dynamical systems similar to the one discussed in appendix A.

It is clear that quantum states that replicate best this restricted dynamics should be characterized by the maximal values $N_b/2$ of the norms of the respective angular momenta \mathbf{j}' and \mathbf{j}'' . We can call such states “spherically localized”, and to uncover them, we can compute the distribution of the respective expectation values $\langle (\mathbf{j}')^2 \rangle$ and $\langle (\mathbf{j}'')^2 \rangle$ of (32), which for $N_b = 6$ should approach $j'(j' + 1) = 12$ or $j''(j'' + 1) = 12$. Results of these calculations for the “Left” and “Right” patterns are shown in fig. 7. For the “Upper Left” graph we find that \mathbf{j}' is maximal along its left boundary, and that together with $k \approx K_1$, they can be “good” quantum numbers corresponding (after normalization) to the “Upper Left” actions. We can also observe, that states with maximal $\langle (\mathbf{j}'')^2 \rangle$ lie on the combined right and bottom boundaries of the \mathcal{EM}^L -lattice. Similarly, for the “Upper Right” graph we conclude that \mathbf{j}'' and K_1 play the role of “good” quantum numbers and are close to the “Upper Right” actions. Furthermore, for the $N_b = 6$ polyad, simple approximate relations

$$j' \approx \frac{1}{2}N_b - n^L(u^+) \quad \text{and} \quad \langle K_1^2 + L_2^2 + K_3^2 \rangle \approx j'(j' + 1), \quad (34a)$$

$$j'' \approx \frac{1}{2}N_b - n^R(u^-) \quad \text{and} \quad \langle K_1^2 + K_2^2 + L_3^2 \rangle \approx j''(j'' + 1). \quad (34b)$$

can be given. It can be conjectured that our “Upper Left” and “Upper Right” constructions begin with and work best for states localized near the C_2 and σ spheres, respectively. After establishing the relations between $[n^L(u^-), n^L(u^+)]$ and $\langle K_1 \rangle, \langle (\mathbf{j}')^2 \rangle$, and between $[n^R(u^-), n^R(u^+)]$ and $\langle K_1 \rangle, \langle (\mathbf{j}'')^2 \rangle$, we can equally express the momentum quantum number used to label the horizontal axes of the “L” and “R” graphs:

$$\mathcal{M}^L = n^L(u^+) - n^L(u^-) = K_1 - 2j' + N_b/2, \quad (35a)$$

$$\mathcal{M}^R = N_b - n^R(u^+) - 3n^R(u^-) = K_1 + 2j'' - N_b/2. \quad (35b)$$

At last, we can also relate the $n^L(u^-)$ and $n^R(u^+)$ de-excitation operators to the ladder operators in the respective \mathbf{j}' and \mathbf{j}'' algebras.

To complete the description, we like to comment briefly on extending our lattice reconstruction to $\ell > 0$. This can be done straightforwardly, and the resulting lattices for each ℓ can be further assembled into the three-dimensional \mathcal{EM} lattice for the entire bending polyad with given N_b as illustrated in fig. 8. Interestingly, as we can see in this figure, the $\ell > 0$ lattices appear more regular because the low j', j'' region becomes inaccessible to them. The mechanism by which axially symmetric pendular rotors avoid the region near their unstable equilibrium for large angular momenta might provide a distant analogy here.

¹⁷Notice that unlike \mathbf{X}^2 and \mathbf{Y}^2 , the quantities $(\mathbf{j}')^2$ and $(\mathbf{j}'')^2$ do not Poisson commute.

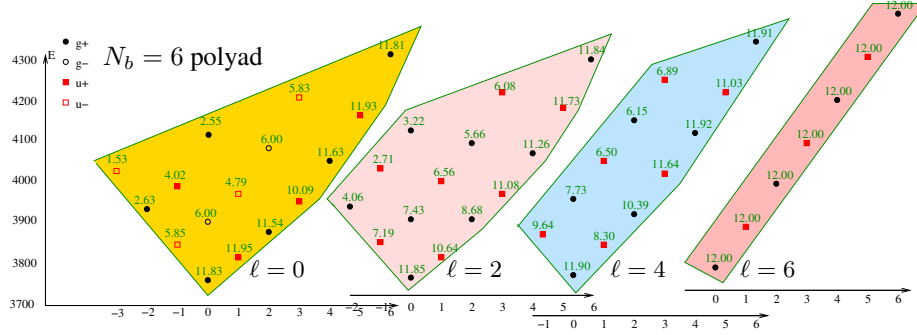


Figure 8: Reconstructed three-dimensional energy level lattice for the entire bending polyad of C_2H_2 with $N_b = 6$ ($n = 4$) sliced into two-dimensional lattices with different possible values of $\zeta = \ell = 0, 2, 4, 6$. The slices are obtained using the “Upper Right” quantum numbers. Average values $\langle (j'')^2 \rangle$ are displayed for each quantum state. Note that quantum number j'' takes integer values in $[\ell/2, N_b/2]$, so that the maximal value of j'' ($j'' + 1$) is 12. The $\ell = 0$ slice repeats fig. 7, bottom right. The \pm states for $\ell > 0$ are degenerate and only g/u symmetries need to be distinguished.

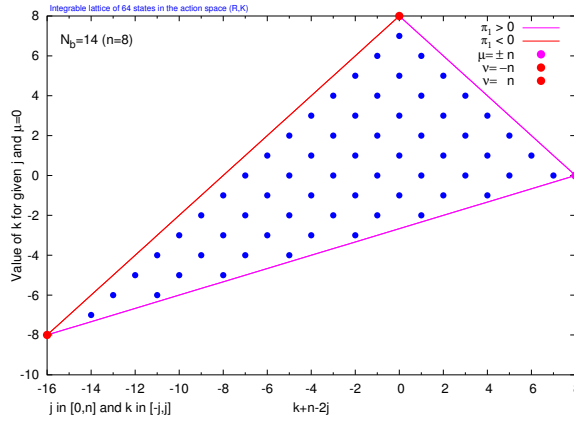


Figure 9: Bending vibrational polyad of C_2H_2 with $N_b = 14$ ($n = 8$) and $\ell = 0$ as a regular lattice in the image of the hypothetical classical integral map (action space plot) obtained with the simple integrable Hamiltonian $\mathcal{H}(j, k)$. Classical relative equilibria (large filled circles), classical relative periodic orbits (solid boundary lines), and the joint integral spectrum of the corresponding quantum system (blue filled circles) are shown. Compare to fig. 3.

4.4 Phenomenological integrable $SO(4) \supset SO(3) \supset SO(2)$ and $SO(4) \supset SO(3)$ models, and their explicit realizations

We return briefly to the phenomenological model Hamiltonian

$$\mathcal{H}_{n,\zeta}(j, k) = c(n, \zeta) + a(n, \zeta) k + b(n, \zeta) j(j + 1) \quad (36)$$

with $j \in [0, n]$ and $k \in [-j, j]$, which was announced in sec. 1.3 and illustrated in fig. 2 and 3 as a simple model which describes remarkably well the internal structure of bending (n, ζ) polyads. In view of the quality of the approximation that (36) provides, even for such high polyad numbers as $N_b = 14$, it calls for a serious scrutiny. This is an integrable model with dynamical symmetry $SO(4) \supset SO(3) \supset SO(2)$, or more

completely, $SU(4) \supset SO(4) \supset SO(3) \supset SO(2)$ and respective momenta (n, ζ) , j , and k which are first integrals of the system. Since in such model, the energy \mathcal{H} is function of first integrals, all states of the polyad form a regular lattice in the image of the *momentum map* illustrated in fig. 9 corresponding to the energy-momentum plot fig. 3. The momentum axis in fig. 2, 3, and 9 is given by

$$\mathcal{M}(n, j, k) = n - 2j + k = n - 2j - \nu,$$

and so, assuming $k = K_1$, it is equivalent to \mathcal{M}^L ; the other action (vertical axis) in fig. 9 is simply k . The image M_n of the classical momentum map in this action space for given n is a triangular domain in \mathbb{R}^2 whose vertices correspond to critical orbits of the system on $\mathbb{S}^2 \times \mathbb{S}^2$. Specifically, for $k = K_1$, the rightmost vertex represents the two equivalent poles with $\mu = \pm n$ where $\nu = j = 0$; the lower left vertex is the image of the $j = \nu = n$ with $\mu = 0$, while the upper vertex (apex) corresponds to the $\nu = -n$ pole with $j = n$ and $\mu = 0$. The boundary ∂M_n can be parameterized as follows. The upper left side of ∂M_n

$$\gamma'_n : [-j, j] \rightarrow \mathbb{R}_{\mathcal{M}, k}^2 : k \mapsto (\mathcal{M}(n, n, k), k)$$

corresponds to maximal j and connects the $K_1 = \pm n$ vertices. The two other sides

$$\gamma''_n : [-j, j] \rightarrow \mathbb{R}_{\mathcal{M}, k}^2 : k \mapsto (\mathcal{M}(n, |k|, k), k).$$

correspond to maximal $|k| = j$. Under the map

$$\Phi_{n, \zeta} : (j, k) \mapsto (\mathcal{M}(n, j, k), \mathcal{H}_{n, \zeta}(j, k)),$$

the domain M_n (for given n and ζ) becomes the triangle-shaped image of the energy-momentum map, illustrated in fig. 2 and 3.

Assuming concrete $k = K_1$, we can see states along γ'_n and γ''_n forming the $j' = n$ and $j'' = n$ multiplets, respectively, and we realize also that the model lattice in fig. 3 does not have monodromy because all four RE's of the corresponding model system (vertices of M_n) are stable. Neither can it account for pitchfork bifurcations of normal mode RE's with $K_1 = \pm n$ (see sec. 3.3). So the interpretation of this model and the relation of its \mathcal{EM} diagram to \mathcal{EM} graphs in sec. 4 requires further investigation.

Near γ'_n , the model (36) corresponds to the ‘‘Upper Left’’ choice of the approximate quantum numbers with $j \approx j'$. However, even there, pitchfork bifurcations shatter all our naive hopes to keep $k = K_1$ on the list of potential approximate integrals of motion in a more qualitatively adequate model. On the other hand, given the substantial detuning term K_1 in (20), and the obvious importance of this term at low N_b , where many states can still be interpreted in terms of normal modes ν_4 and ν_5 , and simply because K_1 is the *only* nontrivial lowest degree term, see (1), it seems reasonable to assume that j is in involution with K_1 . In the resulting integrable approximation, the energy H depends on first integrals n , ζ , j , and functions¹⁸ $\xi : \mathbb{S}^2 \times \mathbb{S}^2 \rightarrow \mathbb{R}$ which Poisson commute with j but not necessarily with K_1 . For such a particular hypothetical $SO(4) \supset SO(3)$ model, we should examine all possible $\mathfrak{so}(3)$ subalgebras that include K_1 as one of the generators, and the respective $SO(3)$ subgroups of $SO(4)$. We can also safely assume that the j^2 term in (36) is of the same order as polynomials of

¹⁸This situation is typical in one-degree-of-freedom reduced systems on \mathbb{S}^2 which transit from the normal modes and a quasi-linear Hamiltonian at low excitations to local modes with a predominantly quadratic Hamiltonian, see, for example, (Kozin et al., 2005).

degree 2 in $\{\mathbf{K}, \mathbf{L}\}$. Furthermore, it becomes clear that the integrable approximation is anisochronous. This is considerably different from the perturbations of the hydrogen atom by constant homogeneous external fields (Efstathiou and Sadovskii, 2010; Fontanari and Sadovskii, 2015; Fontanari et al., 2016).

Further leads in the search for the concrete form of j come from the consequences of the presence of the additional discrete symmetry G_8 (analyzed in sec. 2.4), namely the specific geometry of the low-dimensional subspaces of $\mathbb{S}^2 \times \mathbb{S}^2$ with nontrivial isotropy and the set of G_8 -invariant polynomials of degree 2 in $\{\mathbf{K}, \mathbf{L}\}$. We have seen in sec. 2.4.1 that the action of G_8 on $\mathbb{S}^2 \times \mathbb{S}^2$ has two dynamically invariant spheres with stabilizers C_2 and C_s which correspond to the maximal constant value n of j' and j'' , respectively. Under the flow of any G_8 -invariant Hamiltonian, these spheres are foliated into periodic orbits $\mathbb{S}^1 \subset \mathbb{S}^2 \subset \mathbb{S}^2 \times \mathbb{S}^2$. In an integrable system with the typical fibre \mathbb{T}^2 , the spheres become *critical subspaces* foliated into *critical fibres* \mathbb{S}^1 . The image of the spheres under the integral map of such system with values (h, j) is a critical value set in M_n , a one-dimensional external or internal boundary γ . Recall further that the two spheres intersect at poles $\{K_1 = \pm n\}$. This means that the corresponding critical sets form a closed loop $\gamma' \cup \gamma'' \sim \mathbb{S}^1$ in the image M_n of the integral map. For simplicity reasons, it is plausible that this loop forms, at least partially, the boundary ∂M_n . In an integrable system, we can, and often do, choose one of the local actions I so that it remains constant along the part $\gamma \subset \partial M_n$ of the boundary and thus becomes a global momentum j . All this singles out clearly the momenta j' and j'' , especially after we notice that they are Casimirs of the Poisson algebras $\mathfrak{so}(3)$ generated by $\{L_2, K_3, K_1\}$ and $\{L_3, K_2, K_1\}$, respectively.

Turning to the quadratic G_8 -invariants in sec. 2.3 and their particular choice in sec. 2.5 used by spectroscopists (29), we rewrite

$$(j')^2 = L_2^2 + K_3^2 + K_1^2 = R - H_\ell \quad \text{and} \quad (37a)$$

$$(j'')^2 = L_3^2 + K_2^2 + K_1^2 = R + H_\ell, \quad (37b)$$

with diagonal part

$$R = \frac{1}{2} (n^2 + K_1^2 - L_1^2 + (\zeta/2)^2) \quad \text{and} \quad \hat{R} = R + n, \quad (37c)$$

where the additional term in the quantum analogue \hat{R} accounts for noncommutativity. We introduce two other tensorial terms

$$\xi' = L_2^2 - K_3^2 = H_{DD1} - \frac{1}{2} H_{DD2} \quad \text{and} \quad (38a)$$

$$\xi'' = L_3^2 - K_2^2 = H_{DD1} + \frac{1}{2} H_{DD2} \quad (38b)$$

which Poisson commute with $(j')^2$ and $(j'')^2$, respectively, but not with K_1 . It is the latter terms that can describe pitchfork bifurcations. We realize that any second-degree Hamiltonian is expressed using either $(j')^2$ or $(j'')^2$, and both ξ' and ξ'' together with diagonal terms ζ^2 , L_1^2 , and $(n, K_1)^2$. So it follows nicely that we can have either ‘‘Left’’ or ‘‘Right’’ integrable $\text{SO}(3)$ approximations with integrals (n, ζ, H) and third integral j equal to j' or j'' , and that these approximations have principal perturbations L_1^2 and either ξ'' or ξ' , respectively.

We can see that both integrable approximations are clearly partial, working for large j' and/or j'' and being not applicable at large $|L_1|$, i.e., in the neighbourhoods of the twin poles $\{L_1 = \pm n\}$. In the latter neighbourhoods, all integrability is likely to vanish. This means, in particular, that the respective ‘‘corner’’ of M_n should be disregarded

Term	Parameter cm^{-1}	Term	Parameter cm^{-1}
n	+1332.0664	K_1	+120.34074
$(j')^2$	5.7630334	n^2	-4.1297849
ξ'	-6.1663	nK_1	-11.658435
ξ''	-2.1796779		
L_1^2	+0.05964887	K_1^2	+0.42538738

Table 8: Vibrational bending polyad Hamiltonian of C_2H_2 of maximal degree 2 in $\{\mathbf{K}, \mathbf{L}\}$ expressed using integral j' and restricted to $\ell = 0$; compare to table 4 and eq. (36).

as neither approximation can reach there, and that monodromy can be studied only using two approximations together. Further restrictions on the applicability domains of these approximations come from the requirement for the perturbation ξ to be small. In particular, we should require $|\xi''| \ll (j')^2$ in the “Left” case. This brings us at last to considering concrete parameters in H .

Rewriting the Hamiltonian (19) in terms of j' , ξ' , and ξ'' gives parameters in table 8. We can see immediately, that the concrete parameters of C_2H_2 are such that the contribution of the L_1^2 perturbation term is anomalously small, while the perturbation by ξ'' is moderately small as well. This constitutes the truly dynamical symmetry of the system. The dynamical symmetry and, additionally, the anomalously small parameter of the explicit quadratic contribution K_1^2 are the reasons for the wide range applicability of (36) and, in general, of the $\text{SO}(4) \supset \text{SO}(3)$ models based on j' (“Left” choice). On the other hand, the j'' approximation has large perturbation term ξ' , and is essentially quadratic in K_1 . This is likely to be one of the reasons why the integrable approximation which uses j' works better than the one based on j'' . Further analysis, based on algebraic normal forms, may be due but goes beyond the scope of our present paper.

4.5 Energy-momentum graph regularity in high N_b polyads

We now extend the two different approximate quantum numbers in sec. 4.2 to high- N_b polyads. Knowing of the bifurcations at the two poles with $K_1 = \pm N_b/2$ (sec. 3.3) which create local mode equilibria, we cannot expect K_1 to correspond much longer to (one of) our “Left” and “Right” quantum numbers. We can assume, however, that j' and j'' can still be used at least near the respective founding boundaries of the “Left” and “Right” \mathcal{EM} -graphs. In other words, we can expect that “Left” and “Right” reconstructed lattices continue to be based on the states localized near the respective C_2 - and σ -invariant spheres, and continue to cover a substantial domain of the phase space where either j' or j'' remain large. We can further assume that the “Left” and “Right” numbers provide two overlapping charts of this domain, with correspondence given by (31). In sec. 4.5.1, we exploit the resulting partial regular energy-momentum two-chart lattice in order to uncover quantum monodromy of our system.

In sec. 4.5.2 and 4.5.3, we move to even higher polyads. At the lower energy end of the graphs for these polyads, we observe that the construction becomes quite complicated and even ambiguous. This is quite likely related to the fact that the structure of polyads with $N_b \geq 14$ becomes complicated due to several bifurcations occurring in the low energy region. In particular, it is possible that the non-local Hamiltonian Hopf-like bifurcation creates a new leaf (or “island”, cf. Joyeux et al. (2003); Efsthathiou et al. (2007)) of the local energy-momentum map which should certainly complicate significantly the lattice of quantum states. With regard to future research, one possible way

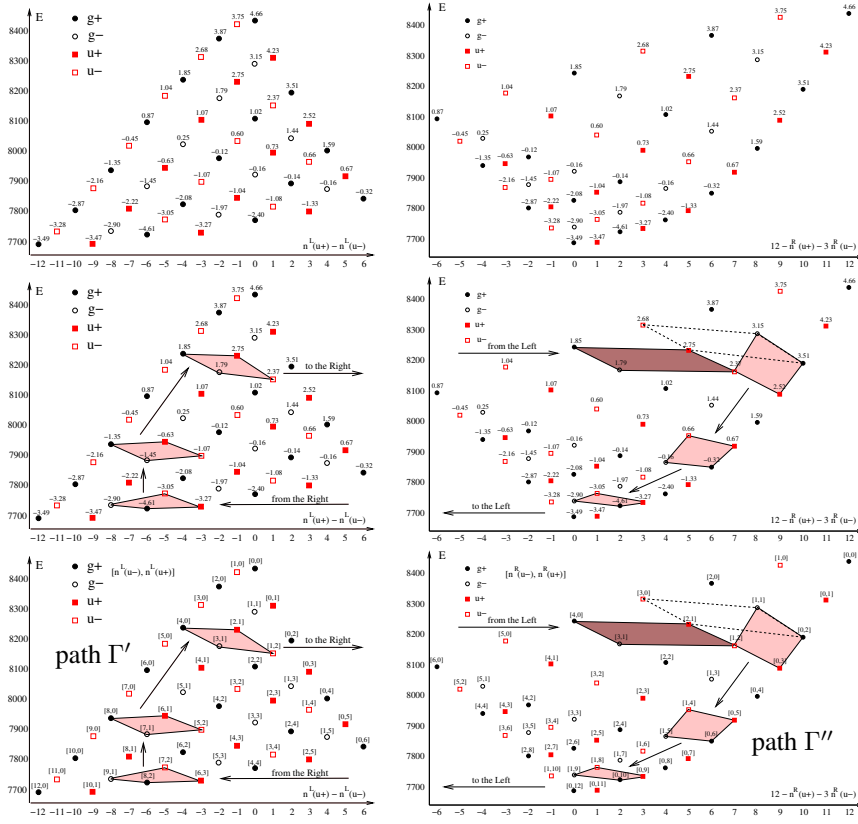


Figure 10: “Upper Left” (left column) and “Upper Right” (right column) energy-momentum graphs for the $N_b = 12$, $\ell = 0$ polyad of C_2H_2 . Average values $\langle K_1 \rangle$ (top and middle rows) and respective quantum numbers $[n^L(u^-), n^L(u^+)]$ and $[n^R(u^-), n^R(u^+)]$ (bottom row) are given near each quantum state. Quantum monodromy is manifested by the evolution of the elementary cell through the lattice of quantum states (middle and bottom rows), see sec. 4.5.1.

to facilitate the analysis of the polyad structure for large N_b may be by using quantum calculations with the same Hamiltonian but with smaller effective value of \hbar , in other words, by increasing the density of states while preserving the system of stationary points and the energy-momentum leaves of the original classical analogue system.

4.5.1 The $N_b = 12$ polyad. Quantum monodromy

The polyad with $N_b = 12$ is the last before cascading bifurcations (fig. 1, sec. 3.3) would likely complicate \mathcal{EM} lattice reconstructions. Both reconstructed \mathcal{EM}^L and \mathcal{EM}^R lattices in fig. 10 are quite regular and are relatively easy to build after confirming the steps in sec. 4.1 by the values of $\langle K_1 \rangle$ and $\langle (j')^2 \rangle$ or $\langle (j'')^2 \rangle$. Along their respective founding boundaries, we can safely assume that our lattices correlate with the underlying classical actions, and that in the open finite neighbourhoods of normal mode poles with $K_1 = \pm n$, at the top and bottom energies where *both* j' and j'' are large, the lattices overlap and we can switch between them using (31). At the same time, we have sufficiently high density of states for an \hbar -small elementary cell to be transported near the founding boundaries. This invites immediately to examine the

evolution of an elementary cell of our partial two-chart quantum lattice reconstruction along the nontrivial closed path $\Gamma = \Gamma' \cup \Gamma''$ that follows near the founding boundaries of the \mathcal{EM} charts, and to investigate quantum monodromy¹⁹. It should be pointed out that Γ loops around the neighbourhood of large $|L_1|$ values where neither of the reconstructed lattices may safely extend, where singularities associated with the twin complex unstable equilibria (sec. 3.3.2) may exist, and where the dynamics might be strongly irregular. Notice also that the two σ - and C_2 -invariant spheres connect at the $K_1 = \pm n$ poles forming a closed singular surface (fig. 5) in $\mathbb{S}^2 \times \mathbb{S}^2$. So lifted to $\mathbb{S}^2 \times \mathbb{S}^2$, the path Γ follows one sphere along Γ'' and then comes back along the other on Γ' .

In fig. 10, we provide four plots to illustrate our monodromy calculation. The middle row plots show elementary cells traveling through the \mathcal{EM}^L and \mathcal{EM}^R lattice charts with all quantum states labeled additionally by $\langle K_1 \rangle$. The latter help identifying the same quantum states in both charts. The bottom plots in fig. 10 show the same evolution but with quantum states labeled by respective quantum numbers $[n^L(u^-), n^L(u^+)]$ and $[n^R(u^-), n^R(u^+)]$. These plots help better visualizing the modification of quantum numbers during the passage of the elementary cell from the \mathcal{EM}^R to the \mathcal{EM}^L representation in the lower energy region governed by (31b). They allow equally to see the conservation of labels when the cell returns to the \mathcal{EM}^R representation in the upper energy part of the lattice where (31a) prescribes that labels in both charts are identical.

As illustrated in fig. 10, with the initial-final point in the upper energy region, we can start down Γ'' in the \mathcal{EM}^R lattice, near its right boundary, and come back up along Γ' in the \mathcal{EM}^R lattice, near its left boundary. Compared to the single-chart \mathcal{EM} lattices with global momenta that were commonly used elsewhere (Sadovskii and Zhilinskiĭ, 1999; Zhilinskiĭ, 2005), we need additionally to switch between the “R” and “L” charts. After coming down on Γ'' into the neighbourhood of $K_1 = -n$, we change the “Right” local labels for the “Left” ones, and the quantum numbers of the vertices of the elementary cell transform according to (31b). As a consequence, the evolution of an elementary cell along Γ manifests monodromy which can be represented, in the appropriately chosen basis of the local \mathbb{Z}^2 lattice, by matrix

$$\begin{pmatrix} 1 & 2 \\ 0 & 1 \end{pmatrix}.$$

Here combining one of the basis elements with *two* others corresponds undoubtedly to the fact, that the *two* complex-unstable equilibria with $L_1 = \pm n$ and $j' = j'' = 0$ are equivalent and Γ loops around the unique \mathcal{EM} image of both of them.

¹⁹Sadovskii and Zhilinskiĭ (2006) review monodromy in molecular physics; see also (Sadovskii and Zhilinskiĭ, 1999) for an early analysis of a model quantum system on $\mathbb{S}^2 \times \mathbb{S}^2$ with monodromy which is in many aspects analogous to the systems in this work. Quantum lattices with monodromy are analyzed in (Zhilinskiĭ, 2005). It is instructive to compare our lattices, specifically the lattices in figs. 2 and 8, 3, 10, 12, to those constructed for the perturbed hydrogen atom (Cushman and Sadovskii, 1999, 2000; Efstathiou et al., 2007) where monodromy was first uncovered in a concrete quantum physical system (see the survey by Efstathiou and Sadovskii (2010)). In addition to the hydrogen atom perturbations, a number of other important systems was analyzed after Richard Cushman used several simple examples (Cushman, 1983; Cushman and Duistermaat, 1988; Bates, 1991) to introduce monodromy to physicists in the mid-1990’s. Known systems with monodromy include rotation of quasilinear molecules, notably H_2O near its unstable linear equilibrium (Child et al., 1999) and others (Winnewisser et al., 2006), the H_2^+ ion (Waalkens et al., 2004), rotating dipolar symmetric top molecules and diatomic molecules subjected to an external electric field (Kozin and Roberts, 2003; Arango et al., 2004), resonant “swing-spring” vibrations of CO_2 (Cushman et al., 2004), and large amplitude vibrations of LiCN (Joyeux et al., 2003).

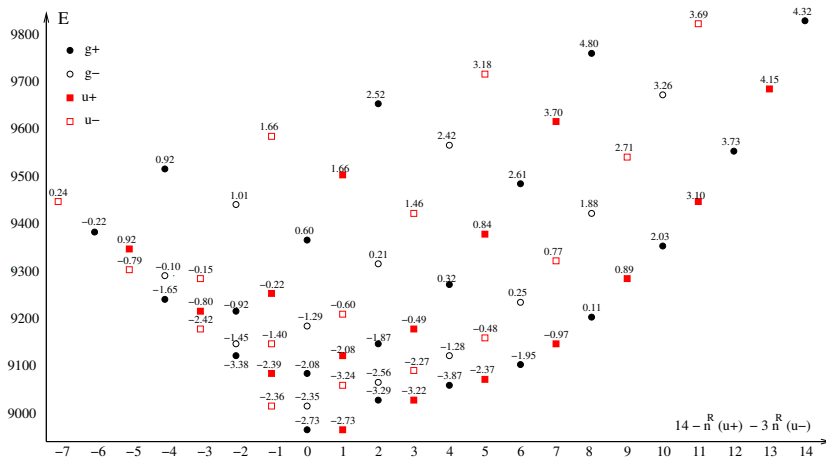


Figure 11: “Upper Right” energy-momentum graph for the $N_b = 14$, $\ell = 0$ polyad of C_2H_2 with average values $\langle K_1 \rangle$ displayed near each quantum state. The corresponding “Upper Left” graph is shown in fig. 3.

4.5.2 The $N_b = 14$ polyad representation

Following the outline in sec. 4.1 and 4.2, we reconstruct the \mathcal{EM}^L and \mathcal{EM}^R graphs for $N_b = 14$ using numerical values of energy and $\langle K_1 \rangle$. The results are displayed in fig. 3 and 11. We like to find both “Left” and “Right” representations exhibiting regular behaviour and to verify the relation (31) between them. The regularity at the bottom energy of the \mathcal{EM}^L graph may be improved by permuting several states at low energies. This requires, however, the reciprocal permutation in the \mathcal{EM}^R graph which worsens its low energy end. These troubles indicate the difficulties of extending the graphs to all states of the polyad, especially at low energies, and of overlapping them.

4.5.3 The $N_b = 16$ polyad representation

The problems, that we encounter at low energies for $N_b = 14$ (sec. 4.5.2), persist and aggravate in higher polyads. To see better how things may evolve, it is interesting to consider the next polyad with $N_b = 16$. Tentative “Left” and “Right” graphs for $N_b = 16$ are shown in fig. 12. In this figure, a thin solid line splits both patterns into top and bottom parts. The line represents the set of states with the same “Left” and “Right” labels $[n^L(u^-), n^L(u^+)] = [n^R(u^-), n^R(u^+)]$, such that $n(u^-) + n(u^+) = N_b/2$ (maximum). Recall that according to (31) all states with the energies above this line have the same “L” and “R” quantum numbers, and that in an “ideal” lattice, all states situated on this line correspond to $K_1 = 0$, see (30). Figure 12 shows that in the upper energy region, the lattice appears very regular in both representations. Conversely, in the lower energy region, the \mathcal{EM}^L lattice still remains quite regular, whereas the \mathcal{EM}^R graph becomes highly nonlinear.

5 Conclusion: types of localized bending states

Michel Herman has played a key part in the study of the rotational-vibrational levels of acetylene and in particular, he has made many important contributions to the global

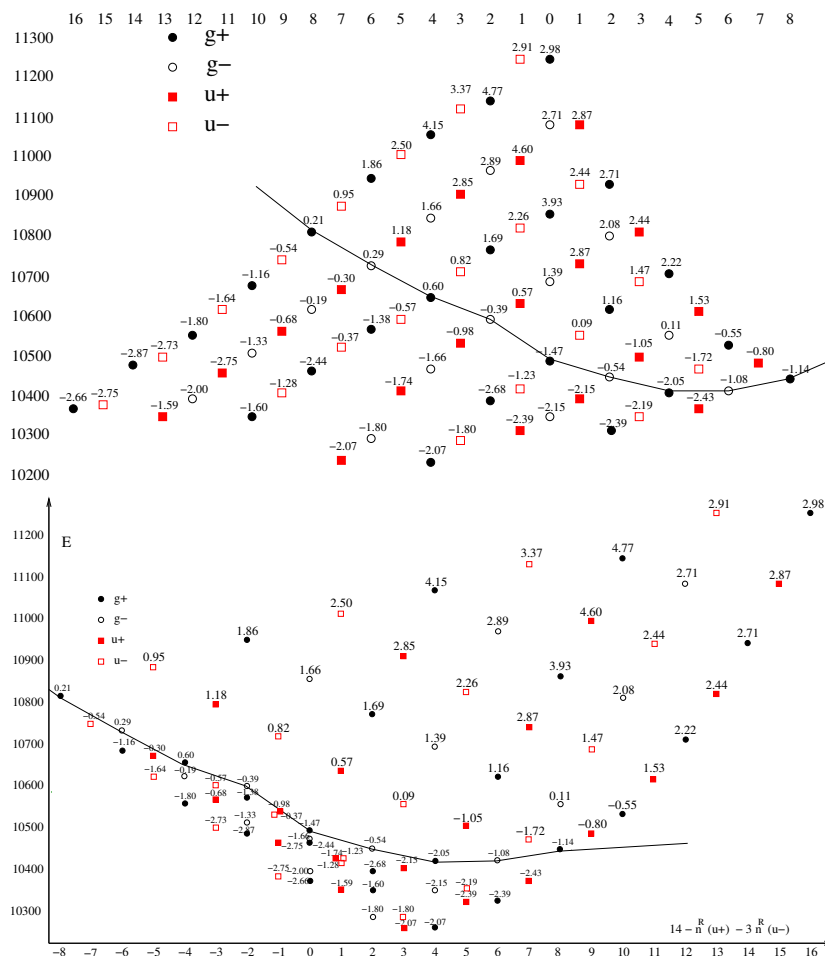


Figure 12: “Upper Left” (top) and “Upper Right” (bottom) energy-momentum graphs for the $N_b = 16$, $\ell = 0$ polyad of C_2H_2 with average values $\langle K_1 \rangle$ displayed near each quantum state.

description and understanding of the vibrational energy levels of this molecule, see (Amyay et al., 2016; Herman, 2011, 2007; Herman et al., 2003; Zhilinskií et al., 2000; Tamsamani et al., 1996; Tamsamani and Herman, 1995) and references therein. In the present article, we rely on the numerical data by Herman et al. (2003) on the vibrational energy levels of C_2H_2 resulting from the global fit of all known experimental information, and reproducing accurately numerous observed spectral transitions. From our many personal encounters, we know well how Michel Herman was always very eager to see the dynamical interpretation and understanding of his data on C_2H_2 and we intend to make a concrete contribution to advance this subject.

We begin with an effective quantum Hamiltonian $\hat{H}_{n,\zeta}$ for bending polyads of C_2H_2 which is similar to that used previously by spectroscopists, notably by Jacobson et al. (1998), and whose parameters are adjusted in order to reproduce the data by Herman et al. (2003) on these vibrational states to available numerical accuracy. Specifically, we reproduce *all* 545 N_b, ℓ -bending vibrational levels from polyads for $N_b \leq 10$ and vibrational angular momentum $\ell = \zeta \leq N_b$ with standard error of 0.05 cm^{-1} , which is the rounding error of the data in (Herman et al., 2003). We focus on polyads with $\ell =$

$\zeta = 0$ and we use $\hat{H}_{n,\zeta}$ for the qualitative analysis of the system of energy levels within these polyads. Such analysis comprises parallel studies of the quantum Hamiltonian, its eigenfunctions, and the classical analogue dynamical system. It involves the detailed analysis of the symmetry group action on classical variables and quantum states, see the discussion by [Michel and Zhilinskii \(2001b\)](#) and references therein. Parts of our analysis reproduce all earlier results by [Kellman and Chen \(1991\)](#); [Rose and Kellman \(1996\)](#); [Jacobson et al. \(1999b,a\)](#); [Ding \(2004\)](#); [Tyng and Kellman \(2006, 2009a,b, 2010\)](#).

First of all, we uncover the correct classical analogue of the C_2H_2 bending polyads which has not been fully described by our predecessors. This classical analogue turns out to be a very fundamental dynamical system and so it merits to be well understood in our context. We show that it is a dynamical Euler–Poisson system on the classical phase space $S^2 \times S^2$ equipped with a standard Poisson algebra $so(3) \times so(3) \sim so(4)$ and classical Hamiltonian function $H_{n,\zeta} : S^2 \times S^2 \rightarrow \mathbb{R}$ which can be expressed as function of two commuting angular momenta \mathbf{X} and \mathbf{Y} . We demonstrate in full detail (sec. 2 and appendices A,B) how this system is obtained from the axially symmetric nearly (1:1):(1:1) resonant oscillator system of bending vibrational modes ν_4 and ν_5 of C_2H_2 after reducing both its axial and approximate dynamical polyad S^1 symmetries with respective first integrals ζ and $N_b = 2n - 1$. For $\zeta = 0$, this is equivalent to a reduced perturbed Keplerian system, such as perturbed hydrogen atom in the n -shell approximation treated within the Kustaanheimo–Stiefel (KS) formalism, see the review by [Efstathiou and Sadovskii \(2010\)](#) and references therein.

Taking into account the full spatio-temporal symmetry G_8 of our system (sec. 2.4), we describe a systematic construction of G_8 -invariant effective Hamiltonians $H_{n,\zeta} : S^2 \times S^2 \rightarrow \mathbb{R}$ in terms of an appropriate polynomial integrity basis. To the lowest essential order with some higher degree diagonal corrections, this gives the spectroscopic Hamiltonians $H_{n,\zeta}$ of [Jacobson et al. \(1998\)](#) and others. Another highly important consequence of the symmetry group presence is the stratification of the $S^2 \times S^2$ phase space (sec. 2.4.1). We uncover a number of isolated points and two-dimensional subspaces with nontrivial isotropy which play a key role in the subsequent analysis of classical function $H_{n,\zeta}$ and of the eigenfunctions of its quantum analogue $\hat{H}_{n,\zeta}$.

The isolated points with nontrivial isotropy are necessarily the equilibria of the reduced system on $S^2 \times S^2$ which correspond to the nonlinear bending normal modes. The study of $\hat{H}_{n,\zeta=0}$ as function of parameter n (polyad number) uncovers series of bifurcations of these equilibria as observed earlier in ([Tyng and Kellman, 2006, 2010](#)). In particular, while some original modes lose stability, new pairs of stable local mode equilibria appear for higher n and the corresponding doublets of quantum states localized near these equilibria appear in the energy spectrum.

The principal, completely new—and somewhat unexpected, results of our study, are related to the presence of the additional approximate dynamical symmetry that we have found in low-to-medium excited bending polyads with $N_b \leq 12$ and that we have observed to persist to a large extent in higher polyads up to $N_b = 20$. This dynamical symmetry appears to be closely related to the existence of two two-dimensional invariant spheres $S^2 \subset S^2 \times S^2$ with isotropy groups C_2 and σ . Because the latter are spatial (non-reversal) groups, the classical dynamics can be contained on these spheres and can serve as the limit to quantum states “localized” (in the phase space sense, i.e., as certain coherent states) in the neighbourhood of one of these 2-spheres. The spheres are defined explicitly in $S^2 \times S^2$ as constant level sets of functions $(j')^2$ and $(j'')^2$, respectively, which attain there their maximal value n^2 . Considering j' and j'' as two approximate first integrals, we uncover, through the computation of averages $\langle (j')^2 \rangle$

and $\langle (j'')^2 \rangle$ on the eigenfunctions of $\hat{H}_{n,\zeta=0}$, the localized states of this new, more general, kind. Energies of quantum states for which new respective approximate quantum numbers can be assigned form two well defined two-dimensional lattices in the energy-momentum domain of the classical system.

The extent to which the approximate integrals j' and j'' and respective regular lattices are justified is further uncovered by continuous propagation of respective local regular energy level patterns and local “good” quantum numbers within the polyad. It turns out that, even in high polyads, the two lattices cover most of the domain in the energy-momentum space except a finite neighbourhood of the critical point with maximal $|L_1| = n$ (and, consequently, minimal $|\mathbf{K}| = 0$) which correspond to the “precessional” nonlinear mode and is complex unstable at low n . Classical dynamics on the preimage of this neighbourhood in $\mathbb{S}^2 \times \mathbb{S}^2$ is chaotic, but is surrounded by nearly integrable dynamics. Using the correspondence between the two lattices, we were able to demonstrate clearly the presence of monodromy²⁰ both in the classical and in the quantum system. While classical analysis reveals Hamiltonian Hopf bifurcations, the study of quantum energy state lattices in two different nearly integrable approximations demonstrates the presence of monodromy directly through the evolution of an elementary lattice cell. This new result is, naturally, very important for the concrete qualitative description of bending polyads, but it is also conceptually important as we seem to deal with a situation, where approximate integrability is not global, is destroyed within a compact submanifold of the phase space, but where monodromy can be still introduced on the remaining Cantor set of the surrounding invariant tori.

Extension of regular energy level patterns indicates the regularity of bending polyads of C_2H_2 even for such relatively high quantum numbers as $N_b = 20$ and suggests further dynamical studies of this dynamical system using normal forms. In this context, further analyzing the dynamics in a one-parameter family of polyads with control parameter N_b which exhibits a series of elementary bifurcations can be of particular interest. Classical studies in this case may be accompanied by quantum calculations with artificially increased density of states (due to formally reduced Planck constant). The qualitative modifications of the thus enhanced quantum energy lattices should definitely improve our understanding of the excited bending dynamics in acetylene and in similar molecules.

A Reminder on the 1:1 oscillator

Perturbations of the 1:1 resonant harmonic oscillator are widely used by molecular physicists, notably by Kellman, to model degenerate and quasi-degenerate vibrations. After reduction of its oscillator symmetry, this system becomes a system with one degree of freedom on the reduced phase space \mathbb{S}^2 equipped with the angular momentum Poisson algebra $\text{so}(3) \sim \text{su}(2)$. It can be studied similarly to the reduced Euler top system and its perturbations (nonrigid rotors). This relation between the two-dimensional oscillator and the rotator has been widely discussed and exploited in many quantum and classical applications. We describe here some tools and notations that will help understanding the higher dimensional case of the 1:1:1:1 oscillator.

²⁰See footnote 19.

A.1 Coordinates

Consider a 4-dimensional symplectic space $T\mathbb{R}_{q,p}^2 \sim \mathbb{R}^4 \sim \mathbb{C}^2$ with coordinates

$$q := (q_x, q_y) \quad \text{and} \quad p := (p_x, p_y),$$

where q 's are the coordinates on the configuration space \mathbb{R}_q^2 and p 's are the corresponding conjugate momenta, and with the standard symplectic form $\omega = dq \wedge dp$. We can use the complex structure $T\mathbb{R}_{q,p}^2 \rightarrow \mathbb{C}^2$ and introduce complex dynamical variables

$$z_s = q_s + ip_s, \quad \bar{z}_s = q_s - ip_s, \quad \text{with } s = x, y, \quad (\text{A.1})$$

Note that the map $(q, p) \mapsto (z, \bar{z})$ multiplies the symplectic form by a factor. In \mathbb{C}^2 , the original Poisson bracket

$$\{q_s, p_s\} = 1, \quad (\text{A.2a})$$

becomes

$$\{z_s, \bar{z}_s\} = \{q_s + ip_s, q_s - ip_s\} = -2i. \quad (\text{A.2b})$$

A.2 Dynamical oscillator symmetry \mathbb{S}^1

Consider the Hamiltonian of the two-dimensional isotropic harmonic oscillator

$$n := \frac{1}{2}(q_x^2 + p_x^2) + \frac{1}{2}(q_y^2 + p_y^2) = \frac{1}{2}z_x\bar{z}_x + \frac{1}{2}z_y\bar{z}_y$$

The dynamical, or oscillator symmetry \mathbb{S}^1 of any system whose Hamiltonian H Poisson commutes with n is defined by the Hamiltonian flow

$$\varphi_n : \mathbb{R}^1 \times \mathbb{C}^2 \rightarrow \mathbb{C}^2 : (t, z) \mapsto \exp(it) z \quad (\text{A.3a})$$

of the vector field X_n ; the conjugate dynamical variable \bar{z} transforms, of course, as

$$(t, \bar{z}) \mapsto \exp(-it) \bar{z}. \quad (\text{A.3b})$$

So the action of φ_n on the complex dynamical variables $(z, \bar{z}) = (z_1, z_2, \bar{z}_1, \bar{z}_2)$ is given by the 4×4 diagonal matrix

$$U_t^{1:1} = \text{diag}(e^{it}, e^{it}, e^{-it}, e^{-it}). \quad (\text{A.3c})$$

Generalizing to an isotropic k -oscillator with dynamical variables z_1, \dots, z_k and $\bar{z}_1, \dots, \bar{z}_k$, we get the $2k \times 2k$ diagonal matrix U_t

$$U_t = \text{diag}(\underbrace{e^{it}, \dots, e^{it}}_{k \text{ times}}, \underbrace{e^{-it}, \dots, e^{-it}}_{k \text{ times}}). \quad (\text{A.3d})$$

It can be seen that all monomials in (z, \bar{z}) that are invariant with respect to φ are of even total degree in (z, \bar{z}) and have equal degrees in z and \bar{z} .

A.3 Coordinates of the diagonal representation

Consider the angular momentum of the two-dimensional oscillator

$$\ell := q_x p_y - p_x q_y = \frac{1}{2i}(\bar{z}_x z_y - z_x \bar{z}_y).$$

Contrary to n , it is not diagonal in the original dynamical variables (z, \bar{z}) . However, it is possible and often convenient to use coordinates $(\mathfrak{z}, \bar{\mathfrak{z}})$ in which both n and ℓ are represented diagonally. To this end, we introduce new canonical variables (q_1, q_2) and conjugate momenta (p_1, p_2) , and the corresponding complex dynamical variables

$$\mathfrak{z}_i = q_i + ip_i, \quad \bar{\mathfrak{z}}_i = q_i - ip_i, \quad \text{with } i = 1, 2, \quad (\text{A.4})$$

such that

$$x = \frac{q_1 + p_2}{\sqrt{2}}, \quad p_x = \frac{-q_2 + p_1}{\sqrt{2}}, \quad y = -\frac{q_2 + p_1}{\sqrt{2}}, \quad p_y = \frac{q_1 - p_2}{\sqrt{2}}. \quad (\text{A.5a})$$

and

$$z_x = \frac{\mathfrak{z}_1 - i\mathfrak{z}_2}{\sqrt{2}}, \quad z_y = \frac{i\mathfrak{z}_1 - \mathfrak{z}_2}{\sqrt{2}}. \quad (\text{A.5b})$$

In other words, we define a linear symplectic isomorphism of \mathbb{C}^2

$$\mathbb{C}^2 \rightarrow \mathbb{C}^2 : z \mapsto \mathfrak{z} = Uz, \quad \text{where } U = U^{-1} = U^\dagger = \frac{1}{\sqrt{2}} \begin{pmatrix} 1 & -i \\ i & -1 \end{pmatrix}$$

In these new variables, ℓ becomes the Hamiltonian of the 2-dimensional harmonic oscillator in 1 : (-1) resonance,

$$\ell(q, p) = \frac{1}{2}(q_1^2 + p_1^2) - \frac{1}{2}(q_2^2 + p_2^2) = \frac{1}{2}\mathfrak{z}_1\bar{\mathfrak{z}}_1 - \frac{1}{2}\mathfrak{z}_2\bar{\mathfrak{z}}_2,$$

while the form of n remains unchanged,

$$n(q, p) = \frac{1}{2}(q_1^2 + p_1^2) + \frac{1}{2}(q_2^2 + p_2^2) = \frac{1}{2}\mathfrak{z}_1\bar{\mathfrak{z}}_1 + \frac{1}{2}\mathfrak{z}_2\bar{\mathfrak{z}}_2.$$

The expression (A.3a) for the flow defined by X_n remains the same albeit for replacing z by \mathfrak{z} . At the same time, the Hamiltonian vector field X_ℓ defines on \mathbb{C}_3^2 the diagonal flow φ_ℓ of the 1:(-1) resonant oscillator. The action of φ_ℓ on the complex dynamical variables $(\mathfrak{z}, \bar{\mathfrak{z}}) := (\mathfrak{z}_1, \mathfrak{z}_2, \bar{\mathfrak{z}}_1, \bar{\mathfrak{z}}_2)$

$$\varphi_\ell : \mathbb{R}^1 \times \mathbb{C}^2 \times \mathbb{C}^2 \rightarrow \mathbb{C}^2 \times \mathbb{C}^2 : (t, \mathfrak{z}, \bar{\mathfrak{z}}) \mapsto U_t^{1:(-1)}(\mathfrak{z}, \bar{\mathfrak{z}})^T \quad (\text{A.6a})$$

is given by the 4×4 diagonal matrix

$$U_t^{1:(-1)} = \text{diag}(e^{it}, e^{-it}, e^{-it}, e^{it}). \quad (\text{A.6b})$$

A.4 The Molien generating function for the invariants of the oscillator \mathbb{S}^1 symmetry

Using the explicit definition (A.3) of the \mathbb{S}^1 action on the initial phase space \mathbb{C}^k of the k -oscillator, we compute the Molien generating function $g(\lambda)$ directly from the Molien theorem by integrating over the group \mathbb{S}^1 (Weyl, 1939)

$$g(\lambda) = \frac{1}{2\pi} \int_0^{2\pi} \frac{dt}{\det(1 - \lambda U_t)}. \quad (\text{A.7})$$

Substituting (A.3d) and changing to the complex unimodular variable

$$\theta = \exp(it), \quad \text{such that} \quad dt = \frac{d\theta}{i\theta}, \quad (\text{A.8})$$

we rewrite (A.7) as a standard Cauchy integral

$$g(\lambda) = \frac{1}{2\pi i} \oint_{|\theta|=1} \frac{\theta^{k-1} d\theta}{(1-\lambda\theta)^k (\theta-\lambda)^k}. \quad (\text{A.9})$$

The formal real variable λ is used to Taylor expand $g(\lambda)$ and the value of λ can be assumed arbitrarily small. When $|\lambda^{-1}| > 1$ our integral has a single pole $\theta = \lambda$ of order $k \geq 1$ within the unit circle $|\theta| = 1$, and the Cauchy integral formula yields

$$g(\lambda) = \frac{1}{(k-1)!} \left. \frac{\partial^{k-1}}{\partial \theta^{k-1}} \frac{\theta^{k-1}}{(1-\lambda\theta)^k} \right|_{\theta=\lambda}. \quad (\text{A.10})$$

In particular we obtain²¹

$$g_{\mathbb{C}^1/\mathbb{S}^1}(\lambda) = 1/(1-\lambda^2), \quad (\text{A.11a})$$

$$g_{\mathbb{C}^2/\mathbb{S}^1}(\lambda) = (1+\lambda^2)/(1-\lambda^2)^3, \quad (\text{A.11b})$$

$$g_{\mathbb{C}^k/\mathbb{S}^1}(\lambda) = \sum_{s=0}^{k-1} \binom{k-1}{s}^2 \lambda^{2s} / (1-\lambda^2)^{2k-1}. \quad (\text{A.11c})$$

Here the formal variable λ represents any of the variables z and \bar{z} . Note that the generating function (A.11a) reflects the fact that any perturbation of a one-dimensional harmonic oscillator can be normalized and represented as a *Birkhoff series* in the action $n = I = \frac{1}{2} z \bar{z}$. Note also that the spaces $\mathbb{C}^k/\mathbb{S}^1$ are complex projective spaces $\mathbb{C}P^{k-1}$. These spaces are compact and C^∞ -smooth, and in particular, $\mathbb{C}^2/\mathbb{S}^1$ is the space $\mathbb{C}P^1$ which is isomorphic to the 2-sphere \mathbb{S}^2 .

A.5 Reduction of the 1:1-oscillator

We have already noticed that any \mathbb{S}^1 -invariant monomial is of even total degree in (z, \bar{z}) and of equal degree in z and \bar{z} . In degree 2, there are four such monomials which can be used to construct four invariants

$$j = \frac{1}{4}(z_1 \bar{z}_1 + z_2 \bar{z}_2) = \frac{1}{2}n, \quad (\text{A.12a})$$

$$j_1 = \frac{1}{4}(z_1 \bar{z}_1 - z_2 \bar{z}_2), \quad (\text{A.12b})$$

$$j_2 = \frac{1}{4}(z_1 \bar{z}_2 + \bar{z}_1 z_2), \quad (\text{A.12c})$$

$$j_3 = \frac{i}{4}(z_1 \bar{z}_2 - \bar{z}_1 z_2), \quad (\text{A.12d})$$

subject to the only algebraic relation

$$2\Phi_n^{1:1} = j_1^2 + j_2^2 + j_3^2 - j^2 = 0. \quad (\text{A.13})$$

The Molien function (A.11b) suggests that the ring of all invariants of the \mathbb{S}^1 action of the 1:1-oscillator system is generated multiplicatively by these four quadratic invariants, and furthermore, that one of (j_1, j_2, j_3) should be used as an auxiliary invariant. Thus we can represent this ring as

$$\mathcal{R}(j, j_1, j_2) \bullet \{1, j_3\}.$$

²¹An alternative derivation was given by Pavlov-Verevkin and Zhilinskiĭ (1988).

It also follows that all \mathbb{S}^1 orbits (A.3a) with fixed value of $n = 2j$ can be labeled by the values of two of the invariants (j_1, j_2, j_3) and the sign of the third one and that the set of these orbits is a 2-sphere \mathbb{S}^2 which can be represented in the ambient space $\mathbb{R}^3_{(j_1, j_2, j_3)}$ using (A.13). This is the *reduced phase space* of the 1:1-oscillator²². Any point on \mathbb{S}^2 lifts to a particular \mathbb{S}^1 orbit in \mathbb{C}^2 .

The Poisson algebra generated by (j_1, j_2, j_3) can be computed directly using definitions (A.12) and (A.2). It is an $\mathfrak{su}(2) \sim \mathfrak{so}(3)$ algebra with the structure matrix

$$\begin{array}{c|cc} & j_2 & j_3 \\ \hline j_1 & j_3 & -j_2 \\ \hline j_2 & & j_1 \end{array} \quad (\text{A.14a})$$

and Casimir j . Note that (A.14a) is conveniently represented by Dirac's formula

$$\{j_a, j_b\} = \sum_c \varepsilon_{abc} \frac{\partial \Phi_n^{1:1}}{\partial j_c}, \quad (\text{A.14b})$$

where the antisymmetric Levi-Civita tensor ε_{abc} equals +1 and -1 for even and odd permutations of (123), respectively.

In this way, any Hamiltonian $H : \mathbb{C}^2 \rightarrow \mathbb{R}$ which Poisson commutes with n becomes a function $\mathcal{H} : \mathbb{S}^2 \rightarrow \mathbb{R}$. We obtain a reduced system with one degree of freedom. The reduced equations of motion are given by the Euler-Poisson equations

$$dj_s/dt = \{j_s, \mathcal{H}\}, \quad s = 1, 2, 3.$$

Note that if H and n do not commute, but H has the form of a series

$$H = H_0 + \epsilon H_1 + \epsilon^2 H_2 + \dots,$$

where $H_0 = n$ and ϵ is a small parameter, H can be first normalized, i.e., transformed into a normal form series \tilde{H} which to any given order in ϵ does Poisson commute with n and which can be reduced. This is a standard approach in molecular vibrations.

A.6 Quantum-classical correspondence

Using the quantum analogues of the classical dynamical variables, we can convert our classical Hamiltonians into their quantum analogues and vice versus. Because we cannot account for non-commutativity, only principal degree terms can be related. Near the classical limit this should be sufficient.

Note that $\bar{z}/\sqrt{2}$ and $z/\sqrt{2}$ or, equally, $\bar{\mathfrak{z}}/\sqrt{2}$ and $\mathfrak{z}/\sqrt{2}$, correspond to the creation-annihilation operators a^+ and a whose action on the oscillator wavefunctions $|n_s\rangle$ with $s = x, y$ or $s = 1, 2$ is

$$a_s^+ |n_s\rangle = \sqrt{n_s + 1} |n_s + 1\rangle \quad \text{and} \quad a_s |n_s\rangle = \sqrt{n_s} |n_s - 1\rangle.$$

These formulae apply directly if quantum wavefunctions are defined as $|n_x, n_y\rangle = |n_x\rangle |n_y\rangle$ with $n = n_x + n_y$ in terms of numbers of quanta in each mode of the oscillator.

²²In the context of molecular vibrations (cf. Kellman (1985) and many others), all quantum states with the same value of $2j = n$ are said to form *n-polyads* (Sadovskii and Zhilinskiĭ, 1995) and this space is often called the *polyad phase space* or the *polyad sphere*. Polyads with even n are analogues of the rotational multiplet of the quantized reduced Euler top.

If, however, quantum wavefunctions are defined as eigenfunctions $|n, l\rangle$ of both n and l , we can work with the \mathfrak{z} coordinates to represent our operators. In this representation, we have $n = n_1 + n_2$ and $l = n_1 - n_2$, where n_i is the number of quanta in mode i of the oscillator. In other words, the wavefunction $|n_1\rangle|n_2\rangle$ is automatically the eigenfunction $|n_1 + n_2, n_1 - n_2\rangle$ of n and l . It follows that

$$a_1^+|n, l\rangle = \sqrt{\frac{n+l+2}{2}}|n+1, l+1\rangle, \quad a_1|n, l\rangle = \sqrt{\frac{n+l}{2}}|n-1, l-1\rangle, \quad (\text{A.15a})$$

$$a_2^+|n, l\rangle = \sqrt{\frac{n-l+2}{2}}|n+1, l-1\rangle, \quad a_2|n, l\rangle = \sqrt{\frac{n-l}{2}}|n-1, l+1\rangle. \quad (\text{A.15b})$$

B The 1:1:1:1 oscillator with axial symmetry

Consider now an 8-dimensional symplectic space $T\mathbb{R}_{q,p}^4$ with coordinates q and respective conjugate momenta p ,

$$q := (q_1, q_2, q_3, q_4) \quad \text{and} \quad p := (p_1, p_2, p_3, p_4), \quad (\text{B.1})$$

and the standard symplectic form $\omega = dq \wedge dp$. Our notation for (q, p) follows the one used in the work on the hydrogen atom for the Kustaanheimo–Stiefel (KS) coordinates, see, for example, (Sadovskii and Zhilinskiĭ, 1998; Cushman and Sadovskii, 2000). Consider an oscillator symmetry \mathbb{S}^1 defined by the flow of the Hamiltonian vector field X_{2n} , where

$$2n = \frac{1}{2} \sum_{i=1}^4 (q_i^2 + p_i^2)$$

is the Hamiltonian of the harmonic 4-oscillator in 1:1:1:1 resonance. Consider another \mathbb{S}^1 action defined by the flow of the Hamiltonian vector field X_ζ , where ζ is the momentum

$$\zeta = q_1 p_4 - q_4 p_1 + q_3 p_2 - q_2 p_3. \quad (\text{B.2})$$

Note that the flow φ_ζ rotates in 2-planes (1, 4) and (2, 3) of $T\mathbb{R}_{q,p}^4$, and that with regard to the bending modes of C_2H_2 (sec. 2.5), the notation can be as follows

$$\begin{aligned} (q_{x'}, p_{x'}) &:= (q_1, p_1), & (q_{y'}, p_{y'}) &:= (q_4, p_4), \\ (q_{x''}, p_{x''}) &:= (q_3, p_3), & (q_{y''}, p_{y''}) &:= (q_2, p_2), \end{aligned} \quad (\text{B.3})$$

and that furthermore,

$$\zeta = \ell = \ell' + \ell''.$$

Similarly to the outline in sec. A.3, the simultaneous diagonal representation of both ζ and n is obtained in new canonical coordinates on $T\mathbb{R}^4$

$$(Q, P)^T = U^T (q, p)^T$$

defined by the symplectic orthogonal matrix

$$U = \frac{1}{\sqrt{2}} \begin{pmatrix} A & -B \\ B & A \end{pmatrix} \quad \text{with} \quad A = \begin{pmatrix} 0 & 0 & 0 & -1 \\ 0 & 1 & 0 & 0 \\ 0 & 0 & 1 & 0 \\ 1 & 0 & 0 & 0 \end{pmatrix} \quad \text{and} \quad B = \begin{pmatrix} 1 & 0 & 0 & 0 \\ 0 & 0 & 1 & 0 \\ 0 & 1 & 0 & 0 \\ 0 & 0 & 0 & -1 \end{pmatrix}.$$

The corresponding complex Hamiltonian coordinates are

$$\mathfrak{z} = Q - iP = W^\dagger U^T(q, p)^T \quad \text{with} \quad W = \begin{pmatrix} 1 & -i \\ 1 & i \end{pmatrix}.$$

Expressed using the new complex dynamical variables $(\mathfrak{z}, \bar{\mathfrak{z}})$, both Hamiltonian functions n and ζ have diagonal representation

$$n = \frac{1}{4}(\mathfrak{z}_1 \bar{\mathfrak{z}}_1 + \mathfrak{z}_2 \bar{\mathfrak{z}}_2 + \mathfrak{z}_3 \bar{\mathfrak{z}}_3 + \mathfrak{z}_4 \bar{\mathfrak{z}}_4) = \frac{1}{2}(n_1 + n_2 + n_3 + n_4), \quad (\text{B.4a})$$

$$\zeta = \frac{1}{2}(-\mathfrak{z}_1 \bar{\mathfrak{z}}_1 - \mathfrak{z}_2 \bar{\mathfrak{z}}_2 + \mathfrak{z}_3 \bar{\mathfrak{z}}_3 + \mathfrak{z}_4 \bar{\mathfrak{z}}_4) = -n_1 - n_2 + n_3 + n_4. \quad (\text{B.4b})$$

B.1 Quadratic polynomial invariants of the $\mathbb{T}_{n, \zeta}^2$ action

It can be seen that—in addition to n and ζ themselves—there are six quadratic $\mathbb{T}_{2n, \zeta}^2$ invariant polynomials in $\mathfrak{z}, \bar{\mathfrak{z}}$. The latter can be constructed most straightforwardly, if we redefine the generators of $\mathbb{T}^2 = \mathbb{S}^1 \times \mathbb{S}^1$ as

$$2x = n - \zeta/2 = n_1 + n_2 \quad \text{and} \quad 2y = n + \zeta/2 = n_3 + n_4 \quad (\text{B.5})$$

and then apply directly the definitions (A.12) for each factor space in $T\mathbb{R}^4 \sim \mathbb{R}^8 = \mathbb{R}^4 \times \mathbb{R}^4$ in order to define the components of the Fock vectors \mathbf{J}_1 and \mathbf{J}_2 such that $\|\mathbf{J}_1\| = x$ and $\|\mathbf{J}_2\| = y$. In our studies of the hydrogen atom perturbed by orthogonal homogeneous constant electric and magnetic fields (Sadovskii and Zhilinskiĭ, 1998; Cushman and Sadovskii, 1999, 2000) and in our subsequent work on more generic field configurations (Efstathiou et al., 2007, 2008, 2009) the \mathbb{T}^2 invariants were chosen as the following components of the Fock vectors²³

$$\mathbf{J}_1 = \frac{1}{4} \begin{pmatrix} 2(n_2 - n_1) \\ i(\mathfrak{z}_1 \bar{\mathfrak{z}}_2 - \bar{\mathfrak{z}}_1 \mathfrak{z}_2) \\ -(\mathfrak{z}_1 \bar{\mathfrak{z}}_2 + \bar{\mathfrak{z}}_1 \mathfrak{z}_2) \end{pmatrix} \quad \text{and} \quad \mathbf{J}_2 = \frac{1}{4} \begin{pmatrix} 2(n_4 - n_3) \\ i(\mathfrak{z}_3 \bar{\mathfrak{z}}_4 - \bar{\mathfrak{z}}_3 \mathfrak{z}_4) \\ -(\bar{\mathfrak{z}}_3 \mathfrak{z}_4 + \mathfrak{z}_3 \bar{\mathfrak{z}}_4) \end{pmatrix}. \quad (\text{B.6})$$

Alternatively, we can define the components of linear combinations

$$\mathbf{L} = \mathbf{J}_1 + \mathbf{J}_2 \quad \text{and} \quad \mathbf{K} = \mathbf{J}_1 - \mathbf{J}_2, \quad (\text{B.7a})$$

such that

$$\mathbf{L}^2 + \mathbf{K}^2 = 2(\mathbf{J}_1^2 + \mathbf{J}_2^2) = n^2 + \zeta^2 \quad \text{and} \quad \mathbf{L} \cdot \mathbf{K} = -2n\zeta, \quad (\text{B.7b})$$

and in particular

$$L_1 = \frac{1}{2}(-n_1 + n_2 - n_3 + n_4) \quad \text{and} \quad K_1 = \frac{1}{2}(-n_1 + n_2 + n_3 - n_4). \quad (\text{B.7c})$$

In the original variables (B.1), these combinations are written as

$$\mathbf{L} = \frac{1}{2} \begin{pmatrix} 2(q_2 p_3 - q_3 p_2) \\ q_2 p_4 - q_4 p_2 + q_3 p_1 - q_1 p_3 \\ q_1 p_2 - q_2 p_1 + q_3 p_4 - q_4 p_3 \end{pmatrix} \quad (\text{B.8a})$$

and

$$\mathbf{K} = \frac{1}{2} \begin{pmatrix} (q_2^2 + p_2^2 + q_3^2 + p_3^2)/2 - (q_1^2 + p_1^2 + q_4^2 + p_4^2)/2 \\ -q_1 q_2 - p_1 p_2 + q_3 q_4 + p_3 p_4 \\ -p_2 p_4 - p_1 p_3 - q_2 q_4 - q_1 q_3 \end{pmatrix}, \quad (\text{B.8b})$$

²³see footnote 6

see, for example, equations (14) and (22) in (Sadovskii and Zhilinskiĭ, 1998). Expressions (B.8) and relations (B.3) are most useful for the correspondence to the C_2H_2 system; they are exploited in sec. 2.4.

The components (B.6) generate a Lie-Poisson algebra with the standard $so(3) \times so(3) \sim so(4)$ structure: for any functions ξ and χ in $(\mathbf{J}_1, \mathbf{J}_2)$ we have the Poisson bracket

$$\{\xi, \chi\}_{\mathbf{J}_1, \mathbf{J}_2} = \mathbf{J}_1 \cdot [\nabla_{\mathbf{J}_1} \xi \times \nabla_{\mathbf{J}_1} \chi] + \mathbf{J}_2 \cdot [\nabla_{\mathbf{J}_2} \xi \times \nabla_{\mathbf{J}_2} \chi] \quad (\text{B.9})$$

In a Keplerian system, ζ equals zero, \mathbf{L} is the angular momentum, and \mathbf{K} is the eccentricity vector²⁴. For the hydrogen atom, the Keplerian integral n and the length $L := \|\mathbf{L}\|$ correspond to the principal quantum number n and orbital momentum l . More precisely, in the semiclassical limit (using atomic units)

$$n_{\text{Kepler}} = n + 1 \quad \text{and} \quad L = \sqrt{l(l+1)} \approx l + \frac{1}{2}.$$

On the other hand, for the 1:1:1 bending polyads of C_2H_2 , $2n$ is the total number of bending quanta, ζ is the total vibrational angular momentum, and

$$\nu = -K_1 \quad \text{and} \quad \mu = L_1, \quad (\text{B.10})$$

give, respectively, the detuning and the difference of the angular momenta of the two 1:1 normal mode subsystems, see sec. 2.

B.2 Symmetrized generating function and integrity basis

We outline the construction of the generating function and the integrity basis for the G_8 -invariant polynomials in the dynamical variables $\{K_1, K_2, K_3, L_1, L_2, L_3\}$ obeying relations (B.7b). The effective G_8 -invariant polyad Hamiltonian of Jacobson et al. (1998, 1999b) is developed to degree 3 in $\{\mathbf{K}, \mathbf{L}\}$ and reproduces all available spectroscopic data (Herman et al., 2003) sufficiently well. We will see below that difficulties in writing this Hamiltonian unambiguously begin in degree 4. For the sake of simplicity, we do not consider explicit dependence on integrals (n, ζ) .

We rely on the techniques of the theory of invariants. The specialized mathematical literature on these techniques is very abundant, and physical applications are quite diverse and are not simply related to our context. An interested reader can find more details and further references in the reviews (Michel and Zhilinskiĭ, 2001b; Zhilinskiĭ, 2001). Further mathematical aspects are presented in (Weyl, 1939; Stanley, 1979; Sturmfels, 1993), while more physically oriented problems are studied, for example, in (Patera et al., 1978; Kim et al., 2001).

For constant n and ζ , relations (B.7b) define a 4-dimensional manifold with topology $\mathbb{S}^2 \times \mathbb{S}^2$ naturally embedded in $\mathbb{R}_{\mathbf{L}, \mathbf{K}}^6$. The group G_8 acting on this manifold (see sec. 2.4) is a finite order-8 commutative group isomorphic to $Z_2 \times Z_2 \times Z_2$ whose characters are given in table 1.

In the absence of any symmetry group action on $\mathbb{S}^2 \times \mathbb{S}^2$ (trivial symmetry group), we consider the generating function for all independent polynomials in $\mathbb{R}_{\mathbf{L}, \mathbf{K}}^6$, use relations (B.7b) as basic (denominator) invariants, and simply remove them from the generating function. Symbolically this can be written as

$$\frac{1}{(1-\lambda)^6} \rightarrow \frac{1+2\lambda+\lambda^2}{(1-\lambda)^4(1-\lambda^2)^2} \rightarrow \frac{1+2\lambda+\lambda^2}{(1-\lambda)^4}$$

²⁴Often called after Laplace-Runge-Lenz, see footnote 4

Table 9: Character table for the reversal order-four symmetry subgroup $G_4^* \subset G_8$ leaving both K_1 and L_1 invariant.

	E	TC_2^y	i	$T\sigma_v^{xz}$	$\{L_\alpha, K_\alpha\}$
A_g	1	1	1	1	K_1, L_1
B_g	1	-1	1	-1	
A_u	1	1	-1	-1	K_2, L_2
B_u	1	-1	-1	1	K_3, L_3

The choice of the concrete integrity basis is, naturally, ambiguous. It is important to choose as six denominator invariants along with two polynomials (B.7b) four other polynomials which form together algebraically independent set of polynomials. This can be done, for example, as

$$\mathbf{K}^2 + \mathbf{L}^2, \mathbf{K} \cdot \mathbf{L}, K_1, L_1, K_2, L_2.$$

After such a choice of algebraically independent polynomials is done, numerator polynomials can be added as

$$L_3, K_3, K_3^2 - L_3^2.$$

Note that we cannot use the product L_3K_3 of the two linear auxiliary (numerator) polynomials as the quadratic auxiliary polynomial because

$$L_3K_3 = \mathbf{K} \cdot \mathbf{L} - L_1K_1 - L_2K_2$$

is a polynomial in the principal (denominator) invariants. At the same time, if we use linear auxiliary invariants $K_3 \pm L_3$, then the quadratic numerator invariant can be taken as their product. As long as we have no additional symmetries, denominator invariants $\{K_1, K_2, L_1, L_2\}$ remain one of several possible choices. Any of these choices allows to generate a complete list of algebraically independent polynomials obeying the two quadratic relations which we want to eliminate.

The same procedure can be applied to eliminate quadratic relations in the presence of symmetry. We begin by taking into account the order-4 reversal group $G_4^* := \{1, \mathcal{T}_2, i, \mathcal{T}_v\}$, which is an index-2 subgroup of the total finite invariance group G_8 . This subgroup is isomorphic to the point group C_{2h} and the abstract group $Z_2 \times Z_2$, and its action on (\mathbf{K}, \mathbf{L}) can be deduced from table 1. This action is equivalent to the standard action of C_{2h} on $\mathbb{R}_{\mathbf{L}, \mathbf{K}}^6$, and its advantage is that each pair $\{K_i, L_i\}$ with $i = 1, 2, 3$, transforms according to one irreducible representation, see table 9.

We construct the generating function for the G_4^* -invariants from the initial representation $A_g \times A_g \times A_u \times A_u \times B_u \times B_u$. From the generating function

$$g_{Z_2 \times Z_2}^{A_g \leftarrow \{2A_g \times 2A_u \times 2B_u\}}(t_{A_g}, t_{A_u}, t_{B_u}) = \frac{1 + t_{A_u}^2 + t_{B_u}^2 + t_{A_u}^2 t_{B_u}^2}{(1 - t_{A_g})^2 (1 - t_{A_u}^2)^2 (1 - t_{B_u}^2)^2} \quad (\text{B.11})$$

written in terms of three auxiliary parameters, we can immediately suggest one possible integrity basis after noticing that its three quadratic terms $t_{A_u}^2$ correspond to $\{K_2^2, L_2^2, K_2L_2\}$, while the three terms quadratic $t_{B_u}^2$ represent $\{K_3^2, L_3^2, K_3L_3\}$. The quartic term $t_{A_u}^2 t_{B_u}^2$ corresponds to the product $K_2L_2K_3L_3$. Such choice suffices if there are no constraints (B.7b). In order to eliminate (B.7b), we should pass to linear combinations and choose those terms as denominator invariants which should be dropped.

The choice of the integrity basis can be done as follows. For the denominator invariants we prefer to choose among six polynomials two terms corresponding to relations to be removed.

$$L_1, \quad K_1, \quad K_2^2 - L_2^2, \quad K_3^2 - L_3^2 \quad (\text{B.12a})$$

$$L_1^2 + L_2^2 + L_3^2 + K_1^2 + K_2^2 + K_3^2, \quad L_1K_1 + L_2K_2 + L_3K_3. \quad (\text{B.12b})$$

The choice is naturally ambiguous. For linear denominator invariants any linear combinations of L_1 and K_1 could be chosen, but we prefer to take denominator invariants in such way that they transform according to irreps of the full symmetry group. This gives unique choice for linear invariants. From these linear invariants it is possible to construct three linearly independent quadratic invariants L_1^2, K_1^2, L_1K_1 . Among other six quadratic invariants $L_2^2, K_2^2, L_2K_2, L_3^2, K_3^2, L_3K_3$. there are four algebraically independent and two linearly independent. When making choice of algebraically independent quadratic invariants we take two of them as relations defining the $\mathbb{S}^2 \times \mathbb{S}^2$ manifold. It is possible because we can form linear combinations with quadratic polynomials constructed from linear algebraically independent invariants. This explains the choice of quadratic denominators made in (B.12).

Note that the integrity basis (B.12) does not correspond exactly to generating function (B.11) with three formal parameters. The integrity basis implied by (B.11) should be chosen so that each invariant polynomial is constructed from variables belonging to the same irreducible representation of G_4^* . The basis (B.12) includes polynomials, specifically the ones corresponding to the $\mathbb{S}^2 \times \mathbb{S}^2$ defining relations (B.7b), which are linear combinations of monomials constructed from variables belonging to different irreducible representations. To see the correspondence between the chosen integrity basis and generating function (B.11) we should replace the three variables $\{t_{A_g}, t_{A_u}, t_{B_u}\}$ of (B.11) by one formal variable λ . The resulting generating function has the form

$$\frac{1 + 2\lambda + \lambda^2}{(1 - \lambda)^2(1 - \lambda^2)^4}.$$

Choosing the numerator invariants, we can easily define quadratic polynomials, but we should pay more attention to the quartic polynomial. Thus it may be tentative to use quartic polynomial $K_2L_2K_3L_3$, or just a product of two quadratic invariant numerator polynomials. The situation here is somewhat similar to the one at the beginning of this appendix where we constructed numerator invariants after removing defining relations of $\mathbb{S}^2 \times \mathbb{S}^2$ and had no additional symmetries. In that simple case we had to choose between L_3K_3 , the product of two auxiliary linear invariants L_3, K_3 , and $K_3^2 - L_3^2$. It was sufficiently evident that L_3K_3 could not be used as quadratic auxiliary invariant for the particular, chosen beforehand (imposed), denominator invariant. Now we face a similar problem at degree 4 and we should analyze it carefully.

The difference between the two suggested choices becomes apparent after classifying invariants by their transformation properties with respect to the complete group G_8 . The G_4^* -invariant numerator polynomial $K_2L_2K_3L_3$ belongs to the A_g representation of G_8 , whereas the product of two auxiliary quadratic G_4^* invariants belongs to the B_{3g} representation of G_8 . These propositions are contradictory.

In order to find out which of the above suggestions is correct, we can construct *all* linearly independent quartic G_4^* -invariant polynomials from linear and quadratic denominator and numerator invariants. As we detail below, this gives 41 polynomials. On the other hand, the generating function (B.11) tells us that there is a total of 42 linearly independent quartic G_4^* -invariant polynomials. It follows that we should find

one additional quartic G_4^* -invariant polynomial in order to complete the set of the 41 already constructed.

The multiplicative ring \mathcal{R} generated freely by principal (denominator) invariants (B.12a) contains 27 quartic and 7 quadratic polynomials. Multiplying the latter by two quadratic auxiliary (numerator) invariants gives further 14 quartic polynomials to make the total of $27 + 14 = 41$. By checking linear dependencies among generated quartic polynomials, we have found that it is necessary to choose $K_2L_2 - K_3L_3$ as principal (denominator) invariant, while the polynomial $K_3^2 - L_3^2$ should be used as auxiliary (numerator) invariant. In such a case, the generating function

$$\frac{1 + \phi_1 + \phi_2 + \phi_1\phi_2}{(1 - K_1)(1 - L_1)(1 - \theta_1)(1 - \theta_2)(1 - \theta_3)(1 - \theta_4)}, \quad (\text{B.13})$$

with

$$\phi_1 = K_2^2 + L_2^2 - K_3^2 - L_3^2, \quad \phi_2 = K_3^2 - L_3^2, \quad (\text{B.14a})$$

$$\theta_1 = K_2^2 - L_2^2, \quad \theta_2 = K_2L_2 - K_3L_3, \quad (\text{B.14b})$$

$$\theta_3 = \mathbf{K}^2 + \mathbf{L}^2 \quad \text{and} \quad \theta_4 = \mathbf{K} \cdot \mathbf{L}, \quad (\text{B.14c})$$

describes correctly all linearly independent G_4^* -invariant polynomials in $\{\mathbf{K}, \mathbf{L}\}$ at least to degree four.

We can now turn to the complete group G_8 . Our numerator and denominator invariants for group G_4^* are constructed so that they belong to the irreducible representations of G_8 , specifically we have

$$(\phi_1)^{A_g}, (\phi_2)^{A_g}, (\phi_1\phi_2)^{A_g}, \quad (\text{B.15})$$

$$(K_1)^{A_g}, (L_1)^{B_{3g}}, (\theta_1)^{A_g}, (\theta_2)^{B_{3g}}, (\theta_3)^{A_g}, (\theta_4)^{B_{3g}}. \quad (\text{B.16})$$

To construct the generating function for the G_8 invariants, we should multiply the numerator and denominator of (B.13) by

$$(1 + L_1)(1 + \theta_2)(1 + \theta_4).$$

This makes all denominator terms G_8 -invariant and increases the number of terms in the numerator, which includes now terms of both A_g and B_{3g} symmetry. Symbolically, this transformation of (B.13) can be represented using two formal parameters (λ, μ) for polynomials of symmetry types A_g and B_{3g} , respectively, as follows

$$\frac{1 + 2\lambda^2 + \lambda^4}{(1 - \lambda)(1 - \mu)(1 - \lambda^2)^2(1 - \mu^2)^2} = \frac{(1 + 2\lambda^2 + \lambda^4)(1 + \mu)(1 + \mu^2)^2}{(1 - \lambda)(1 - \mu^2)(1 - \lambda^2)^2(1 - \mu^4)^2}. \quad (\text{B.17})$$

Here, in the numerator, μ stands for linear covariant L_1 of type B_{3g} , while the two μ^2 terms correspond to two quadratic covariants θ_2 and θ_4 of symmetry B_{3g} . In the denominator, μ^2 corresponds to the invariant L_1^2 , while the two μ^4 factors correspond to two invariants, θ_2^2 and θ_4^2 . In order to obtain the generating function for G_8 invariants, we should retain only terms of symmetry A_g in the numerator. The symbolic form of this functions is

$$\frac{(1 + 2\lambda^2 + \lambda^4)(1 + 2\lambda^3 + \lambda^4)}{(1 - \lambda)(1 - \lambda^2)^3(1 - \lambda^4)^2},$$

or, more explicitly,

$$\text{Numerator: } (1 + \phi_1 + \phi_2 + \phi_1\phi_2)(1 + L_1\theta_2 + L_1\theta_4 + \theta_2\theta_4), \quad (\text{B.18a})$$

$$\text{Denominator: } (1 - K_1)(1 - L_1^2)(1 - \theta_1)((1 - \theta_2^2)(1 - \theta_3)(1 - \theta_4^2)). \quad (\text{B.18b})$$

Fixing (excluding) relations θ_3 and θ_4 , we obtain

$$\frac{(1 + 2\lambda^2 + \lambda^4)(1 + \lambda^3)}{(1 - \lambda)(1 - \lambda^2)^2(1 - \lambda^4)} = \frac{1 + 2\lambda^2 + \lambda^3 + \lambda^4 + 2\lambda^5 + \lambda^7}{(1 - \lambda)(1 - \lambda^2)^2(1 - \lambda^4)} \quad (\text{B.19})$$

with denominator invariants

$$K_1, \quad L_1^2, \quad \theta_1, \quad \theta_2^2, \quad (\text{B.20a})$$

and numerator invariants

$$\phi_1, \quad \phi_2, \quad L_1\theta_2, \quad \phi_1\phi_2, \quad \phi_1L_1\theta_2, \quad \phi_2L_1\theta_2, \quad \phi_1\phi_2L_1\theta_2, \quad (\text{B.20b})$$

where ϕ_i and θ_i are defined in (B.14).

References

- R. Abraham and J. Marsden. *Foundation of Mechanics*. Addison-Wesley, Reading, MA, 1978.
- B. Amyay, A. Fayt, M. Herman, and J. V. Auwera. Vibration-rotation spectroscopic database on acetylene, $\tilde{X}^1\Sigma_g^+$ ($^{12}\text{C}_2\text{H}_2$). *J. Phys. Chem. Ref. Data*, **45(2):023103**, 2016.
- C. A. Arango, W. W. Kennerly, and G. S. Ezra. Quantum monodromy for diatomic molecules in combined electrostatic and pulsed nonresonant laser fields. *Chem. Phys. Lett.*, **392(4):486–492**, 2004. ISSN 0009-2614.
- V. I. Arnold. *Geometrical Methods in the Theory of Ordinary Differential Equations*, volume 250 of *Grundlehren der mathematischen Wissenschaften*. Springer-Verlag, Berlin, 1983.
- V. I. Arnol'd. *Mathematical methods of classical mechanics*, volume 60 of *Graduated Texts in Mathematics*. Springer-Verlag, New York, 2 edition, 1989. Translated by K. Vogtmann and A. Weinstein.
- V. I. Arnol'd. *Catastrophe theory*. Springer-Verlag, Berlin, 1992.
- V. Bargmann. Zur Theorie des Wasserstoffatoms (on the theory of the hydrogen atom). *Z. Phys.*, **99:576–582**, 1936.
- L. M. Bates. Monodromy in the champagne bottle. *Z. Angew. Math. Phys.*, **42:837–847**, 1991. ISSN 1420-9039.
- B. A. Bernevig. *Topological insulators and topological superconductors*. Princeton Univ. Press, Princeton, 2013.
- P.-L. Buono, F. Laurent-Polz, and J. Montaldi. Symmetric Hamiltonian bifurcations, based on lectures by J. Montaldi. In J. Montaldi and T. Ratiu, editors, *Geometric Mechanics and Symmetry : The Peyresq Lectures*, volume 306 of *London Mathematical Society Lecture Note Series*. Cambridge University Press, Cambridge, UK, 2005.
- M. S. Child and L. Halonen. *Advances in Chemical Physics*, volume 57, chapter Overtone Frequencies and Intensities in the Local Mode Picture, pages 1–58. John Wiley & Sons, Inc., New York, 1984. doi: 10.1002/9780470142813.ch1.
- M. S. Child, T. Weston, and J. Tennyson. Quantum monodromy in the spectrum of H_2O and other systems: new insight into the level structure of quasi-linear molecules. *Mol. Phys.*, **96:371–379**, 1999.

- H. Crogman, V. Boudon, and D. A. Sadovskii. Local modes of silane within the framework of stretching vibrational polyads. *Europ. Phys. J. D*, **42**:61–72, 2007.
- R. H. Cushman and L. Bates. *Global aspects of classical integrable systems*. Birkhäuser, Basel, 1997.
- R. H. Cushman and J. J. Duistermaat. The quantum-mechanical spherical pendulum. *Bull. Am. Math. Soc.*, **19**:475–479, 1988.
- R. H. Cushman and D. A. Sadovskii. Monodromy in perturbed Kepler systems: hydrogen atom in crossed fields. *Europhys. Lett.*, **47**:1–7, Jul 1999.
- R. H. Cushman and D. A. Sadovskii. Monodromy in the hydrogen atom in crossed fields. *Physica D*, **142**:166–96, Aug 2000.
- R. H. Cushman, H. R. Dullin, A. Giacobbe, D. D. Holm, M. Joyeux, P. Lynch, D. A. Sadovskii, and B. I. Zhilinskiĭ. CO₂ molecule as a quantum realization of the 1:1:2 resonant swing-spring with monodromy. *Phys. Rev. Lett.*, **93**:024302/1–4, Jul 2004.
- R. H. Cushman. Geometry of the energy-momentum mapping of the spherical pendulum. *Centrum voor Wiskunde en Informatica Newsletter*, 1:4–18, 1983.
- X. Ding. *Generalized critical points analysis of acetylene vibrational dynamics*. PhD thesis, University of Oregon, Department of Chemistry, University of Oregon, March 2004. URL <http://darkwing.uoregon.edu/~meklab/DingThesis/Thesis.pdf>. switch $\pm \leftrightarrow \mp$ in the rhs of the matrix element definition for V_{ℓ} .
- A. J. Dorney and J. K. G. Watson. Forbidden rotational spectra of polyatomic molecules: Stark effects and $\Delta J = 0$ transitions of t_d molecules. *J. Mol. Spectrosc.*, **42**(1):135–148, 1972. ISSN 0022-2852.
- K. Efstathiou and D. A. Sadovskii. Perturbations of the 1:1:1 resonance with tetrahedral symmetry: a three degree of freedom analogue of the two degree of freedom Hénon-Heiles hamiltonian. *Nonlinearity*, **17**:415–46, Mar 2004.
- K. Efstathiou and D. A. Sadovskii. Normalization and global analysis of perturbations of the hydrogen atom. *Rev. Mod. Phys.*, **82**(3):2099–2154, Aug 2010.
- K. Efstathiou, D. A. Sadovskii, and R. H. Cushman. Linear Hamiltonian Hopf bifurcation for point-group-invariant perturbations of the 1:1:1 resonance. *Proc. Roy. Soc. London, Ser. A*, **459**:2997–3019, Dec 2003.
- K. Efstathiou, D. A. Sadovskii, and B. I. Zhilinskiĭ. Analysis of rotation-vibration relative equilibria on the example of a tetrahedral four atom molecule. *SIAM J. Appl. Dyn. Syst. (SIADS)*, **3**:261–351, 2004.
- K. Efstathiou, D. A. Sadovskii, and B. I. Zhilinskiĭ. Classification of perturbations of the hydrogen atom by small static electric and magnetic fields. *Proc. Roy. Soc. London, Ser. A*, **463**:1771–1790, Jul 2007.
- K. Efstathiou, O. V. Lukina, and D. A. Sadovskii. Most typical 1:2 resonant perturbation of the hydrogen atom by weak electric and magnetic fields. *Phys. Rev. Lett.*, **101**:253003/1–4, Dec 2008.
- K. Efstathiou, O. V. Lukina, and D. A. Sadovskii. Complete classification of qualitatively different perturbations of the hydrogen atom in weak near orthogonal electric and magnetic fields. *J. Phys. A: Math. Theor.*, **42**:055209/1–29, 2009.

- V. Fock. Zur Theorie des Wasserstoffatoms (on the theory of the hydrogen atom). *Z. Phys.*, **98**: 145–154, 1935.
- D. Fontanari and D. Sadovskii. Perturbations of the hydrogen atom by inhomogeneous static electric and magnetic fields. *J. Phys. A: Math. Theor.*, **48(9)**:095203, 3 2015.
- D. Fontanari, F. Fassò, and D. A. Sadovskii. Quantum manifestations of Nekhoroshev stability. *Phys. Lett. A*, **380**:3167–3172, Aug 2016.
- R. Gilmore. *Catastrophe Theory for Scientists and Engineers*. Dover books on advanced mathematics. Dover Publications, New York, 1993. ISBN 9780486675398.
- H. Goldstein. Prehistory of the Runge-Lenz vector. *Am. Jour. Phys.*, **43**:735–738, 1975.
- H. Goldstein. More on the prehistory of the Runge-Lenz vector. *Am. Jour. Phys.*, **44**:1123–1124, 1976.
- W. G. Harter and C. W. Patterson. Rotational energy surfaces and high- J eigenvalue structure of polyatomic molecules. *J. Chem. Phys.*, **80(9)**:4241–61, 1984.
- B. Hartke, A. E. Janza, W. Karrlein, J. Manz, V. Mohan, and H.-J. Schreier. Local versus hyperspherical modes of water and formaldehyde: Effect of molecular complexity on mode-selective structures and dynamics. *J. Chem. Phys.*, **96(5)**:3569, 1992.
- M. Herman. The acetylene ground state saga. *Mol. Phys.*, **105(17-18)**:2217–2241, 2007.
- M. Herman, A. Campargue, M. I. E. Idrissi, and J. V. Auwera. Vibrational spectroscopic database on acetylene, $\tilde{X}^1\Sigma_g^+$ (12 C₂H₂, 12 C₂D₂, and 13 C₂H₂). *J. Phys. Chem. Ref. Data*, **32(3)**:921–1361, 2003.
- M. Herman. *High-resolution Infrared Spectroscopy of Acetylene: Theoretical Background and Research Trends*. John Wiley & Sons, Ltd, London, 2011. ISBN 9780470749593. doi: 10.1002/9780470749593.hrs101.
- D. R. Herrick. Symmetry of the quadratic zeeman effect for hydrogen. *Phys. Rev. A*, **26**:323–329, 1982.
- M. P. Jacobson, C. Jung, H. S. Taylor, and R. W. Field. State-by-state assignment of the bending spectrum of acetylene at 15.000 cm⁻¹: A case study of quantum-classical correspondence. *J. Chem. Phys.*, **111**:600–618, 1999a.
- M. P. Jacobson, R. J. Silbey, and R. W. Field. Local mode behavior in the acetylene bending system. *J. Chem. Phys.*, **110**:845–859, 1999b.
- M. P. Jacobson, J. P. O'Brien, R. J. Silbey, and R. W. Field. Pure bending dynamics in the acetylene $\tilde{X}^1\Sigma_g^+$ state up to 15 000 cm⁻¹ of internal energy. *J. Chem. Phys.*, **109(1)**:121–133, July 1998.
- C. Jaffé and P. Brumer. Local and normal modes: A classical perspective. *J. Chem. Phys.*, **73(11)**:5646–5658, 1980.
- M. Joyeux, D. A. Sadovskii, and J. Tennyson. Monodromy of the LiNC/NCLi molecule. *Chem. Phys. Lett.*, **382**:439–42, Dec 2003.
- M. E. Kellman. Algebraic resonance dynamics of the normal/local transition from experimental spectra of ABA triatomics. *J. Chem. Phys.*, **83(8)**:3843–3858, 1985.
- M. E. Kellman and G. Chen. Approximate constants of motion and energy transfer pathways in highly excited acetylene. *J. Chem. Phys.*, **95(11)**:8671–8672, 1991.

- J. S. Kim, L. Michel, and B. I. Zhilinskiĭ. The ring of invariant real functions on the Brillouin zone. *Physics Reports*, **341(16):337–376**, 2001. ISSN 0370-1573. Symmetry, invariants, topology.
- I. N. Kozin and R. M. Roberts. Monodromy in the spectrum of a rigid symmetric top molecule in an electric field. *J. Chem. Phys.*, **118(23):10523–10533**, 2003.
- I. N. Kozin, D. A. Sadovskii, and B. I. Zhilinskiĭ. Assigning vibrational polyads using relative equilibria: application to ozone. *Spectrochim. Act. A*, **61:2867–85**, Oct 2005.
- L. D. Landau and E. M. Lifshitz. *Quantum mechanics (nonrelativistic theory)*, volume III of *Theoretical physics*. Fizmatlit, Moscow, 5 edition, 2002. in Russian.
- D. Larese, M. A. Caprio, F. Prez-Bernal, and F. Iachello. A study of the bending motion in tetratomic molecules by the algebraic operator expansion method. *J. Chem. Phys.*, **140(1):014304**, 2014.
- R. T. Lawton and M. S. Child. Local mode vibrations of water. *Mol. Phys.*, **37(6):1799–1807**, 1979.
- J. Ma, D. Xu, H. Guo, V. Tyng, and M. E. Kellman. Isotope effect in normal-to-local transition of acetylene bending modes. *J. Chem. Phys.*, **136(1):014304**, 2012.
- L. Michel and B. I. Zhilinskiĭ. Rydberg states of atoms and molecules. Basic group-theoretical and topological analysis. *Phys. Rep.*, **341:173–264**, 2001a.
- L. Michel and B. I. Zhilinskiĭ. Symmetry, invariants, topology. Basic tools. *Phys. Rep.*, **341:11–84**, 2001b.
- I. M. Mills and A. G. Robiette. On the relationship of normal modes to local modes in molecular vibrations. *Mol. Phys.*, **56(4):743–765**, 1985.
- J. Montaldi and R. M. Roberts. Relative equilibria of molecules. *J. Nonlin. Sci.*, **9(1):53–88**, Feb 1999. ISSN 1432-1467.
- J. Montaldi, R. M. Roberts, and I. Stewart. Periodic solutions near equilibria of symmetric Hamiltonian systems. *Phil. Trans. R. Soc. London Ser. A*, **325:237–293**, 1988.
- J. Montaldi, R. M. Roberts, and I. Stewart. Existence of nonlinear normal modes of symmetric hamiltonian systems. *Nonlinearity*, **3(3):695–730**, 1990.
- J. Patera, R. T. Sharp, and P. Winternitz. Polynomial irreducible tensors for point groups. *J. Math. Phys.*, **19(11):2362–2376**, 1978.
- C. W. Patterson, A. S. Pine, and B. J. Krohn. ν_3 vibrational ladder of sf_6 . *Opt. Lett.*, **6(1):39–41**, Jan 1981.
- W. Pauli. Über das Wasserstoffspektrum vom Standpunkt der neuen Quantenmechanik (the hydrogen spectrum from the view point of the new quantum mechanics). *Z. Phys. A*, **36:336–363**, 1926.
- I. M. Pavlichenkov. Bifurcations in quantum rotational spectra. *Phys. Rep.*, **226(4-5):173–279**, 1993. ISSN 0370-1573.
- I. M. Pavlichenkov and B. I. Zhilinskiĭ. Rotation of molecules around specific axes: axes reorientation under rotational excitation. *Chem. Phys.*, **100:339–354**, 1985.
- I. M. Pavlichenkov and B. I. Zhilinskiĭ. Critical phenomena in rotational spectra. *Ann. Phys. (N.Y.)*, **184:1–32**, 1988.

- V. E. Pavlov-Verevkin and B. I. Zhilinskiĭ. Effective Hamiltonians for vibrational polyads: integrity basis approach. *Chem. Phys.*, **126(2)**:243–253, 1988. ISSN 0301-0104.
- J. Plřva. Molecular constants for the bending modes of acetylene $^{12}\text{C}_2\text{H}_2$. *J. Molec. Spectrosc.*, **44(1)**:165–182, 1972.
- J. P. Rose and M. E. Kellman. Bending dynamics from acetylene spectra: Normal, local, and precessional modes. *J. Chem. Phys.*, **105(24)**:10743–10754, 1996.
- D. A. Sadovskii and B. I. Zhilinskiĭ. Qualitative study of a model three-level Hamiltonian with $\text{SU}(3)$ dynamical symmetry. *Phys. Rev. A*, **48**:1035–44, Aug 1993a.
- D. A. Sadovskii and B. I. Zhilinskiĭ. Group-theoretical and topological analysis of localized rotation-vibration states. *Phys. Rev. A*, **47**:2653–71, Apr 1993b.
- D. A. Sadovskii and B. I. Zhilinskiĭ. Counting levels within vibrational polyads: generating function approach. *J. Chem. Phys.*, **103**:10520–36, Dec 1995.
- D. A. Sadovskii and B. I. Zhilinskiĭ. Tuning the hydrogen atom in crossed fields between the Zeeman and Stark limits. *Phys. Rev. A*, **57**:2867–84, Apr 1998.
- D. A. Sadovskii and B. I. Zhilinskiĭ. Monodromy, diabolic points, and angular momentum coupling. *Phys. Lett. A*, **256**:235–44, Jun 1999.
- D. A. Sadovskii and B. I. Zhilinskiĭ. Quantum monodromy and its generalizations and molecular manifestations. *Mol. Phys.*, **104**:2595–615, Aug 2006.
- D. A. Sadovskii, D. N. Kozlov, and P. P. Radi. Direct absorption transitions to highly excited polyads 8, 10, and 12 of methane. *Phys. Rev. A*, **82**:012503/1–17, Jul 2010.
- R. P. Stanley. Invariants of finite groups and their applications to combinatorics. *Bull. Amer. Math. Soc.*, **1(3)**:475–511, 1979.
- B. Sturmfels. *Algorithms in invariant theory*. Springer Verlag, Berlin, 1993.
- M. A. Tamsamani and M. Herman. The vibrational energy levels in acetylene $^{12}\text{C}_2\text{H}_2$: Towards a regular pattern at higher energies. *J. Chem. Phys.*, **102(16)**:6371–6384, 1995.
- M. A. Tamsamani, M. Herman, S. A. B. Solina, J. P. O’Brien, and R. W. Field. Highly vibrationally excited $^{12}\text{C}_2\text{H}_2$ in the $\tilde{X}^1\Sigma_g^+$ state: Complementarity of absorption and dispersed fluorescence spectra. *J. Chem. Phys.*, **105(24)**:11357–11359, 1996.
- D. J. Thouless. *Topological Quantum Numbers in Nonrelativistic Physics*. World Scientific, Singapore, 1998.
- V. Tyng and M. E. Kellman. Bending dynamics of acetylene: new modes born in bifurcations of normal modes. *J. Phys. Chem. B*, **110(38)**:18859–71, Sep 2006.
- V. Tyng and M. E. Kellman. Catastrophe map and the role of individual resonances in C_2H_2 bending dynamics. *J. Chem. Phys.*, **130(14)**:144311, April 14 2009a.
- V. Tyng and M. E. Kellman. Critical points bifurcation analysis of high- ℓ bending dynamics in acetylene. *J. Chem. Phys.*, **131(24)**:244111, Dec 2009b.
- V. Tyng and M. E. Kellman. Bifurcation phase diagram for c_2h_2 bending dynamics has a tetra-critical point with spectral patterns. *J. Phys. Chem. A*, **114(36)**:9825–9831, June 2010.
- G. Valent. The hydrogen atom in electric and magnetic fields: Pauli’s 1926 article. *Am. J. Phys.*, **71**:171–175, 2003.

- J. van der Meer. The Kepler system as a reduced 4D harmonic oscillator. *J. Geom. Phys.*, **92** (Suppl. C):181–193, 2015.
- H. Waalkens, H. R. Dullin, and P. H. Richter. The problem of two fixed centers: bifurcations, actions, monodromy. *Physica D*, **196**:265–310, 2004.
- H. Weyl. *Classical groups, their invariants and representations*. Princeton University Press, New Jersey, 1939.
- M. Winnewisser, B. P. Winnewisser, I. R. Medvedev, F. C. De Lucia, S. C. Ross, and L. M. Bates. The hidden kernel of molecular quasi-linearity: Quantum monodromy. *J. Mol. Struct.*, **798**:1–26, 2006. ISSN 0022-2860.
- L. Xiao and M. E. Kellman. Catastrophe map classification of the generalized normal-local transition in Fermi resonance spectra. *J. Chem. Phys.*, **93**(8):5805–20, 15 Oct 1990.
- B. I. Zhilinskiĭ, M. I. E. Idrissi, and M. Herman. The vibrational energy pattern in acetylene (VI): Inter- and intrapolyad structures. *J. Chem. Phys.*, **113**(18):7885–7890, 2000.
- B. I. Zhilinskiĭ. Qualitative analysis of vibrational polyads: N -mode case. *Chem. Phys.*, **137**(1):1–13, 1989. ISSN 0301-0104.
- B. I. Zhilinskiĭ. Symmetry, invariants, and topology in molecular models. *Phys. Rep.*, **341**(1):85–171, 2001.
- B. I. Zhilinskiĭ. Interpretation of quantum Hamiltonian monodromy in terms of lattice defects. *Acta Appl. Math.*, **87**(1):281–307, May 2005.